Ion Exchange in Porous Crystals

by

Brian Marsden Munday

A thesis submitted for the Degree of

Doctor of Philosophy of the University

of London

Department of Chemistry
Imperial College of Science
and Technology
London, S.W.7.

July, 1969

Abstract

Ion exchange equilibria at 25° C have been studied in the natural zeolite phillipsite, and in the synthetic zeolites Na-P (cubic) and K-F. Exchange isotherms are presented for the following ion pairs:

Phillipsite: Na-Li, Na-K, Na-Rb, Na-Cs, Na-Ca, Na-Sr, Na-Ba
Na-P : Na-Li, Na-K, Na-Rb, Na-Cs, Na-Sr, Na-Ba
K-F : Na-Li, K-Li, Na-K, Na-Cs, K-Cs, Na-Ca, Na-Sr, Na-Ba, K-Ba.

The selectivity series found for exchanges in phillipsite (based on the thermodynamic equilibrium constant) was

$$Li \ll Ca < Sr < Na < Rb \sim K < Cs \ll Ba.$$

The Na-Ba exchange was highly selective for Ba (giving quantitative removal of Ba from solution up to a Ba loading of 0.6) but was irreversible under the experimental conditions.

In zeolite P the selectivity series was found to be

$$Li \ll Na < K \sim Rb \sim Cs \sim Sr \ll Ba$$

All exchanges in zeolite P appeared to be reversible, although accompanied by considerable changes in unit cell size and symmetry. Complete replacement of Na by Cs could not be obtained. In all exchanges in phillipsite and Na-P, the selectivity coefficient varied with the cation loading. The variation was linear in several cases, and Kielland constants were calculated. A positive Kielland constant was found for the Na-K exchange in zeolite P.

In zeolite F, only the K-Li and Na-Cs isotherms were completely reversible. The Na-Li and Na-K isotherms exhibited small, but well-defined hysteresis loops. All other isotherms were found to be irreversible, or to show pronounced hysteresis.

This unusual behaviour has been interpreted in terms of two types of exchange site . The hysteresis and irreversibility in some exchanges have been qualitatively explained as arising from unusually large differences in the unit cell sizes of the various cationic forms of this zeolite.

Exchanges involving the ions K-Li, K-Na, and K-Ba are also presented for zeolite K-F containing various amounts of occluded potassium chloride.

Solid phase activity coefficients and thermodynamic equilibrium constants have been calculated for all reversible exchanges using a computer program "CALCIS" written for this work.

Acknowledgements

I wish to express my thanks to Professor R.M. Barrer, F.R.S. for his constant encouragement and guidance during the course of this work.

I am also indebted to my colleagues in these laboratories for many helpful suggestions and discussions. In particular I wish to thank Hans Villiger for his assistance with computer programming and X-ray powder diffraction.

Finally I should like to thank the Colonial Sugar Refining Company Limited, Australia, without whose generous sponsorship I could not have undertaken this work.

Nomenclature

The following symbols and conventions are used throughout this thesis:-

Symbols

A, B	cations.
z_A, z_B	valencies of A, B.
A_z, B_z	equivalent cation fractions of A and B in a zeolite.
A_s, B_s	equivalent cation fractions of A and B in solution.
m_A, m_B	molalities of A and B in solution.
γ_A, γ_B	molal ionic activity coefficients of A and B in solution.
$\gamma_{\pm AX}$, $\gamma_{\pm BX}$	mean ionic activity coefficients of salts AX and BX in solution.
$\gamma_{\pm AX}^{(BX)}$, $\gamma_{\pm BX}^{(AX)}$	mean ionic activity coefficients of salts AX and BX in mixed solution (AX + BX).
f_A, f_B	rational activity coefficients of A and B in the zeolite.
$a_{A(z)}$, $a_{B(z)}$	activities of A and B in the zeolite.
$a_{A(s)}$, $a_{B(s)}$	activities of A and B in solution.
n_A, n_B, n_w	moles of A, B, and water.
μ_i	chemical potential of species i.
I	ionic strength of solution.
K_c	selectivity coefficient.
K_c'	"corrected" selectivity coefficient.
K_a	rational thermodynamic equilibrium constant.

Conventions

1. Subscripts (z) and (s) refer to the zeolite and solution respectively.

2. The description of an ion exchange reaction as proceeding "from A to B" (written A ⟶ B) refers to the conversion of the exchanger from the A form to the B form.

3. For the exchange equilibrium

$$z_B A_{(s)} + z_A B_{(z)} \rightleftharpoons z_B A_{(z)} + z_A B_{(s)}$$

(i) the selectivity coefficient K_c is defined by

$$K_c = \frac{A_z^{z_B} \cdot m_B^{z_A}}{B_z^{z_A} \cdot m_A^{z_B}}$$

Note that zeolite ion concentrations are expressed as equivalent fractions, whereas solution concentrations are molalities,

(ii) the "corrected" selectivity coefficient K_c' is defined by

$$K_c' = K_c \cdot \frac{\gamma_B^{z_A}}{\gamma_A^{z_B}}$$

(iii) the rational thermodynamic equilibrium constant K_a is given by

$$K_a = K_c' \cdot \frac{f_A^{z_B}}{f_B^{z_A}}$$

4. The logarithm of a quantity x to base 10 is written as log x. Logarithms to base e are written as ln x.

5. Exchange isotherms are plotted with A_s as the ordinate, and A_z as the abscissa.

Contents

1. Introduction

Historical Development

Phenomena which may now be ascribed to ion exchange processes have been observed from the days of Aristotle onwards. Most of these observations involved the partial purification of brackish water after passage through mineral sands and soils.

The ion exchange basis of this effect was first proposed in 1850 by Thompson (1) and Way (2), who described it as "base-exchange". Lemberg (3), and later Wiegner (4) attributed this behaviour to the presence of glauconites, clays, zeolites, and humic acids in the soil. It is interesting, in the light of later developments, to note that both inorganic and organic substances were then known to exhibit ion exchange behaviour.

The investigation and utilisation of ion exchange materials have increased greatly in the last thirty years, following the development of polymeric organic resin exchangers. Work on inorganic exchangers has also been expanding, but has tended to be overshadowed by the rapid advances in resin exchanger technology. In recent years however, ion exchange processes involving high temperatures or the presence of ionising radiation (conditions to which organic resin exchangers are not generally suited) have lead to a renewal of interest in inorganic exchangers.

Many inorganic materials exhibit ion exchange behaviour (5). Apart from the further development of the "soil-based" exchangers, compounds such as molybdo- and tungsto- phosphates, arsenates and silicates, hydrous oxides of polyvalent metals, zirconium phosphate and antimonate, and rare earth vanadates, have all been investigated as ion exchangers. A comprehensive discussion of the synthesis and properties of these interesting compounds has been presented by Amphlett (6).

The Zeolites

As noted above, zeolites were among the first materials known to function as ion exchangers; the original synthetic exchangers were also of this type. Gans (7) was responsible for much of the development of "permutites", partially crystalline sodium aluminosilicate gels, widely used for water purification.

All silicate minerals are essentially based on the tetrahedral SiO_4^{4-} structural unit. These units may be linked, by sharing oxygen atoms, to form the various classes of the silicate minerals (8). Of these, the tectosilicates are characterised by a three-dimensional framework resulting from the joining of each tetrahedron to four other such tetrahedra, giving a resultant composition $(SiO_2)_n$. However, because of the similarity of the Si-O and Al-O bond lengths (approximately 1.63 Å and 1.73 Å respectively), and the ability of aluminium to enter into four-fold co-ordination, replacement of silicon by aluminium can occur in these silicates. The extent of this replacement is limited by Loewenstein's Rule (9), which states that the maximum ratio of tetrahedrally co-ordinated aluminium to silicon is 1:1, as the linkage of two AlO_4^{5-} tetrahedra is not permitted.

Such replacement of Si by Al occurs in the felspars, zeolites, and felspathoids. In these minerals the excess negative charge created by the introduction of tripositive aluminium atoms is balanced by the incorporation of an equivalent number of cations. The felspars have compact framework structures, and the cations are not normally accessible for exchange. In the zeolites and felspathoids however, the framework atoms are linked in such a way as to create large cavities and channels in the structure. These voids contain the cations and water in the case of zeolites, and cations and entrapped salt molecules in the felspathoids. There is a great diversity of cavity types and sizes in the zeolite minerals. Meier (10) has recently described those zeolites for which the structure is known, and many examples of the various types of cavity known to occur may be found in his paper.

These unique structural features of the zeolites account for their most interesting and technically important properties. The water in the cavities and channels of most zeolites may be removed under vacuum or by moderate heating, without the collapse of the framework. The "outgassed" zeolites so formed behave as excellent sorbents for water and other molecules. Moreover, because the cavities and pores are of fixed dimensions for any particular zeolite, sorption is governed by the size and configuration of the sorbate. Thus zeolites are known as 'molecular sieves'. Many zeolites, particularly in the hydrogen or rare-earth exchanged form, are very active catalysts, and are widely used as such in the petroleum industry and elsewhere (11).

The property most relevant to the present work is that of ion exchange. Because the cations are electrostatically bound to the framework, and are potentially accessible via the channel systems, they may be exchanged for other cations, provided these are not excluded by the molecular sieve action.

Extensive research, particularly by Barrer in this country, and by chemists of the Union Carbide Corporation in the United States, has resulted in the synthesis and investigation of several zeolites, some of which have natural counterparts, and others which are novel species. Many of these zeolites have found important applications in industry (12).

The structures of most of the natural zeolites, and an increasing number of synthetic zeolites, have now been determined (10). This detailed structural knowledge has provided a sound basis for understanding the mechanisms of many of thereactions in which zeolites are involved, including fundamental sorption and solid state reactions (e.g.(13)).

Our eventual understanding of the behaviour of the zeolites, and through them, of more complicated systems, will result from research into every facet of their behaviour - synthesis, structure, sorption, and ion exchange.

The work described in this thesis is concerned with the ion exchange properties of three zeolites:- the natural mineral phillipsite, and the synthetic zeolites named Na-P (cubic) (14) and K-F (15) by Barrer. Exchange isotherms have been determined at 25° C, with ion pairs selected from the alkali and alkaline earth metals. In all cases the solution concentration was constant and equal to 0.100 equivalents per litre.

2. Ion Exchange in Zeolites

The ion exchange properties of several zeolites have been investigated in recent years, mainly by Barrer and co-workers in this country, and by Sherry and Ames, in the U.S.A. Much of this work has been concentrated on the commercially important synthetic zeolites A, X, and Y, produced by the Union Carbide Corporation.

A partial list of the felspathoids and zeolites studied includes:

Analcite	(16), (17), (33)
'Basic' Cancrinite	(17)
'Basic' Sodalite	(17)
Chabazite	(18), (19), (33)
Clinoptilolite	(20), (21), (22)
Mordenite	(23), (20), (21)
Erionite	(20), (21)
Phillipsite	(20), (21)
Zeolite 'A'	(24), (25), (20), (21)
Zeolite 'X'	(20), (21), (26), (27), (28), (29), (30), (31)
Zeolite 'Y'	(28), (29), (31), (32)

These investigations have revealed that ion exchanges in zeolites often exhibit several distinctive features, which arise directly or indirectly from the unique structural characteristics of these materials.

Ion Exclusion

In this most extreme form of several 'ion-sieve' effects, a particular ion, because of its size, may be completely excluded from entering the zeolite. Some examples of this effect are given in Table 2.1.

Table 2.1

Exchanger	Exchanged	Not Exchanged
Ultramarine (34)	K^+	Cs^+
Analcite (16)	Rb^+	Cs^+
Basic cancrinite (17)	Rb^+	Cs^+
Chabazite (18)	Cs^+	$\overset{+}{N}Me_4$
Faujasite (26)	$\overset{+}{N}Me_4$	$\overset{+}{N}Et_4$

The exclusion of Cs^+ by basic cancrinite (17) is of particular interest, sincethe diameter of the Cs^+ ion is less than that of the cancrinite channels. Barrer and Falconer have suggested that the exclusion of Cs^+ in this case results from the "two-way traffic' requirements for ion exchange in cancrinite, when the channels are not interconnected. There is insufficient room for Cs^+ to "pass" another ion in the channels, and therefore exchange does not occur.

Ion exclusion may also result from a valency effect. Barrer and Sammon (18) reported that lanthanum was excluded from chabazite. This could not be explained on a purely steric basis, since Rb^+, of greater size, was not excluded. The reason advanced in this case was that exchange of sodium by tripositive lanthanum would lead to regions of excess positive charge in the vicinity of the La^{3+} ion, and regions of negative charge at the sites vacated by two of the three sodium ions replaced by the lanthanum. Such a situation would be energetically unfavourable, and exchange therefore did not occur.

Incomplete exchange can occur if the entering ions, although of a diameter small enough to enable them to enter the crystal, occupy so much space that complete replacement of the original ions is impossible. This effect was strikingly demonstrated by the work of Barrer et al. on alkylammonium ion exchange in zeolite NaX. Using solutions of alkyl

ammonium chlorides, they found that the maximum percentage of exchange fell from 92%, for ammonium ions, to 23% for $\overset{+}{N}Me_4$. No exchange occurred with $\overset{+}{N}Et_4$ (26). For tetramethyl ammonium ions, the available interstitial volume in the crystal would be fully occupied by 33 $\overset{+}{N}Me_4$ cations, whereas complete exchange would require 86 cations per unit cell.

Ion-sieve effects in zeolites have led to important applications. Silver analcite has been used as a reagent for separating Cs^+ from other alkali metal cations (35). Complete removal of Na^+ from mixed (Na, Cs) solutions was obtained at 100° C. The ion-sieve effect is also the basis of an identification reaction for zeolites, proposed by Helferrich (36). In this test the mineral under investigation is first treated with silver nitrate in neutral solution for 30 minutes. The solid is separated, and shaken with tetra-n-butyl ammonium bromide solution. The pH of the supernatant liquid is then measured. With zeolites, this pH is normally 9 to 11. The reactions occurring are:

$$M^+(z) + Ag^+(s) \rightleftharpoons Ag^+(z) + M^+(s)$$

$$Ag^+(z) + \overset{+}{N}Bu_4 + Br^- + H_2O \longrightarrow H^+(z) + AgBr\downarrow + OH^- + \overset{+}{N}Bu_4.$$

The tetraalkylammonium cation is excluded by the zeolite. Hydrogen (or hydronium) ion exchange occurs as the silver ions are removed by precipitation.

The same type of reaction can be used to produce hydrogen exchanged forms of zeolites for the very important catalytic applications.

Selectivity in Zeolite Ion Exchangers

Various affinity sequences have been found for uni-univalent cation exchanges on zeolites, many of the sequences falling into one or other of the eleven affinity series predicted by Eisenman (37).

In many zeolite systems, however, selectivity series quoted must

be regarded with caution, since selectivity coefficients often vary with cation loading. Series quoted on the basis of the thermodynamic equilibrium constant K_a can also be misleading, as K_a is a constant reflecting the overall exchange behaviour. For any two isotherms giving the same K_a, the selectivity coefficient can vary significantly, and selectivity reversal may occur.

Barrer and Meier have classified the behaviour of the selectivity coefficient in three categories:-

I $\dfrac{d \log K'_c}{d A_z} = 0$, i.e., selectivity coefficient constant.

II $\dfrac{d \log K'_c}{d A_z}$ = constant, log selectivity coefficient varies linearly with cation loading.

III $\dfrac{d \log K'_c}{d A_z}$ not constant: general case.

Many examples of all three types of behaviour have been reported. Constant selectivity coefficients have been found for the Na-Li exchange in ultramarine (34), Na-Li, Na-K, Na-Ag and Li-K exchanges in basic sodalite (17), and several others. One very interesting example was the Na-Ag exchange in Zeolite A, in which an apparent selectivity reversal was shown by Barrer and Meier to be due to the presence of two types of exchange site, each having ideal (constant K'_c) behaviour.

Examples of type II are quite common, and include the Na-Rb, Na-Tl, K-Ag exchanges in chabazite (18). The theoretical basis of a linear variation of log K_c with cation loading is discussed in Section 3.

Limited Solid Solubility

The Na-K, Na-Tl and K-Tl isotherms in analcite, studied by Barrer and Hinds (16) exhibited considerable hysteresis, the forward and reverse isotherms following different paths. Within the hysteresis

loop two phases co-existed, one representing one end-member of exchange, and the other the second end-member. The hysteresis loop was therefore indicative of a miscibility gap in the mixed end-member solid solutions, and the hysteresis resulted from the difficulty of nucleating one phase in the presence of the other. (In the Na-K exchange, the end-members are actually known as distinct minerals, the sodium form being analcite, the potassium form leucite.) Limited solid solubility has also been observed by Sherry in the Na-Sr ion exchange in Zeolite X (30). In this work, a very elegant investigation, by X-ray crystallography, demonstrated the existence of two phases, and related their appearance to changes in cation positions in the unit cell. Further examples of limited solid solubility, and hysteresis, were observed in the present work, and are discussed in Section 7.

Ion Exchange in Phillipsite, Na-P, and K-F

Phillipsite

Ames has reported ion-exchange isotherms for a Nevada phillipsite, involving the ion pairs Na-Cs, Na-K, K-Cs (20), and Na-Sr, Na-Ca, Sr-Ca (21). The silica-alumina ratio for this sample was given as 4:1. All exchanges were complete, and (assumed) reversible, and were conducted at a constant solution concentration of 1.0 N.

Hoss and Roy (38) prepared Li, Na, K, Ca, and Ba exchanged forms from a sample of phillipsite of non-sedimentary origin, with $SiO_2 : Al_2O_3$ equal to 3.5:1. Exchange was incomplete in all cases, ranging from about 90% for Na and Ca, to 25% for Ba. The original phillipsite was calcium-rich. No quantitative exchange isotherms are given.

Barrer, Bultitude and Kerr (39) have discussed the relationship between the minerals phillipsite, wellsite, and harmotome, and the zeolites of the 'P' group. The Ca and Ba derivatives of tetragonal Na-P showed considerable similarity to the derivatives of the natural harmotome zeolites. The similarity between potassium phillipsite and

the synthetic zeolite K-M (40) was again apparent. A structural scheme for zeolites of the P group, harmotome and phillipsite was proposed, as discussed in Section 4.

Zeolite Na-P (cubic)

No quantitative ion exchange isotherms have been found in the literature for zeolites of the P group. (The relationships between cubic and tetragonal forms of Na-P synthesised by Barrer (41) are discussed in Section 4.)

In an extensive study of the synthesis and properties of the P zeolites, Taylor and Roy found miscibility gaps in the Na-Ca and Na-K exchange reactions of tetragonal Na-P (42)(43).

Zeolite K-F

In the original work on the synthesis of zeolite K-F, Barrer and Baynham (40) prepared the Na and Ca derivatives. X-ray diffraction studies showed no appreciable change in the lattice dimensions when these ions were introduced (40). The Rb and Cs forms of zeolite F were synthesised directly by Barrer, Cole, and Sticher (44) ("Rb-D and Cs-D"). The rubidium zeolite had previously been made by Barrer and McCallum (45). The relationship between Rb-D, Cs-D and K-F was demonstrated by the identity of the X-ray patterns of the Rb and Cs derivatives of K-F, although both these exchanges were incomplete at room temperature. Lattice expansion was observed to occur during both exchanges.

Barrer, Cole, and Sticher also reported an exchange isotherm at 25° C for the K⟶Na exchange in zeolite F. This isotherm had a discontinuity between approximately $0.6 < K_2 < 0.9$. The reverse isotherm (Na⟶K) was not determined. This appears to be the only quantitative exchange isotherm reported for this zeolite.

A mixed (Na,Li) form of zeolite F has recently been synthesised by Borer (46).

3. Theoretical Treatment of Ion Exchange Equilibria

Many theoretical models of ion exchange behaviour have been advanced, ranging from purely empirical equations to thermodynamic and statistical mechanical theories. The approaches adopted have depended largely on the type of exchanger under consideration.

Several theories have been developed to account for ion exchange in resin exchangers, where swelling of the exchanger and solute uptake can be significant. The more important theories in this category are discussed by Helferrich (47).

The effects of swelling and (if dilute solutions are employed) of solute and solvent uptake are of very minor importance in zeolite exchangers, and can be neglected in most cases.

This discussion will therefore be limited to those theories which have been successfully applied to zeolite exchangers.

The Exchange Equation

The ion exchange equilibrium to be discussed may be represented by the equation:

$$z_B{}^{z_A+}A_{(s)} + z_A{}^{z_B+}B_{(z)} \rightleftharpoons z_B{}^{z_A+}A_{(z)} + z_A{}^{z_B+}B_{(s)}$$

Application of the law of mass action gives, for the equilibrium constant K_a,

$$K_a = \frac{a_{A(z)}^{z_B} \cdot a_{B(s)}^{z_A}}{a_{B(z)}^{z_A} \cdot a_{A(s)}^{z_B}}$$

The solution activities may be expressed in the usual way as a concentration term multiplied by an ionic activity coefficient. The

concentration units used in this work are molalities, and the activity coefficients are therefore molal ionic activity coefficients.

Thus
$$K_a = \frac{a_{A(z)}^{z_B} \cdot m_B^{z_A} \cdot \gamma_B^{z_A}}{a_{B(z)}^{z_A} \cdot m_A^{z_B} \cdot \gamma_A^{z_B}}$$

If the zeolite components are regarded as comprising a solid solution $(A,B)_z$, the activity terms for the zeolite phase may be similarly expressed in terms of concentration and activity coefficient. The convention used in this thesis is that equivalent fractions are used for the zeolite phase concentrations, and the associated activity coefficients are therefore rational activity coefficients

$$K_a = \frac{A_z^{z_B} \cdot f_A^{z_B} \cdot m_B^{z_A} \cdot \gamma_B^{z_A}}{B_z^{z_A} \cdot f_B^{z_A} \cdot m_A^{z_B} \cdot \gamma_A^{z_B}} \qquad \text{Equation 3.1}$$

$$= K_c' \cdot \frac{f_A^{z_B}}{f_B^{z_A}} \quad \text{by definition of } K_c' .$$

K_c' thus defined is the corrected selectivity coefficient. In the above expression for K_a (equation 3.1), the quantities A_z, B_z, m_A and m_B are determined experimentally, leaving the activity coefficients γ and f to be evaluated.

Evaluation of Solution Phase Activity Coefficients

The activity coefficients γ_A and γ_B are individual ion activity coefficients, and as such cannot be determined. The ratio $\Gamma = \gamma_B^{z_A}/\gamma_A^{z_B}$ can however be evaluated.

The mean ionic activity coefficient of an electrolyte $A_{p+}X_{p-}$ is given by

$$\gamma_{\pm AX} = \left(\gamma_A^{p+} \cdot \gamma_X^{p-}\right)^{\frac{1}{p+ + p-}}$$

where p+ and p- are the number of cations and anions respectively. If the cation A has a valency z_A, and the anion X a valency z_X, then

$$p+ = z_X; \quad p- = z_A$$

$$\gamma_{\pm AX} = \left(\gamma_A^{z_X} \cdot \gamma_X^{z_A}\right)^{\frac{1}{z_X+z_A}} \qquad \text{Equation 3.2}$$

Similarly

$$\gamma_{\pm BX} = \left(\gamma_B^{z_X} \cdot \gamma_X^{z_B}\right)^{\frac{1}{z_X+z_B}} \qquad \text{Equation 3.3}$$

By raising both sides of equation 3.2 to the power $\frac{z_B(z_X+z_A)}{z_X}$, and both sides of equation 3.3 to the power $\frac{z_A(z_X+z_B)}{z_X}$, and dividing

$$\Gamma = \frac{\gamma_B^{z_A}}{\gamma_A^{z_B}} = \frac{\gamma_{\pm BX}^{z_A(z_B+z_X)/z_X}}{\gamma_{\pm AX}^{z_B(z_A+z_X)/z_X}} \qquad \text{Equation 3.4}$$

In the case of two univalent cations A and B, and a common univalent anion X, this reduces to

$$\Gamma = \frac{\gamma_B}{\gamma_A} = \frac{\gamma_{\pm BX}^2}{\gamma_{\pm AX}^2}$$

Strictly, however, the mean activity coefficients required are those for the salts AX and BX in mixed solution (A,B)X. Glueckauf (48) has derived an expression for the required mean ionic activity coefficients in terms of the activity coefficients

of the pure salts at the ionic strength of the mixed solution:-

$$\log \gamma_{\pm AX}^{(BX)} = \log \gamma_{\pm AX} - \frac{m_B}{4I}\left[k_1 \log \gamma_{\pm AX} - k_2 \log \gamma_{\pm BX} - \frac{k_3}{1+I^{\frac{1}{2}}}\right]$$

Equation 3.5

and

$$\log \gamma_{\pm BX}^{(AX)} = \log \gamma_{\pm BX} - \frac{m_A}{4I}\left[k_1' \log \gamma_{\pm BX} - k_2' \log \gamma_{\pm AX} - \frac{k_3'}{1+I^{\frac{1}{2}}}\right]$$

Equation 3.6

where

$k_1 = z_B(2z_B - z_A + z_X)$

$k_2 = z_A(z_B + z_X)^2 (z_A + z_X)^{-1}$

$k_3 = \frac{1}{2} z_A . z_B . z_X (z_A - z_B)^2 (z_A + z_X)^{-1}$

$k_1' = z_A(2z_A - z_B + z_X)$

$k_2' = z_B(z_A + z_X)^2 (z_B + z_X)^{-1}$

$k_3' = \frac{1}{2} z_B . z_A . z_X (z_B - z_A)^2 (z_B + z_X)^{-1}$

I = ionic strength of the mixed solution.

The ionic strength I may be expressed in terms of the constant total normality T_N and the solution concentration A_s by using the relations

$$I = \frac{1}{2} \Sigma m_i z_i^2$$

$$m_A = \frac{T_N . A_s}{z_A} \; ; \; m_B = \frac{T_N . B_s}{z_B}$$

$$A_s + B_s = 1.$$

Thus

$$I = \frac{T_N}{2}\left[z_X + z_B + A_s(z_A - z_B)\right]$$

Substitution of these terms in equations 3.5 and 3.6 enables $\log \gamma_{\pm AX}^{(BX)}$ and $\log \gamma_{\pm BX}^{(AX)}$ to be calculated. The $\gamma_{\pm AX}$ and $\gamma_{\pm BX}$ inserted must be the mean ionic activity coefficients of the salts AX and BX at the

ionic strength I, and must therefore be known as a function of I.

The required function Γ is given by

$$\log \Gamma = \frac{z_A(z_B + z_X)}{z_X} \log \gamma_{\pm BX}^{(AX)} - \frac{z_B(z_A + z_X)}{z_X} \log \gamma_{\pm AX}^{(BX)}$$

For uni-univalentexchanges using 1:1 electrolytes the equations reduce to:-

(i) $k_1 = k_2 = k_1' = k_2' = 2;\ k_3 = k_3' = 0.$

(ii) $I = T_N.$

(iii) $$\log \gamma_{\pm AX}^{(BX)} = \log \gamma_{\pm AX} - \frac{B_s}{4}\left[2 \log \gamma_{\pm AX} - 2 \log \gamma_{\pm BX}\right].$$

(iv) $$\log \gamma_{\pm BX}^{(AX)} = \log \gamma_{\pm BX} - \frac{A_s}{4}\left[2 \log \gamma_{\pm BX} - 2 \log \gamma_{\pm AX}\right]$$

(v) $$\log \Gamma = \log \gamma_{\pm BX} - \log \gamma_{\pm AX}.$$

Therefore for uni-univalent exchanges conducted at a constant total concentration,

$$\Gamma = \gamma_{\pm BX}/\gamma_{\pm AX} \quad \text{for all } A_s$$

Evaluation of Solid Phase Activity Coefficients

If the assumption is made that the ratio of the solid phase activity coefficients is constant, then for uni-univalent exchanges (in which, as shown above, the ratio of solution phase activity coefficients is constant)

$$\frac{A_z \cdot B_s}{B_z \cdot A_s} = \text{constant}.$$

This is the simplest form of the law of mass action, and has been found to apply in several zeolite exchanges (for example the Na-Tl exchange in Linde zeolite A (25), and the Na-Ag, Na-Li, and Na-K exchanges in

basic sodalite (17)).

In most cases, however, the selectivity coefficient is not constant, but is a function of A_z. Kielland (49) proposed the following semi-empirical equations to take account of this dependence:-

$$\log f_A = C.B_z^2 \; ; \; \log f_B = C.A_z^2$$

where C is a constant (the "Kielland constant"). These equations were derived for uni-univalent exchanges only. (Note that logarithms used are to base 10.) Substitution in the mass action equation 3.1 gives

$$K_a = K_c' \, e^{2.3C(B_z^2 - A_z^2)}$$

$$= K_c' \, e^{2.3C(1-2A_z)} \quad \text{since } A_z + B_z = 1$$

$$\log K_a = \log K_c' + C(1-2A_z) \qquad \text{Equation 3.7}$$

Thus a plot of $\log K_c'$ versus A_z should, by this theory, produce a straight line of gradient 2C and intercept on the $\log K_c'$ axis of $(\log K_a - C)$.

This equation 3.7 has been found to hold for many uni-univalent exchanges in zeolites. All values of the constant C so far reported have been negative, and mainly in the range 0 to -1. (If C = 0, equation 3.7 reduces to the simple mass action equation.)

Barrer and Sammon (18), for example, have reported linear $\log K_c'$ versus A_z plots for the Na-Rb, Na-Tl, and K-Ag exchanges in chabazite.

In 1956, Barrer and Falconer developed a statistical mechanical theory of ion exchange (17). They assumed that

(a) when two entering ions, B, occupy adjacent sites in a A-rich lattice, an additional change in the energy of the crystal occurs.

(b) This change is negligible when ions A, B occupy adjacent sites

relative to the state when two A ions occupy adjacent sites.

(c) The change in energy is additive with respect to the number of pairs (B,B) independently of whether these occur in clusters or singly.

(d) Apart from this energy change, all other interactions between the energy change and the partition functions of ions A and B in the framework, and of the framework, are neglected.

(e) The distribution of ions on sites is random.

(f) The amount of intracrystalline water is unaltered by exchange.

The energy change occurring when two B ions occupy adjacent sites was set equal to $\frac{2w}{z}$, where w is an energy term, and z the co-ordination number of any site.

The statistical mechanics treatment leads to the following expression in the case of two ions of equal valencies:-

$$\log \frac{A_z.B_s}{A_s.B_z} = \log \frac{j_A(T)}{j_B(T)} + \frac{1}{2.303}\left[\frac{\mu^0_{A_s} - \mu^0_{B_s}}{kT} + \frac{E_A - E_B}{kT}\right] + \frac{2B_z}{2.303}\,\frac{(N_A+N_B)}{N}\,\frac{w}{kT}$$

Equation 3.8

where $j_A(T)$ and $j_B(T)$ are the partition functions of the ions A and B in the zeolite, N is the total number of available sites, and N_A, N_B are the number of ions A or B in the crystal. E_A and E_B are the energies of the ions in the crystal relative to their energies in a convenient reference state, and excluding pair interactions.

A similar treatment has recently been used by Birch, Redfern, and Salmon for uni-divalent anion exchanges (75).

Equation 3.8 is of the same form as equation 3.7, derived from Kiellands equations. For identity

$$K_a = \frac{j_A(T)}{j_B(T)} \exp\left[\frac{\mu^0_{A_s} - \mu^0_{B_s} + (E_A - E_B)}{kT} + \frac{w(N_A + N_B)}{NkT}\right]$$

$$C = -\frac{w(N_A + N_B)}{2.303\ N\ kT}$$

Thus the Barrer and Falconer treatment provides a sound explanation of Kielland's equations.

The equation for a uni-univalent exchange isotherm according to the Kielland and Barrer and Falconer theory becomes

$$K_a = \frac{A_z.B_s}{B_z.A_s}\ \Gamma\ \exp\left\{2.3\ C(1-2\ A_z)\right\} \qquad \text{Equation 3.9}$$

This equation is an explicit function of A_s, but an implicit function of A_z.

Rearrangement of equation 3.9 gives

$$A_s = \frac{\Gamma\ A_z\ \exp\left\{2.3C(1-2\ A_z)\right\}}{K_a(1-A_z) + \Gamma\ A_z\ \exp\left\{2.3C(1-2\ A_z)\right\}} \qquad \text{Equation 3.10}$$

Differentiation with respect to A_z gives

$$\frac{dA_s}{dA_z} = \frac{K_a\Gamma \exp\left\{2.3C(1-2A_z)\right\}.\ (4.6C\ A_z^2 - 4.6C\ A_z + 1)}{\left[K_a(1-A_z) + \Gamma A_z\ \exp\left\{2.3C(1-2A_z)\right\}\right]^2}$$

$$\frac{dA_s}{dA_z} = 0 \qquad \text{when} \qquad 4.6C\ A_z^2 - 4.6C\ A_z + 1 = 0$$

i.e., when $A_z = 0.5 \pm \sqrt{\frac{4.6C-4}{4x4.6C}}$

The roots of this equation are real when

$$4.6C > 4$$
$$C > 0.87$$

Since the sum of the roots of the quadratic = 1, and the product of the roots = $\frac{1}{4.6C}$, both roots for $C > 0.87$ lie in the range $0 < A_z < 1$. Thus for $C > 0.87$, the isotherm has a maximum and a minimum, and, as

in the the analogous case in adsorption discussed by Fowler and Guggenheim (50) conditions are satisfied for phase separation. This would be expected to lead to miscibility gaps in the isotherm.

Figure 3.1 shows the isotherm contours calculated from equation 3.10 for two values of K_a, and several values of C. It can be seen that negative values of C can lead to sigmoidal isotherms. In cases where $C > 0.87$, the two-phase regions of the isotherm correspond to the dotted horizontal lines. If $C = 0.87$, the isotherm has a saddle point at $A_z = 0.5$.

It is apparent from equation 3.10, that when $A_z = 0.5$, A_s is given by

$$\underset{(A_z=0.5)}{As} = \frac{0.5\Gamma}{0.5(K_a+\Gamma)}$$

i.e. $$K_a = \frac{\Gamma(1-A_s)}{A_s} \quad \text{for } A_z = 0.5, \text{ and for all C.}$$

Thus $\log K_a$ may be found from the "Kielland plot" of $\log K_c'$ versus A_z, since

$$\log K_a = \log K_c' \quad \text{when } A_z = 0.5.$$

The Kielland-Barrer-Falconer theory described above is applicable in many cases of uni-univalent exchanges in zeolites. There are some cases however, particularly involving uni-divalent exchanges, where $\log K_c'$ is neither constant, nor varies linearly with A_z. The general thermodynamic theory of ion exchange equilibria can then be used to evaluate the activity coefficients required.

General Thermodynamic Theory of Ion Exchange

A simplified thermodynamic approach to the evaluation of activity coefficients in the solid phase has been developed by Ekedahl, Högfeldt and Sillen (51,52), andby Argersinger, Davidson and Bonner (53). They considered the solid phase as a binary solution (A,B)z. The standard

Figure 3.1

Kielland Isotherms

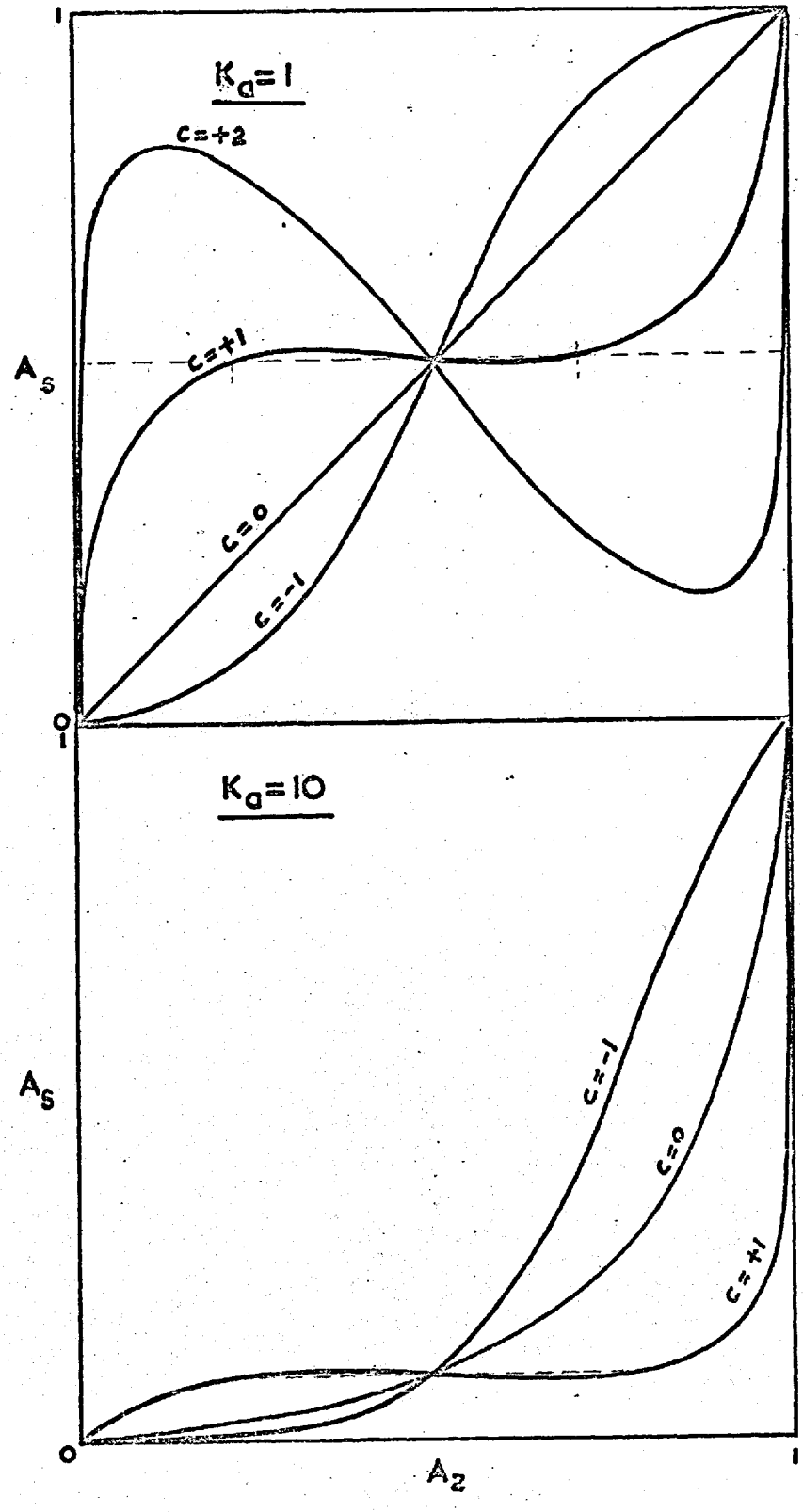

states of the components were taken as the pure components $A_{(z)}$ and $B_{(z)}$ in equilibrium with dilute solutions of AX and BX respectively. The water content of the exchanger phase was assumed constant.

The activity coefficients f_A and f_B were derived in terms of the mole fractions (x_A, x_B) of $A_{(z)}$ and $B_{(z)}$ in the mixed exchanger. The subsequent treatment led to the following expressions for f_A, f_B, and K_a:-

$$\log f_A = -\int_{K'_{c_1}}^{K'_c} x_B \, d \log K'_c \qquad K'_{c_1} = K_c \text{ when } x_B = 0$$

$$\log f_B = \int_{K'_{c_0}}^{K'_c} x_A \, d \log K'_c \qquad K'_{c_0} = K'_c \text{ when } x_A = 0$$

$$\log K_a = \int_0^1 \log K'_c \, d x_A .$$

The above results apply to uni-univalent exchanges, and in this case $x_A = A_z$, $x_B = B_z$.

For uni-divalent exchanges, the mole fractions x_A and x_B are not equal to the equivalent fractions A_z and B_z, and hence the expressions derived by the above authors for uni-divalent exchanges cannot be directly applied to the present work.

A similar treatment, using equivalent fractions as concentration units, and considering water as an additional component in the exchanger, was undertaken by Gaines and Thomas (54), Argersinger (55), and Högfeldt (56). The approach of Gaines and Thomas is most directly applicable here.

The standard states for the exchanger were taken to be the pure exchangers $A_{(z)}$ and $B_{(z)}$ in equilibrium with infinitely dilute solutions of the pure salts AX and BX (i.e., pure water). The standard state

for the water was defined such that its activity at equilibrium was the same in all three phases, exchanger, liquid and vapour. For the electrolytes in solution the standard state was the "hypothetical ideal 1 molal solution" in which the solute has a mean activity coefficient of unity at atmospheric pressure and at all temperatures.

The chemical potential of the exchanger components $A_{(z)}$ and $B_{(z)}$ are therefore given by

$$\mu_{A_{(z)}} = \mu^0_{A_{(z)}} + RT \ln f_A . A_z$$

$$\mu_{B_{(z)}} = \mu^0_{B_{(z)}} + RT \ln f_B . B_z$$

In the solution

$$\mu_{A_{(s)}} = \mu^0_{A_{(s)}} + RT \ln m_A \gamma_A$$

$$\mu_{B_{(s)}} = \mu^0_{B_{(s)}} + RT \ln m_B \gamma_B$$

At equilibrium, the chemical potential of the water is the same in all phases, and the change in free energy is zero.

The Gibbs-Duhem equation can be applied to the exchanger phase to give

$$n_A \, RT \, d \ln A_z . f_A + n_B \, RT \, d \ln B_z . f_B + n_w \, RT \, d \ln a_w = 0$$

where the subscript w refers to the water component. Cancelling the RT terms, and multiplying throughout by $\frac{z_A z_B}{z_A n_A + z_B n_B}$ yields

$$\frac{z_A n_A}{z_A n_A + z_B n_B} \cdot z_B \, d \ln A_z . f_A + \frac{z_B n_B}{z_A n_A + z_B n_B} \cdot z_A \, d \ln B_z . f_B + \frac{n_w z_A z_B}{z_A n_A + z_B n_B} \, d \ln a_w =$$

But $z_A n_A + z_B n_B = 1$; $\frac{z_A n_A}{z_A n_A + z_B n_B} = A_z$; $\frac{z_B n_B}{z_A n_A + z_B n_B} = B_z$;

$$\therefore \; z_B A_z \, d \ln A_z f_A + z_A B_z \, d \ln B_z f_B + n_w z_A z_B \, d \ln a_w = 0$$

Separation of the logarithmic terms and rearranging gives

$$z_B\, d\, A_z + z_A\, d\, B_z + A_z\, d \ln f_A^{z_B} + B_z\, d \ln f_B^{z_A} + n_w z_A z_B\, d \ln a_w = 0$$

Equation 3.11

As before

$$K_a = K_c' \cdot \frac{f_A^{z_B}}{f_B^{z_A}}$$

$$\therefore \ln K_a = \ln K_c' + \ln f_A^{z_B} - \ln f_B^{z_A}$$

$$\therefore \quad 0 = d \ln K_c' + d \ln f_A^{z_B} - d \ln f_B^{z_A} \qquad \text{Equation 3.12}$$

Combining equations 3.11 and 3.12 results in the relations

$$d \ln f_A^{z_B} = (z_B - z_A)\, d\, B_z - B_z\, d \ln K_c' - n_w\, z_A z_B\, d \ln a_w$$

$$d \ln f_B^{z_A} = -(z_B - z_A) d\, A_z + A_z\, d \ln K_c' - n_w\, z_A z_B\, d \ln a_w.$$

These expressions are then integrated. In the case of zeolite exchangers however, the water activity term can be neglected. Swelling in these exchangers is small or insignificant, and if dilute solutions are used for exchange, the error introduced by neglecting the water activity terms (of the order of 5 cals/gm equiv. in free energy) is negligible when compared to the experimental errors involved.

Integration then gives

$$\ln f_A^{z_B} = (z_B - z_A) B_z - \int_{K_{c_1}'}^{K_c'} B_z\, d \ln K_c \qquad (K_c' = K_{c_1}' \text{ when } B_z = 0)$$

Equation 3.13

$$\ln f_B^{z_A} = -(z_B - z_A) A_z + \int_{K_{c_0}'}^{K_c'} A_z\, d \ln K_c' \qquad (K_c' = K_{c_0}' \text{ when } A_z = 0)$$

Equation 3.14

$$\ln K_a = \ln K_c' + \ln f_A^{z_B} - \ln f_B^{z_A}$$

$$= (z_B - z_A) + \int_0^1 \ln K_c' \, d A_z \qquad \text{Equation 3.15}$$

Equations 3.13 and 3.14 may be transformed to give the more useful forms

$$\log f_A^{z_B} = 0.4343(z_B - z_A)B_z - B_z \log K_c' + \int_0^{B_z} \log K_c' \, d B_z \, .$$

$$\therefore \log f_A^{z_B} = 0.4343(z_B - z_A)B_z - \log K_c' + A_z \log K_c' + \int_{A_z}^1 \log K_c' \, d A_z$$

Equation 3.16

and

$$\log f_B^{z_A} = -0.4343(z_B - z_A)A_z + A_z \log K_c' - \int_0^{A_z} \log K_c' \, d A_z$$

Equation 3.17

$$\log K_a = 0.4343(z_B - z_A) + \int_0^1 \log K_c' \, d A_z \qquad \text{Equation 3.18}$$

Equations 3.16, 3.17, and 3.18 are then all expressed in terms of the experimentally determined quantities $\log K_c'$ and A_z, and the integrals may be evaluated easily from a plot of $\log K_c'$ versus A_z, as shown in Figure 3.2. If the relationship betweeen $\log K_c'$ and A_z is linear, of the form $\log K_c' = 2CA_z + g$, then equations 3.16 and 3.17 reduce, in the case of uni-univalent exchanges, to the Kielland equations

$$\log f_A = C.B_z^2$$

$$\log f_B = C.A_z^2 \, .$$

In the ideal case (i.e. C = 0) the equations become

$$\log f_A = \log f_B = 0 \quad (f_A = f_B = 1).$$

Figure 3.2

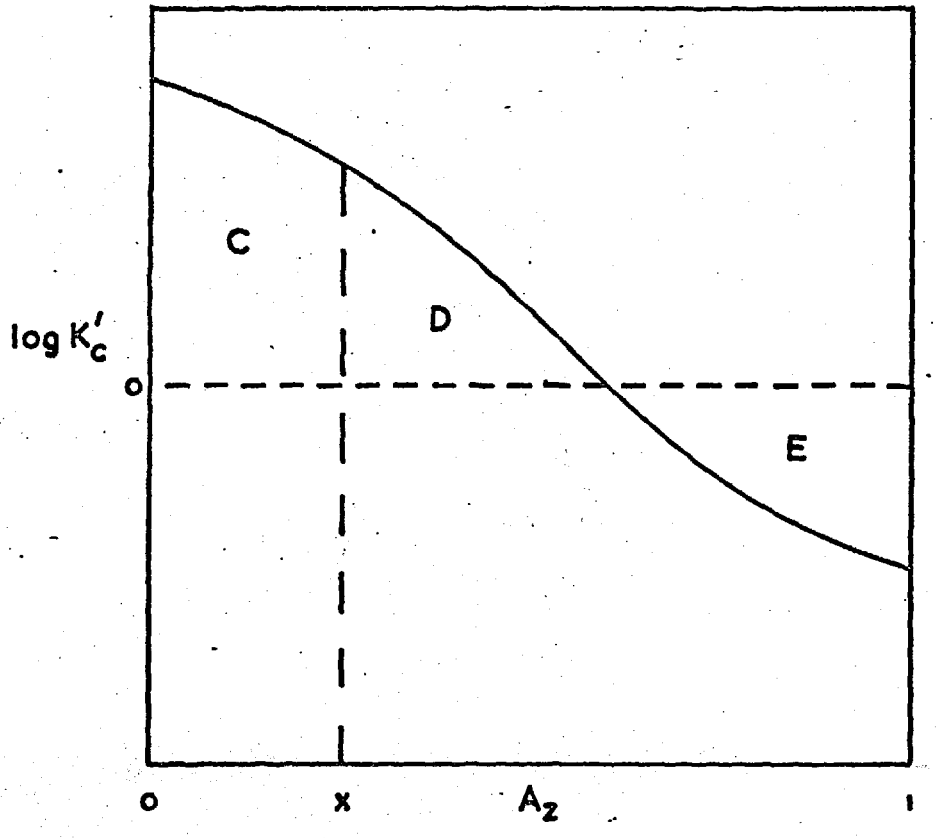

At $A_Z = x$:

$$\int_x^1 \log K_c' \, dA_Z = D - E$$

$$\int_0^x \log K_c' \, dA_Z = C$$

$$\int_0^1 \log K_c' \, dA_Z = C + D - E$$

In all cases, the standard free energy of exchange per equivalent of exchanger is given by

$$\Delta G^0 = - \frac{RT}{z_A \cdot z_B} \ln K_a .$$

4. Materials

Phillipsite

The phillipsite used in this work was a sample of the natural mineral from Pine Valley, Nevada, U.S.A. Zeolite deposits from this locality are alteration products of volcanic tuffs originally deposited in an alkaline lake environment (57). The sample as received consisted of small slabs of fine, loosely cemented crystals, in layers of about 1/4" thickness, varying in colour from pale yellow to dark brown.

X-ray powder diffraction photographs of the mineral showed that the major contaminant was erionite (revealed by weak to very weak reflections at d-values 11.7 and 6.6, corresponding to the two strongest lines of erionite, (100) and (110)). The erionite impurity tended to be greatest in the darker layers of the sample.

Light-coloured portions of the sample were selected, and ground to pass a 100 mesh sieve. The ground material was extracted with hot water for 1-2 hours in a Sohxlet apparatus. It was then dried at 80° C, and stored over saturated ammonium chloride solution to reach a constant water content.

X-ray photographs of the extracted material still showed faint erionite lines, estimated to correspond to about 3% to 5% of this impurity. Further purification was not attempted.

The composition of phillipsite appears to depend on its paragenesis. Before the discovery of extensive sedimentary deposits, most samples of phillipsite studied were of igneous origin, occurring as crystalline linings in vugs within basaltic rocks. The $SiO_2 : Al_2O_3$ ratio for these specimens was reported to be in the range 2.6-4.4 (38)(58)(59) corresponding to the formulae $(\frac{1}{2}M^{++}, M^{+})_2O.Al_2O_3.2.6SiO_2.nH_2O$ to $(\frac{1}{2}M^{++}, M^{+})_2O.Al_2O_3..4.4SiO_2.nH_2O$. The cationic composition also varies widely, samples of non-sedimentary origin being rich in Ca^{++}, together

with Na^+ and K^+, whereas samples of sedimentary origin have fewer divalent cations, and K^+ often dominates over Na^+ (57).

The silica:alumina ratio in sedimentary deposits is also much higher, (5.5-6.9) (57), although Ames has reported a ratio of 4 for a Nevada phillipsite (20). The $SiO_2:Al_2O_3$ ratio has a considerable effect on the ion-exchange properties of the zeolite. The higher this ratio, the fewer the cations needed to balance the excess framework charge, and therefore the greater the space available per cation.

The unit cell of phillipsite has been reported as monoclinic $P2_1/m$ or $P2_1$ (a = 10.02Å, b = 14.28Å, c = 8.64Å, $\beta = 125^0 40'$) by Strunz (60) and as orthorhombic B2mb by Steinfink (61) (a = 9.965, b = c = 14.25Å). Steinfink determined the structure of this phillipsite, a crystal from pelagic sediments in the Pacific Ocean. The composition of the specimen was

$$(K_xNa_{1-x})_5 Al_5 Si_{11} O_{32} \cdot 10H_2O.$$

The orthorhombic unit cell contained two formula weights.

The framework structure can be regarded as consisting of a fundamental unit of two tetrahedra linked head to head through an apical oxygen atom. Ten of these double units are then linked together by sharing corners into an "S" shaped configuration approximately 14Å long, 7Å wide, and 4.5Å high. In Figure 4.1, tetrahedra labelled 1 to 10 constitute this "S" configuration. Adjacent 'S' units (tetrahedra 1 to 10 and 1' to 10') are then linked at the circled points by sharing oxygen atoms between tetrahedra 1, 3'; 6, 4'; 7, 5'; 8, 10'; as shown. This linkage is formed between the upper strand of the first 'S' and the lower strand of the second, i.e., the first and second S units are staggered vertically by $\frac{1}{2}a$. The height of two of these staggered S units is therefore approximately 9Å, and the area in the b-c plane is approximately 14Å x 14Å. The resulting channel framework is apparent from Figure 4.1. The free diameter of the main octagonal channels is approximately 4Å.

Figure 4.1

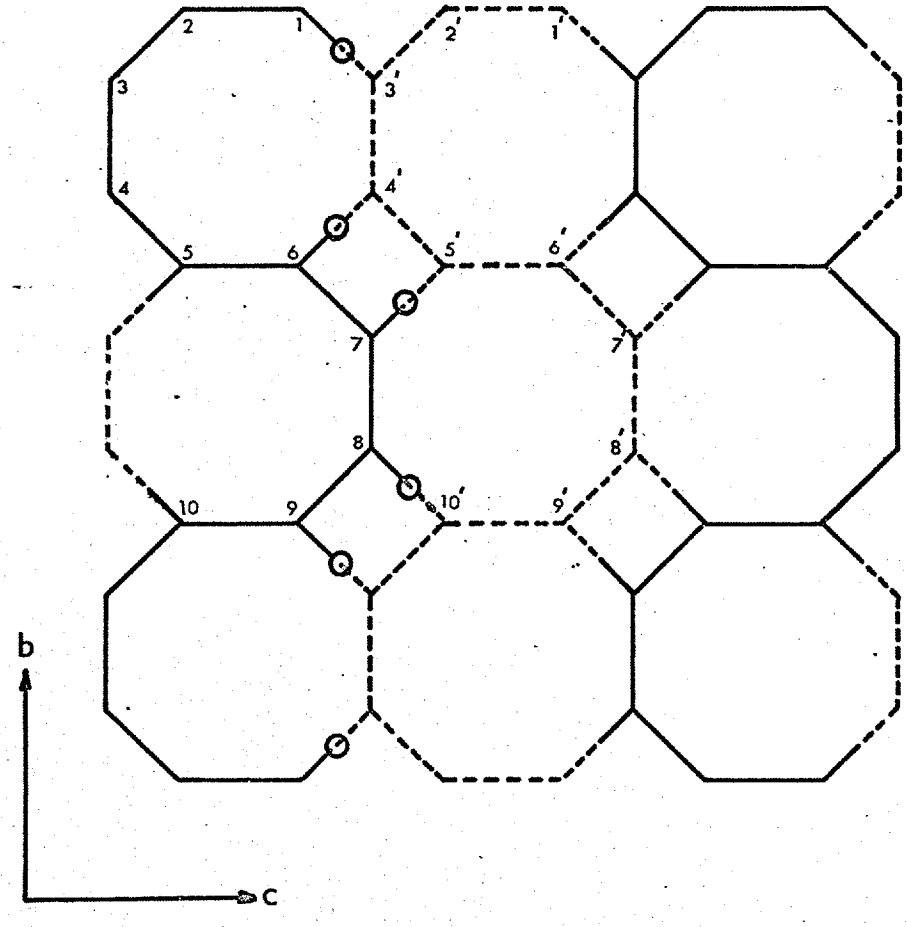

MAIN CHANNEL SYSTEM IN PHILLIPSITE

This description is necessarily idealised, since it assumes Si-O-Si bond angles of 180° in the basic double-tetrahedra units. Further details of individual bond distances and angles may be found in Steinfink's paper.

The barium zeolite harmotome has a very similar structure (62).

NaP (cubic)

The "P" group of zeolites was first prepared by Barrer et al (41) by hydrothermal crystallisation of gels. The gels were of the composition $Na_2O.Al_2O_3.nSiO_2.mH_2O$ (n = 1-12) with a 200-300% excess of sodium hydroxide, and were crystallised at temperatures ranging from 60°-250° C. The composition of the products varied from Na_2O, Al_2O_3, $3.3SiO_2$, $4.3H_2O$ to Na_2O, Al_2O_3, $5.3SiO_2$, $5.7H_2O$. Three distinct crystal habits were found - cubic, tetragonal, and (rarely) orthorhombic. The orthorhombic form in particular had an X-ray powder pattern very similar to that of phillipsite.

These "P" zeolites have since been synthesised and investigated by Barrer, Bultitude and Kerr (39), Regis et al (63), and, particularly the tetragonal species Na-P_T, by Taylor and Roy (42),(43). The Linde zeolite B prepared by Breck in 1956 has since been identified as a P zeolite (64).

The zeolite Na-P used in this work was synthesised from kaolinite and added silica, by a method developed by J.F. Cole in these laboratories. The composition of the reactant mixture was as follows:-

Kaolinite	0.1 moles
Silica (B.D.H. pure precipitated)	0.2 moles
Sodium hydroxide	0.6 moles
Water	250 ml

The silica was dissolved in a solution of the alkali, and the kaolinite then added. The mixture was transferred to a polypropylene bottle

and rotated end-over-end in an oven maintained at 80° C, for a period of three weeks.

The white crystalline product was filtered on a sintered glass filter, washed thoroughly with distilled water, then dried at 80° C.

The X-ray powder diffraction pattern of the product showed that only the cubic Na-P phase was present, together with muscovite mica (an impurity in the kaolinite used in the synthesis). The mica was separated by repeated sedimentation and decantation in distilled water. The purified product showed no trace of mica on the X-ray pattern.

The zeolite was equilibrated over saturated ammonium chloride solution in a desiccator for one week before analysis and use, and was stored in this desiccator (as were all the zeolites used in this work).

The X-ray powder pattern was indexed to give a body-centred cubic unit cell, with a = 10.0 Å. Observed and calculated d-spacings are given in Appendix 1.

A structure for the cubic Na-P zeolite, and its possible relationship to the other P zeolites, and harmotome and phillipsite, was suggested by Barrer, Bultitude and Kerr (39). The basic building unit for this structure consisted of eight $(SiO_4)^{4-}$ tetrahedra linked to form a cube. These cubic units were positioned at the corners and centre of the cubic unit cell and joined by bridging oxygen atoms. This framework contained 16 (Al+Si) and 32 oxygens per unit cell.

The oxygen-atom framework structure is shown in Figure 4.2. Atoms above the plane of the tetrahedra marked ABCD are not shown. The main channels have 8-ring openings, with a free diameter of about 3.3Å. These channels run parallel to all three crystal axes, and are all interlinked.

This structure has recently been verified in all essential detail by Borer (46). In the ideal structure, the Si-O-Si bonds linking the basic cubic building units along the three-fold axes of the unit cell

Figure 4.2

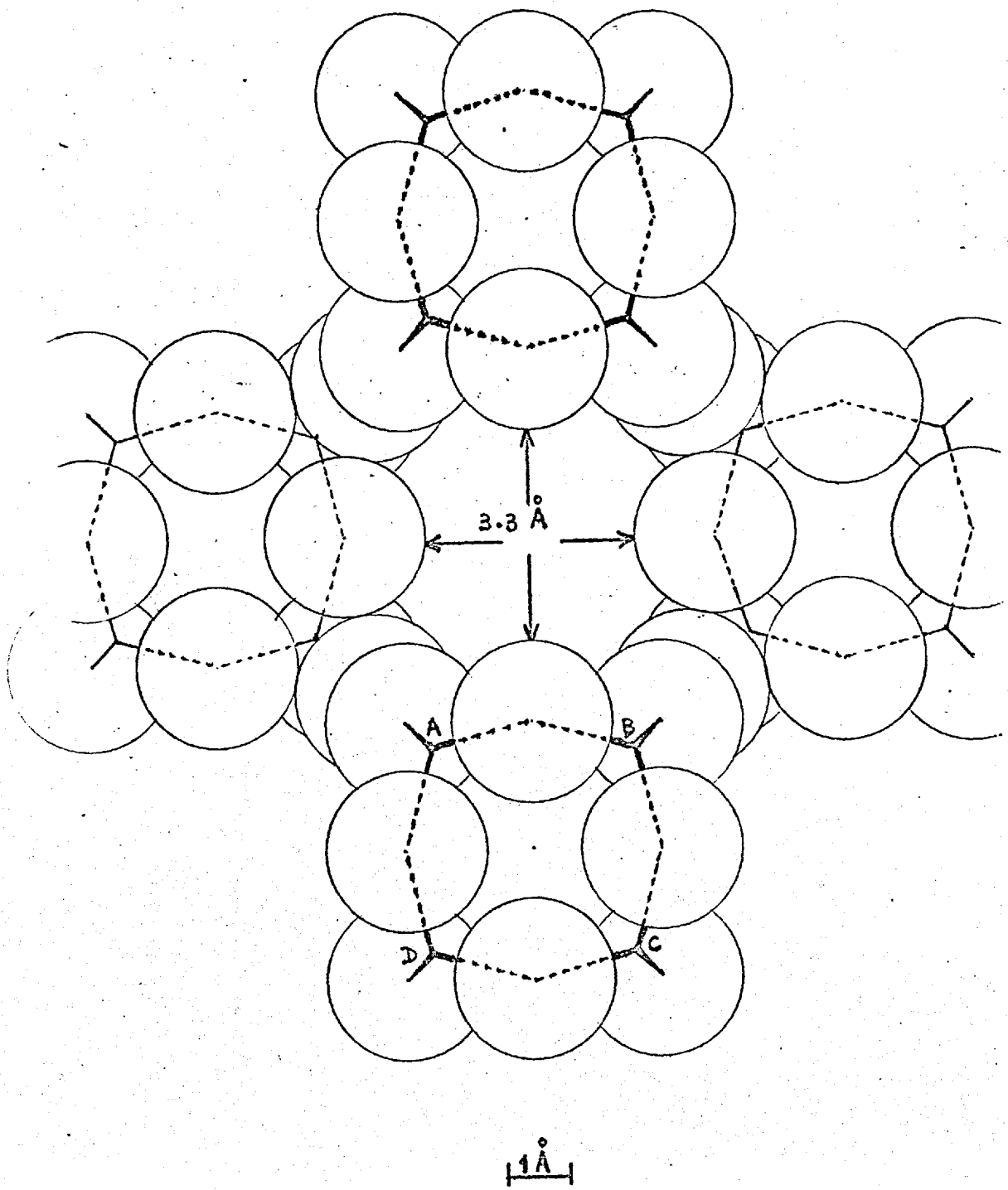

OXYGEN ATOM FRAMEWORK IN ZEOLITE P

have bond angles of 180^0. In the actual structure these angles are reduced to below 150^0 by staggering of oxygen atoms about the body diagonals of the cell. This in turn implies that the true symmetry of the unit cell is lowered. Least-squares refinement of the structure gave an R-value (based on structure factor) of 0.29. The six cations and twelve water molecules in Borer's sample ($Na_6 Al_6 Si_{10} O_{32} . 12H_2O$) were assigned by partial occupancy to the 48-fold (y, z, 0) positions, with y = 0.1, z = 0.42 (i.e., to either side of the centre of the main channels).

Barrer, Bultitude and Kerr (39) also suggested that the tetragonal form of Na-P (Na-P_T) had a slightly distorted cubic Na-P structure, giving the tetragonal unit cell a = 10.0Å, c = 9.8$_8$Å.

In an extensive investigation of the P zeolites, Taylor and Roy (43) found that the cubic and tetragonal forms of P were related by a reversible displacive transition. Ion-exchanged forms of Na-P_T displayed three types of symmetry, classified by Taylor and Roy (42) as

P^1 : Primitive cell, $a \geqslant c$; tetragonal Li, Na; cubic Mg,Co,Ni,Cu

P^2 : "Body centred" cell, $a > c$; tetragonal K,Rb,Cs,Ag

P^3 : Body centred cell, $c \geqslant a$; tetragonal Ca,Sr,Ba, cubic Cd

Solid solution gaps were found to exist at room temperature in the Na-K, Na-Ca, Na-Ba, and probably K-Ca, exchange systems.

Barrer et al. (39) have reported that the Ca and Ba forms of Na-P_T have powder patterns different to those derived from the cubic phase. The Na-P_T derivatives were similar to the Ca and Ba forms of harmotome.

Borer (46) has recently attempted to determine the structure of Na-P_T using X-ray powder diffraction methods. He found that the X-ray pattern of tetragonal Na-P could not be accounted for by a slight distortion of the basic structure found for cubic Na-P, and concluded that the two phases have different framework structures. This conclusion is contrary to the results of Taylor and Roy discussed above, since

it is highly improbable that the low temperature reversible transition between cubic and tetragonal Na-P, found by Taylor and Roy, could involve breaking of Si-O bonds.

The actual relationship between the cubic and tetragonal phases is therefore still uncertain. Evidence presented in this thesis (Chapter 7) tends to support Taylor and Roy's work.

Zeolite K-F

This synthetic potassium zeolite, $K_2O.Al_2O_3.2SiO_2.3H_2O$, was prepared by hydrothermal crystallisation of aluminosilicate gels by Barrer and Baynham (40) and by Ovsepyan and Zhdanov (65). More recently it has been made by low temperature hydrothermal treatment of kaolinite with potassium hydroxide, by Barrer, Cole, and Sticher (44). The rubidium and caesium forms of this zeolite (Rb-D and Cs-D) were also synthesised directly.

The latter method of synthesis was used in this work. The reaction mixture consisted of 26% K_2O, 3% kaolinite, and 70% water. The mixture was placed in a polypropylene bottle and rotated in an oven at 80° C for 12 days. The product was filtered and washed with distilled water to a pH of approximately 7. It was then ground to pass a 100 mesh sieve after drying at 80° C.

The zeolite was stored over a saturated solution of ammonium chloride in a desiccator.

The X-ray pattern of the product was similar to that reported for K-F by Barrer, Cole, and Sticher. A list of observed d-spacings and intensities is given in Appendix 1. The X-ray powder pattern of this zeolite has not been indexed, nor has the structure been determined.

Zeolite K-F(Cl)

Barrer et al, (44) have recently reported the synthesis of zeolite K-F containing occluded potassium chloride and potassium bromide

(K-F(Cl) and K-F(Br)). These phases were synthesised from kaolinite and potassium hydroxide, as for K-F above, in the presence of relatively strong (1-4M) solutions of the halides. The amount of KCl or KBr incorporated in the K-F crystals increased with increasing salt concentration, and also with increasing base concentration. For a base concentration of 4 molal, the maximum weight % potassium halide incorporated was about 6%, using salt concentrations of 4 molal. The compositions of these salt-rich specimens were

$$K_2O,\ Al_2O_3,\ 2SiO_2,\ 0.3KCl,\ 2.5H_2O$$

and

$$K_2O,\ Al_2O_3,\ 2SiO_2,\ 0.23KBr,\ 2.5H_2O.$$

The authors also found that in the presence of mixed halide solutions, potassium chloride was preferentially occluded.

Part of the work, on the synthesis of the potassium chloride-bearing zeolite, was repeated in the present study. Two potassium hydroxide concentrations were used, 4 molal, and 10 molal. The weight of kaolinite used was 5g. At each base concentration reaction mixtures of kaolinite, base, and salt were prepared, the salt concentrations ranging from 0.05 molal to saturated. All syntheses were performed in polypropylene bottles, rotated in an oven at 80° C for 12 days. At the end of this time the mixtures were filtered, washed with distilled water until no chloride could be detected in the washings, then dried at 80° C. The samples were then equilibrated over saturated ammonium chloride solution in a desiccator before analysis.

The results of this work are discussed in Section 7. Three of the samples prepared were reserved for a limited investigation of their ion-exchange properties.

5. Experimental Methods

Preparation of Monocationic Derivatives

Alkali metal and alkaline earth exchanged forms of all three zeolites were prepared by treatment of the zeolite with concentrated aqueous solutions of the appropriate metal chlorides. Several treatments, usually at 80° C, were used for each zeolite. Each treatment lasted from 25 to 48 hours. The products were filtered, and washed with cold distilled water until the washings showed no trace of chloride ions. The exchanged zeolites were dried at 80° C and stored over saturated ammonium chloride solution.

Analysis of Parent Zeolites

Phillipsite was analysed for SiO_2, Al_2O_3, Fe_2O_3, and CaO by the standard gravimetric methods of silicate analysis given by Groves (66) and Vogel (67). Each determination was done in triplicate.

An estimate of the iron content of the phillipsite was obtained by a visual colorimetric titration of the filtrate from the silica determination using potassium thiocyanate. Details are given by Vogel (67).

The SiO_2 and Al_2O_3 contents of K-F and Na-P were also measured by the standard methods, oxine being used in the gravimetric determination of the aluminium.

The alkali metal contents (except Cs) of all three zeolites were determined by flame photometry, using a Unicam SP90 dual absorption-emission instrument. The sample preparation was as follows:-

An accurately weighed amount of sample (approximately 0.2g) was treated in a platinum dish with 5 ml 10% H_2SO_4, and 40 ml concentrated hydrofluoric acid. The mixture was evaporated to dryness over a steam bath, and the procedure repeated. The solid residue from the second

evaporation was dissolved by adding 5 ml concentrated HCl and water, and heating for half an hour on the steam bath. The clear solution was cooled, transferred to a 250 ml volumetric flask, and made up to volume with distilled water. This solution was then diluted to a suitable concentration for the flame photometric analysis.

The alkaline earth metals, Ca, Sr, and Ba, were measured by atomic absorption photometry, using the same instrument. The sample preparation was similar to that described above, with perchloric acid (3 ml of 70%) substituted for the sulphuric acid.

Standards for these determinations were prepared from A.R. grade metal chlorides, or in the case of Rb and Li, chlorides of the highest available purity. Aluminium was added to all alkali metal standards (as the sulphate) in an amount equivalent to the appropriate alkali metal or alkaline earth content, as the sample solutions contained the framework aluminium of the zeolite.

Aluminium interference was suppressed in the case of solutions containing Ca, Sr, and Ba, by the addition of lanthanum chloride solution, giving a final lanthanum chloride concentration of 0.4% w/v. The efficiency of suppression was checked by using solutions of known Ca, Sr, or Ba content. Recovery in each case averaged over 99%.

Water contents were determined using a Stanton thermobalance, and were calculated as the % loss in weight after heating to 800° C.

Analysis of K-F(Cl)

The chloride contents of the various preparations of zeolite K-F containing occluded potassium chloride were determined as follows:

The sample (0.5-1.0g) was weighed accurately into a 150 ml conical flask. 5ml of 6M HNO_3 and 5 ml distilled water were added, and the zeolite decomposed by heating on a steam bath. (Decomposition was rapid, as K-F has a 2:1 $SiO_2:Al_2O_3$ ratio.) Silica remained in

colloidal suspension. An excess of standard 0.1N $AgNO_3$ was added by pipette (20 ml), and the silver chloride formed was coagulated by gentle boiling for one or two minutes. The mixture was then cooled, and titrated against approximately 0.05M KSCN (previously standardised against the silver nitrate solution) using ferric alum indicator (saturated ferric alum acidified with a few drops of concentrated nitric acid). Magnetic stirring was used throughout the titration, and the end point was quite distinct, but faded rapidly, because of the slow dissolution of the silver chloride precipitate in the absence of excess silver ion at the end-point. This fading can be eliminated by filtration of the zeolite solution plus silver chloride before titration. This was attempted, but filtration proved to be virtually impossible in the presence of the colloidal silica.

The accuracy of the method used (with filtration) was checked by analysing mixtures of zeolite K-F (without occluded KCl) and a known amount of potassium chloride. Recovery of the salt in duplicate determinations was 99% and 100%.

Exchange Isotherms

All exchange isotherms were measured at 25° C using a constant solution concentration of 0.100 equivalents per litre. The batch technique was used.

Accurately weighed quantities of a monocationic zeolite (usually approximately 0.5g) were weighed into polypropylene bottles of 60 ml capacity. A known volume (usually 40 ml) of a 0.100 N solution containing a known proportion of the competing ions was added by pipette. The bottles were then closed using the polypropylene tops, and placed into clips on an axle attached to a rigid framework. The axle was rotated through a chain drive by a small electric motor secured to the top of the framework. The framework was then placed in position over a glass trough filled with water. The temperature of the water was controlled to 25 $\pm$0.5° C by means of a silica-sheathed heating element and a

bimetallic strip temperature controller, through an electric relay.

The rotating bottles on the driven shaft provided vigorous stirring. The end-over-end rotation of the bottles themselves ensured that the zeolite and solution charges were thoroughly mixed.

A period of from three to seven days was allowed to ensure equilibrium in the case of uni-univalent exchanges. The equilibration time given for uni-divalent exchanges was two weeks. (Equilibrium was undoubtedly reached in much shorter times.)

After equilibration, the bottles were removed from the water bath, and the zeolite allowed to settle.

Aliquots of two (2) ml of the supernatant solution were then pipetted into 500 ml volumetric flasks, and made up to volume using distilled water. These solutions were then analysed directly by flame photometry or atomic absorption spectrophotometry for each of the cations. The exception to this procedure was the case of isotherms involving caesium. For (Na, Cs) isotherms, sodium only was measured, as the instrument wavelength range was insufficient for the measurement of caesium. For (K, Cs) isotherms, a gravimetric method was used. Aliquots (20 ml) of the supernatant solutions were pipetted into weighed 100 ml beakers, and evaporated to dryness in an air oven at 100^0 C. After cooling in a desiccator, the beaker was re-weighed, and the weight of residue (KCl + CsCl) calculated. The residue was then dissolved in 20 ml distilled water, and the total chloride content found by titration with standard 0.05 N $AgNO_3$ using chromate-dichromate indicator.

From the weight of the mixed chlorides, and the total chloride content, the proportions of potassium and caesium were readily calculated. (The chloride concentration was theoretically constant and equal to 0.100 N. The titration results indicated total chloride contents of 0.098 to 0.102 N. Such deviations may easily arise through experimental error, or evaporation of the supernatant solution.)

The standard solutions for the flame photometric analysis were prepared from the same mixed cation solutions that were added to the zeolite samples. The normal range of mixed cation solutions employed varied from pure 0.100 N solution of one cation, to pure 0.100 N solution of the other, with intermediate proportions 0.1 to 0.9 in steps of 0.1. The standard 0.1 N solutions were prepared from the A.R. grade metal chlorides (or nitrates for some exchanges in K-F(Cl)). The normality was checked by a total chloride titration.

The reproducibility of the whole procedure was found to depend almost entirely on the reproducibility of the flame photometric measurement. Errors in weighing and dilution were negligible. The reproducibility of the flame photometer varied approximately linearly over the 100% transmission scale, fluctuations of ± 0.5 division being common at about 100% transmission (i.e., at solution cation fractions of about 1.0). Assuming an approximately linear calibration curve (% transmission versus cation fraction in solution) this resulted in a fairly constant relative error in cation fraction of about 1%. Thus the errors in the solution cation fractions were greater at both ends of the isotherm (since a high cation fraction of one ion implies a low cation fraction of the other).

In practice, using the normalisation procedure described in Section 6, A_s values of duplicate determinations were found to agree within 0.005 (cation fraction), even when the measured total cation concentration in solution varied from 0.097 N to 0.103 N. Normalised duplicate A_z values (calculated from solution concentrations) were found to differ by no more than 0.01 in cation fraction.

Errors of this magnitude, although reasonably small in absolute terms, can represent large relative errors at the ends of the isotherm. These errors further lead to large deviations in $\log K_c'$, which accounts for the considerable scatter observed in plots of $\log K_c'$ versus A_z at low and high A_z values.

The extent of agreement between isotherm contours measured in the forward and reverse directions is determined largely by the accuracy of the exchange capacities of the starting materials (the two end-members for the relevant exchange). The exchange capacity, expressed in milliequivalents per gram of zeolite, varies from one cationic form of a zeolite to another, because of differing water contents and the equivalent weights of the ions. (The exchange capacity expressed as milliequivalents per gram of water- and cation-free zeolite is, of course, constant).

In this work exchange capacities were measured by direct cation analysis of the hydrated cation-exchanged forms. For caesium-based zeolites the exchange capacity was calculated from the known exchange capacity and water content of the sodium form, and the measured water content of the caesium form, using the relationship

$$q_B = \frac{q_A(100-w_B)}{(100-w_A)+0.1q_A(e_B-e_A)}$$

where q_A, q_B are the exchange capacities of the A and B forms, w_A and w_B are the water contents (weight %) and e_A and e_B are the equivalent weights of ions A and B.

X-ray Powder Diffraction Methods

If a^*, b^*, c^*, α^*, β^*, γ^* define the reciprocal dimensions of a general cell in reciprocal space, then

$$Q_{hkl} = h^2 a^{*2} + k^2 b^{*2} + l^2 c^{*2} + 2hka^*b^* \cos \gamma^* + 2klb^*c^* \cos \alpha^* + 2hlc^*a^* \cos \beta^* \qquad \text{Equation 5.1}$$

where h, k, and l are the Miller indices of the crystal planes. If d_{hkl} is the interplanar spacing of a plane hkl, and θ_{hkl} is the Bragg diffraction angle, ~~and then~~

$$Q_{hkl} = \frac{1}{d^2_{hkl}} = \frac{4 \sin^2 \theta_{hkl}}{\lambda^2}$$

where λ is the X-ray wavelength.

Indexing a given X-ray powder diffraction pattern consists in finding reciprocal cell constants and hkl's such that equation 5.1 is satisfied for all observed Q_{hkl}'s.

For cubic, tetragonal and orthorhombic crystals, equation 5.1 reduces to

$$\text{cubic} : Q_{hkl} = (h^2 + k^2 + l^2) a^{*2}$$

$$\text{tetragonal} : Q_{hkl} = (h^2 + k^2) a^{*2} + l^2 c^{*2}$$

$$\text{orthorhombic:} \quad Q_{hkl} = h^2 a^{*2} + k^2 b^{*2} + l^2 c^{*2} \quad .$$

Details of the various graphical and analytical methods which can be used to index general diffraction patterns may be found in standard texts (68). The successful application of any of these methods depends on the collection of accurate data (Q, d, or θ values).

All X-ray powder diffraction photographs in this work were taken using a Guinier de Wolff camera, and copper K_{α} radiation. The above camera enables four separate patterns to be recorded simultaneously on a single piece of film.

For quantitative work, lead nitrate was used as a standard in one of the four sample positions.

The distance of each diffraction arc from the zero mark on the film was measured using a Hilger vernier film measuring device. Several measurements were made for each line, and an estimation of the standard deviation obtained. For the camera used, these distances (in mm) correspond to Bragg angles of 4θ.

The 4θ measurements obtained were corrected for film shrinkage

using the observed and calculated values found for the lead nitrate standard. In the early work this correction was made manually by graphical methods. Later a computer program LCLSQ (69) performed the correction using a polynomial least-squares fitting procedure. This program also tabulated corrected Q, d, and 4θ values, and, if the pattern had been indexed, found the unit cell parameters a, b, c, α, β, and γ.

Finally, another computer program APOL (70), written by J.F. Cole and H. Villiger in these laboratories, was used to calculate all the possible reflections for the unit cell found, for comparison with the observed reflections.

6. Calculation of Results

The isotherm co-ordinates A_z and A_s were calculated from the measured equilibrium solution concentrations as follows:

Let w = weight of zeolite taken (g)
q = exchange capacity (meq/g)
V = volume of solution added (ml)
a_1 = initial concentration of ion A in solution (meq/ml)
a_2 = final " " A " "
b_1 = initial " " B " "
b_2 = final " " B " "

Consider the exchange A ⟶ B. For this exchange q is the exchange capacity of the zeolite in the A form.

All exchanges were conducted using solutions of constant total normality TN (0.1 meq/ml).

$$\therefore \quad a_1 + b_1 = 0.1$$

However, because of experimental error and other factors, the measured final total concentration $a_2 + b_2$ was often not exactly 0.1, but varied in the range 0.097 to 0.103. The equilibrium solution concentrations were therefore corrected to a total concentration of 0.100 meq/ml:-

$$\text{Corrected } a_2 = a_2' = \frac{a_2}{a_2 + b_2} \times 0.100$$

$$\text{Corrected } b_2 = b_2' = \frac{b_2}{a_2 + b_2} \times 0.100$$

Then $A_s = 10 \times a_2'$

$B_s = 10 \times b_2'$

(This "normalising" procedure was found to improve the agreement

between duplicate measurements, and to reduce the scatter on the resultant isotherm.)

Initial meq of ion A in solution = Va_1

Final " " " " = Va_2

∴ meq A displaced from zeolite (Δa), which equals the meq B entering the zeolite, is given by

$$\Delta a = V(a_2 - a_1).$$

Total available meq in zeolite = wq

$$\therefore \quad B_z = \frac{V(a_2 - a_1)}{wq}$$

$$A_z = 1 - B_z$$

The exchange isotherm A_s versus A_z was then plotted.

As discussed in Section 3, the calculation of the thermodynamic equilibrium constant for the exchange reaction involves the evaluation of solution and solid phase activity coefficients:

$$K_a = \frac{A_z^{z_B} \cdot m_B^{z_A} \cdot \gamma_B^{z_A} \cdot f_A^{z_B}}{B_z^{z_A} \cdot m_A^{z_B} \cdot \gamma_A^{z_B} \cdot f_B^{z_A}}$$

$$= K_c' \cdot \frac{f_A^{z_B}}{f_B^{z_A}}$$

The molalities m_A and m_B were taken as being equal to molarities, as dilute solutions were used. They were calculated from the relations

$$m_A = \frac{TN \cdot A_s}{z_A}; \quad m_B = \frac{TN \cdot B_s}{z_B}$$

where TN is the total solution concentration (meq/ml). Solution

activity coefficients were calculated by means of Glueckauf's equation (see Section 3). For uni-univalent exchanges with a univalent anion the required ratio of solution activity coefficients Γ was calculated from

$$\Gamma = \frac{\gamma_{\pm BX}}{\gamma_{\pm AX}}$$

where $\gamma_{\pm BX}$ and $\gamma_{\pm AX}$ are the mean ionic activity coefficients of the salts BX and AX at the ionic strength of the mixed solution (which is constant and equal to the normality (0.1) in this case). The values of $\gamma_{\pm}$ used were obtained from Conway (71) and are given in Table 6.1.

For uni-divalent exchanges the $\gamma_{\pm}$ terms required are a function of the ionic strength I, which varied from 0.10 (pure BX) to 0.15 (pure AX_2) for the constant total normality 0.1 meq/ml. From published values of $\gamma_{\pm}$ at various ionic strengths (Conway (71), Harned and Owen (72), Robinson and Stokes (73)) a linear interpolation was made over the small range of ionic strength encountered.

The linear function was expressed in the form of an equation

$$\gamma_{\pm MX}(I) = \gamma_{\pm MX}(I_{TN}) + g_{MX}(I - I_{TN})$$

where $\gamma_{\pm}(I_{TN})$ is the mean ionic activity coefficient of the electrolyte at the ionic strength corresponding to the concentration TN.

Values of g calculated are also given in Table 6.1

Table 6.1

Values of $\gamma_{\pm}(I_{TN})$ and the factor "g_{MX}"

Salt MX	$\gamma_{\pm}(I_{TN})$	g_{MX}	I_{TN}
$LiNO_3$	0.788	---	0.100
LiCl	0.790	-0.29	0.100
$NaNO_3$	0.762	---	0.100

Continued .....

NaCl	0.778	-0.43	0.100
KNO_3	0.739	---	0.100
KCl	0.770	-0.52	0.100
RbCl	0.764	-0.55	0.100
CsCl	0.756	-0.63	0.100
$CaCl_2$	0.518	-0.80	0.150
$SrCl_2$	0.515	-1.02	0.150
$BaCl_2$	0.508	-1.37	0.150

The evaluation of Γ by means of Glueckauf's equations was then performed. All these calculations, and the subsequent calculations of $\log K'_c$, f_A, f_B and K_a were made on the Imperial College IBM 7090/4 computer, using a Fortran IV program "CALCIS" written for this purpose.

After the evaluation of Γ, $\log K'_c$ was calculated:

$$\log K'_c = \log \frac{A_z^{z_B} \cdot m_B^{z_A}}{B_z^{z_A} \cdot m_A^{z_B}} \cdot \Gamma$$

The "Kielland plot" data, $\log K'_c$ versus A_z, were then analysed by a least-squares method to find three polynomial equations of fit, linear, quadratic, and cubic. Polynomial equations were selected (rather than any other form, e.g., exponential) because the simpler theoretical relationships were of a polynomial form - the "ideal" case being a polynomial of zero order in A_z, the Kielland case of first degree. A theoretical justification for the use of a polynomial has also been given by Freeman (74).

The least-squares procedure found the "best" polynomial equation of fit, for each of the three orders. Each of these three equations was then integrated to calculate the terms needed for the evaluation of f_A, f_B, and K_a, namely

$$\log f_A^{z_B} = 0.4343(z_B - z_A)B_z - \log K_c' + A_z \log K_c' + \int_{A_z}^{1} \log K_c' \, d A_z$$

$$\log f_B^{z_A} = -0.4343(z_B - z_A)A_z + A_z \log K_c' - \int_{0}^{A_z} \log K_c' \, d A_z$$

$$\log K_a = 0.4343(z_B - z_A) + \int_{0}^{1} \log K_c' \, d A_z$$

The derivation of these equations has been discussed in Section 3.

A guide to the error of fit in each case was provided by an "R factor" defined by

$$R = \sqrt{\left[\frac{\sum\left[\log K_c'(\text{observed}) - \log K_c'(\text{calculated})\right]^2}{N - M - 1}\right]}$$

where N is the number of pairs of $\log K_c$, A_z values and M is the order of the polynomial.

The expression for $\log K_c$ is extremely sensitive to small changes in A_z or A_s, particularly near the isotherm axes. This leads to considerable scatter in plots of $\log K_c'$ versus A_z at each end of the curve. Moreover, a symmetrical positive or negative error in either A_z or A_s produces a non-symmetrical error in $\log K_c'$. Thus the error of fit found for the $\log K_c'$ vs A_z polynomial is not necessarily a good indication of the actual error in terms of the isotherm itself. For this reason, it was desirable to calculate A_s versus A_z from the polynomial Kielland equations. This calculation is straightforward for uni-univalent exchanges, since

$$K_c' = \frac{A_z \cdot m_B \cdot \gamma_{\pm BX}}{B_z \cdot m_A \cdot \gamma_{\pm AX}}$$

$$= \frac{A_z(1-A_s) \cdot \gamma_{\pm BX}}{(1-A_z)A_s \cdot \gamma_{\pm AX}}$$

$$\therefore A_s = \frac{A_z \gamma_s}{K'_c(1-A_z) + A_z\gamma_s}$$

where $$\gamma_s = \gamma_{\pm BX}/\gamma_{\pm AX}$$

In the case of uni-divalent exchanges however, the $\gamma_{\pm}$ terms calculated from Glueckauf's equation are themselves complex functions of A_s, and A_s cannot therefore be directly calculated for a given A_z and log K'_c. This problem was overcome by defining a quantity S as

$$S = \frac{m_B^{z_A} \cdot \gamma_B^{z_A}}{m_A^{z_B} \cdot \gamma_A^{z_B}}$$

$$= K'_c \cdot \frac{B_z^{z_A}}{A_z^{z_B}}$$

$$= \frac{K'_c\,(1-A_z)^{z_A}}{A_z^{z_B}}$$

Thus S could be calculated for any given A_z and log K'_c.

By using a separate computer program "SVAS", values of S were calculated for $0.001 \leqslant A_s \leqslant 0.999$ in steps of 0.001. These tables of S values were prepared for each uni-divalent ion pair encountered (Na-Ca, Na-Sr, Na-Ba where A_s refers to the divalent ion).

There are certain dangers in using a least-squares polynomial fitting program in this work. These arise because the experimental values of A_z do not usually cover the entire range $0 < A_z < 1$. The polynomial fit only applies in the experimental range of A_z, and is not constrained outside this range (except in the case of a linear (Kielland) polynomial). Thus a polynomial which gave a perfect fit

in the experimental range of A_z, say $a_1 < A_z < a_2$, could have maxima or minima in $0 < A_z < a_1$ and $a_2 < A_z < 1$ which would not be consistent with the actual log K_c' versus A_z function. It is important to consider the behaviour of the polynomial function over the whole range $0 < A_z < 1$ before proceeding to integrate the equation to obtain f_A, f_B and K_a.

This danger can be minimised if, instead of using experimental A_z and log K_c' values, a smooth curve is drawn through the experimental isotherm points, and several values are read off this curve over the whole range of A_z. One disadvantage of this method is that it prejudices the objectivity of the mathematical procedure. In the case of an isotherm which shows a strong selectivity for one of the ions, the method may nevertheless be the only way to obtain consistent values of log K_c' and A_z over the whole range of the isotherm.

A complete listing of the "CALCIS" and "SVAS" programs is given in Appendix 2.

7. Results and Discussion

7.1. Phillipsite

Analysis

The results of analysis of the extracted phillipsite were as follows:

	%	moles
SiO_2	54.18	0.902
Al_2O_3	16.29	0.160
Fe_2O_3	1.26	0.008
Na_2O	7.04	0.114
K_2O	2.87	0.030
CaO	0.26	0.005
H_2O	16.46	0.914
	98.36	

The total % of constituents determined is significantly less than 100%. The difference is assumed to be due to other constituents (TiO_2, MnO etc.) not determined. It is also apparent that the total cation content accounts for only 93% of the alumina content, whereas for a pure zeolite the mole ratio $Al_2O_3 : M_2O$ should be 1.0. In this case the low ratio is probably caused by slight hydrolysis of the sample during the extraction procedure.

The $SiO_2 : Al_2O_3$ ratio of 5.6, and the predominance of alkali metal cations over alkaline earth cations, is typical of phillipsites of sedimentary origin, particularly for samples from the California/Nevada region of the U.S.A.(57).

The analysis corresponds to an approximate oxide formula of $(Na,K,\frac{1}{2}Ca)_2O,Al_2O_3,5.6SiO_2,5.7H_2O$. The phillipsite structure determined by Steinfink (61) and described in Section 4 contained 32(Al+Si) atoms

per orthorhombic unit cell. On this basis, the unit cell contents, for the phillipsite used in this work, are approximately described by the formula

$$(Na,K,\tfrac{1}{2}Ca)_8.Al_8Si_{24}O_{64}.24H_2O.$$

The cation density of eight monovalent cations per unit cell is two less than that for Steinfink's sample, for which the unit cell formula was $(Na,K)_{10}Al_{10}Si_{22}O_{64}.20H_2O$. Cation analyses for the mono-cationic exchange forms of the phillipsite gave the following exchange capacities (expressed in meq/g of hydrated zeolite):-

Li :	3.22	Cs :	2.23 (calculated)
Na :	2.76	Ca :	2.51
K :	2.78	Sr :	2.46
Rb :	2.70	Ba :	2.47

The relationship between the water content of these exchange forms, and the cation radius, is shown in Figure 7.1. As expected, there was a smooth decrease in water content with increasing cation size, and the water contents of the alkaline earth exchange forms were higher than those for monovalent cations of similar size.

Ion Exchange Equilibria

The results of the ion-exchange equilibria studies in phillipsite are given in graphical form in Figures 7.2 to 7.9. For reversible isotherms three graphs are shown:

(a) Exchange isotherm (A_s versus A_z)
(b) "Kielland plot" (log K_c' versus A_z)
(c) Variation of solid phase activity coefficients with cation loading (f versus A_z).

If the isotherm was found to be irreversible, the exchange isotherm only is shown. Unless stated otherwise, the solid line curves shown on each of the figures were obtained from the least-squares refinement

Figure 7.1

Water contents of Phillipsite derivatives

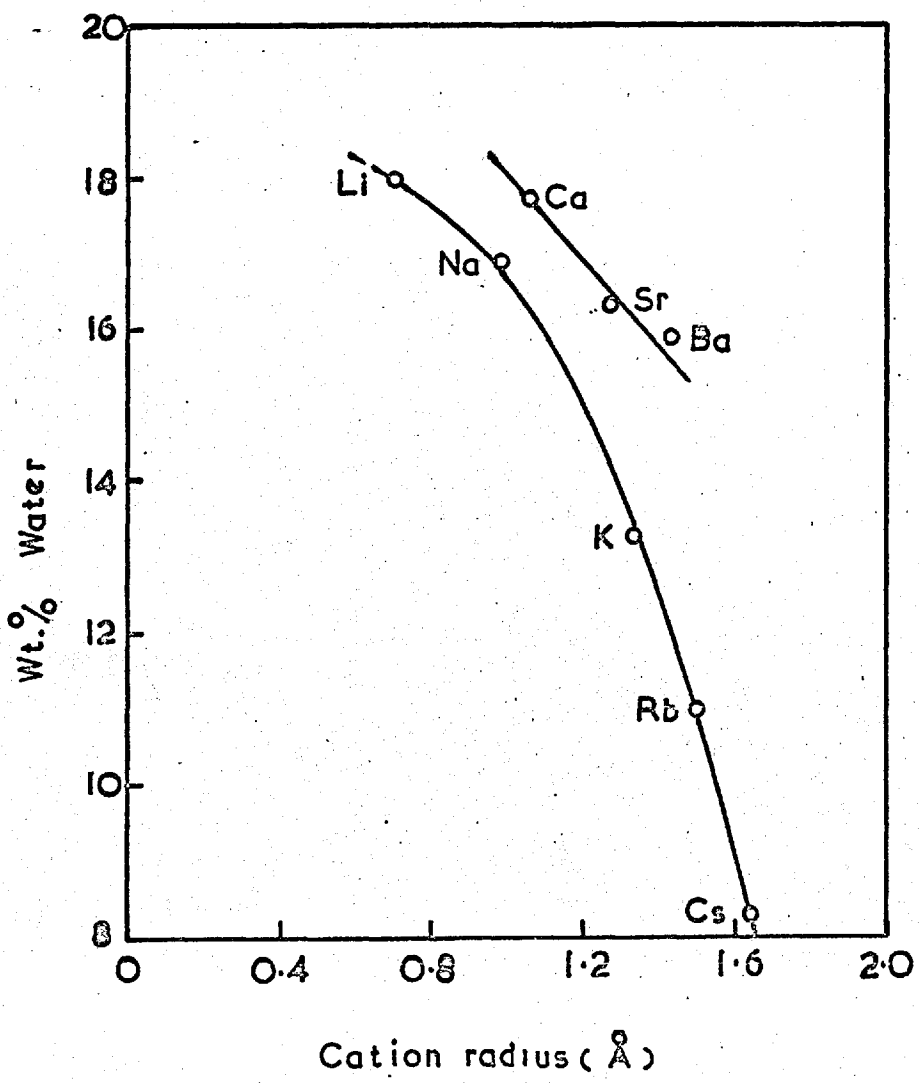

of the experimental data. For example, on an exchange isotherm, the continuous isotherm contour shown is the isotherm calculated from the best least-squares polynomial fit between log K_c' and A_z.

Na-Li Exchange

The exchange isotherm, Figure 7.2(a) was reversible, and showed a high selectivity for sodium. The corrected selectivity coefficient varied considerably with cation loading, and was best represented by the cubic equation

$$\log K_c' = -1.325 + 0.741\ Li_z - 7.830\ Li_z^2 + 5.292\ Li_z^3 .$$

The reliability of fit factor, R, defined in Section 6 was 0.109. (The lower the value of R, the better the fit.)

Integration of the above equation gave the thermodynamic equilibrium constant K_a for the reaction Na⟶Li, as

$$K_a = 0.006.$$

The standard free energy of exchange, ΔG^0, was evaluated using the relationship $\Delta G^0 = -RT \ln K_a$, giving

$$\Delta G^0 = +3{,}000 \text{ cal/g equivalent.}$$

Solid phase activity coefficients were computed from the log K_c' versus Li_z equation above, using the methods described in Section 6. The variation of the solid phase activity coefficients f_{Na} and f_{Li} is shown in Figure 7.2(c). Because the calculation of these coefficients involves the integration of the log K_c' versus Li_z equation, the equation describing the variation of f_{Na} (or f_{Li}) with Li_z is a complex one. If log K_c' is a polynomial function of order n in Li_z, then log f_{Na} (or log f_{Li}) is a polynomial function of order n+1 in Li_z.

On the basis of the K_a value, phillipsite showed a greater selectivity for sodium ~~and~~ over lithium than chabazite, for which Davies (76)

Figure 7·2: Na–Li Exchange in Phillipsite

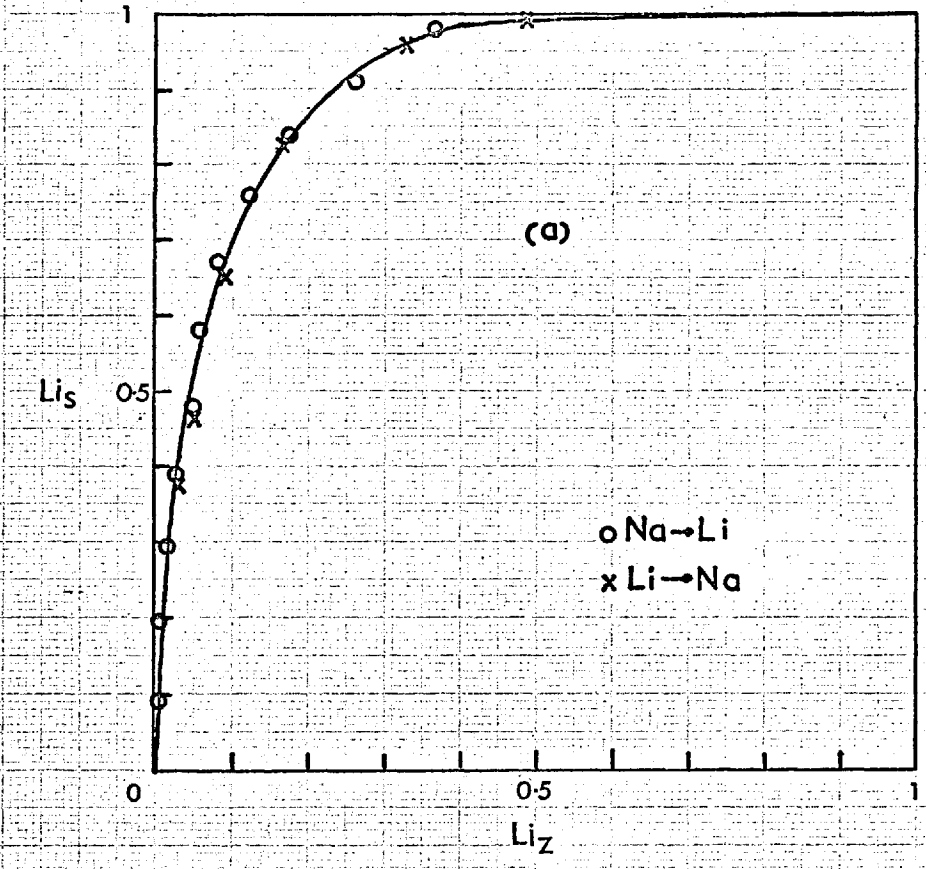

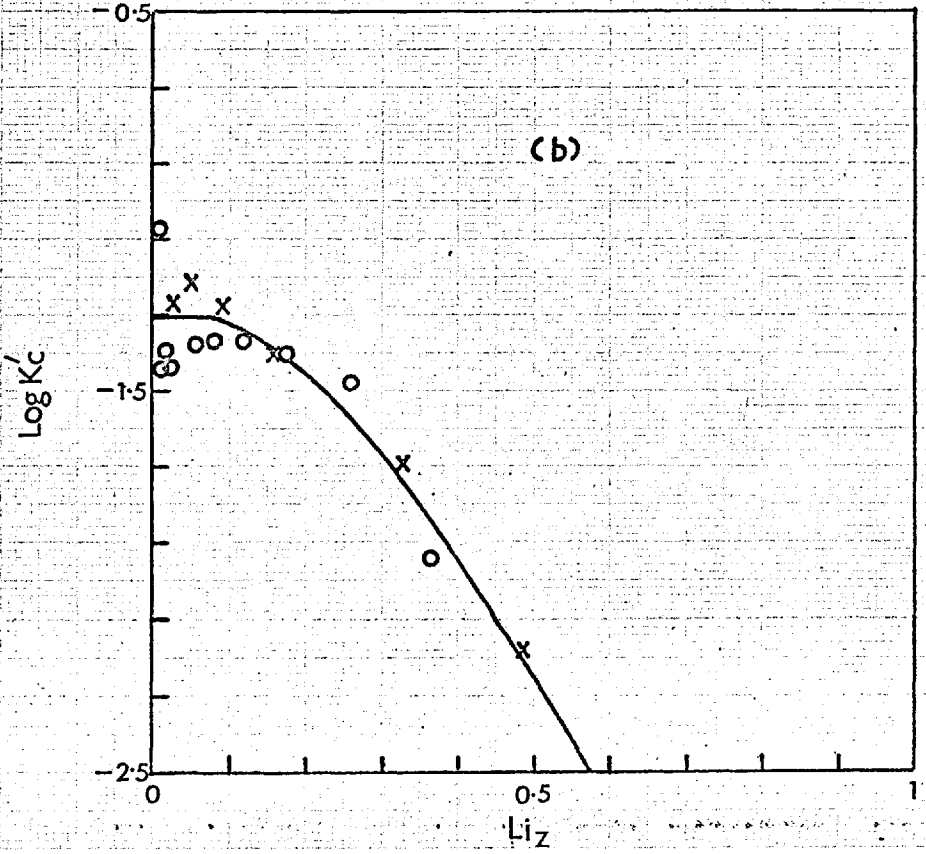

Figure 7·2c

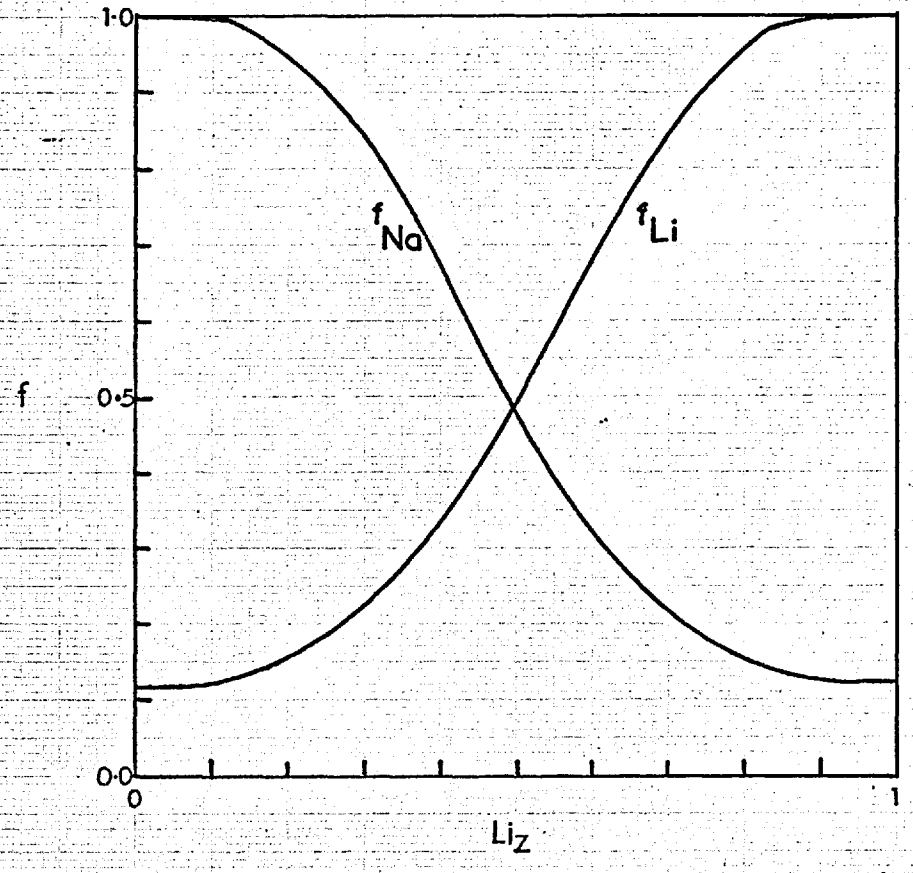

found $K_a = 0.055$. Of several Na-Li exchanges reported for zeolites, phillipsite is the most selective for sodium, the order being (76):-

Phillipsite > Chabazite > NaY > NaX > NaA > basic sodalite > basic cancrinite

Na-K Exchange

The Na-K exchange was complete and reversible. The isotherm, Figure 7.3(a), showed that potassium was the preferred ion. The corrected selectivity coefficient varied linearly with potassium loading, thus satisfying the conditions of Kielland's theory. The linear equation of fit was

$$\log K_c' = 1.804 - 1.385\, K_z \qquad (R = 0.090).$$

The Kielland constant C was evaluated as 0.5 x gradient of the line, and K_a was calculated by integration of the above equation between the limits $K_z = 0$ and $K_z = 1$. Thus

$$C = -0.69$$
$$K_a = 12.9$$

The standard free energy of exchange was calculated from K_a in the usual way, giving

$$\Delta G^0 = -1{,}500 \text{ cal/g equivalent.}$$

The solid phase activity coefficients in this case could be calculated using Kielland's equations

$$\log f_{Na} = C.K_z^2$$
$$\log f_K = C.Na_z^2 .$$

The results are shown in Figure 7.3(c).

These results may be compared to those reported by Ames (20) for a Nevada phillipsite. The phillipsite studied by Ames had a silica/alumina ratio of 4, and an exchange capacity of 2.3 meq/g. The Na-K isotherm was similar in shape to Figure 7.3(a), but gave a lower K_a value of 5.26, and ΔG^0 of -1000 cal/g equiv. The total solution

Figure 7.3 : Na–K Exchange in Phillipsite

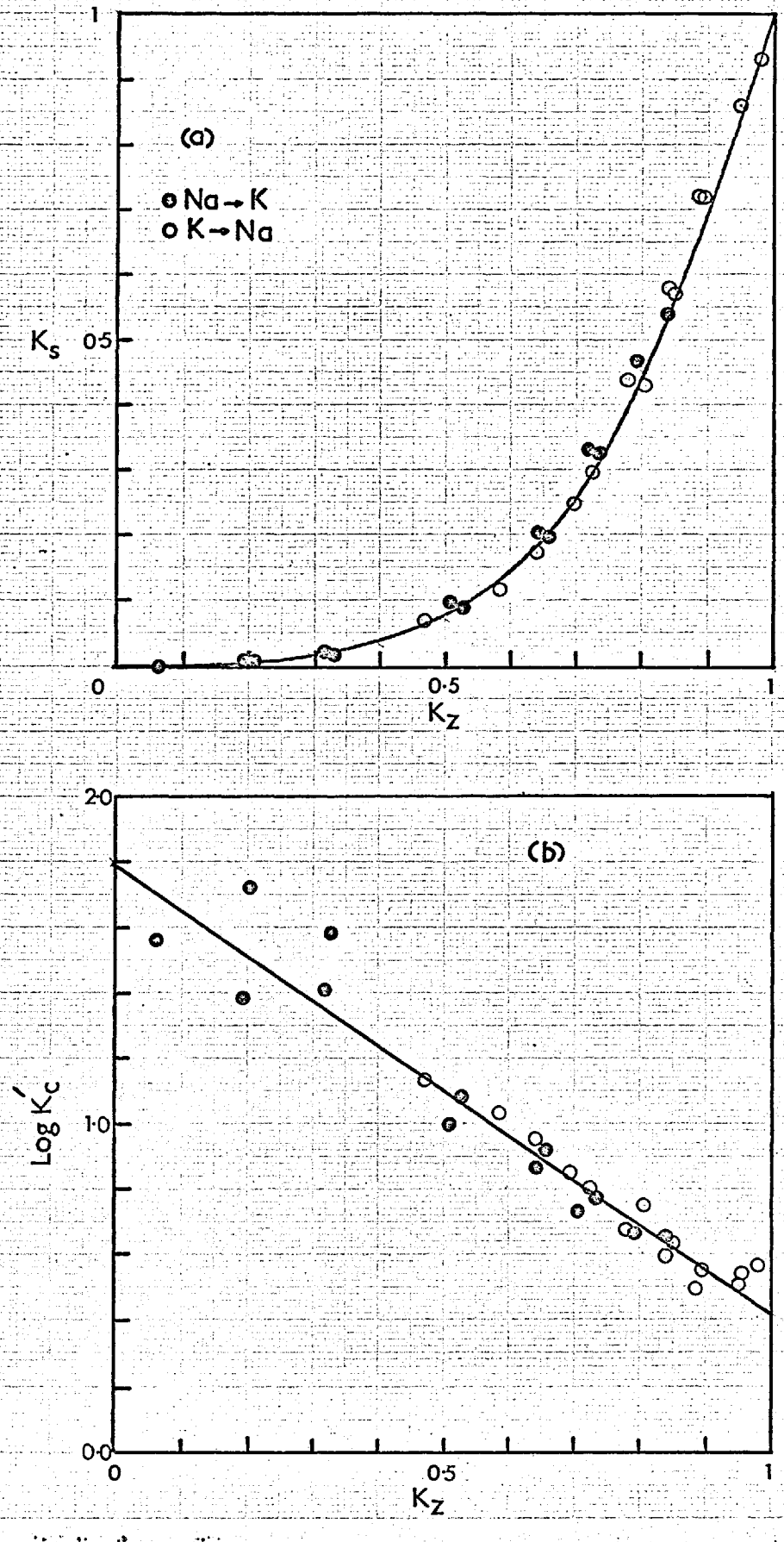

Figure 7·3c

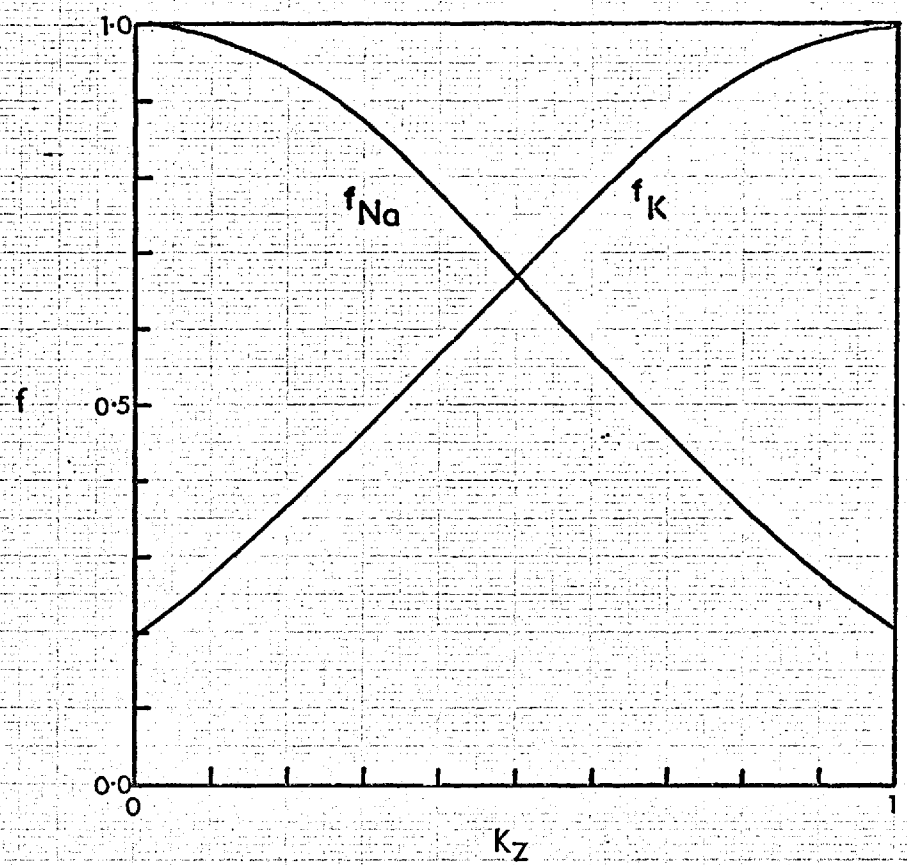

concentration was 1.0 N, compared to 0.1 N in this work. However, for uni-univalent exchanges, K_a should be independent of the solution concentration. The poor agreement between the two sets of results must presumably be due to differences in sample composition, exchange capacity and technique (Ames used a radiometric column flow method).

A further comparison may be made with results obtained for the Na-K exchange in a synthetic phillipsite (prepared by J.F. Cole in these laboratories*).

This sample had an exchange capacity, determined by analysis of the sodium and potassium exchanged forms, of 3.20 meq/g. The silica/alumina ratio was not measured. If the water content is assumed to have been 24 H_2O per unit cell, as for the natural phillipsite, then the composition of the sample would be $Na_2O, Al_2O_3, 5.2SiO_2, 5.4H_2O$. An X-ray photograph of this material showed that it was contaminated with traces of synthetic zeolite "L".

The Na-K exchange isotherm obtained for this synthetic phillipsite is shown in Figure 7.4(a). The selectivity coefficient varied linearly with potassium content, following the equation

$$\log K_c' = 2.402 - 1.908\ K_z \qquad (R = 0.047)$$

K_a and ΔG^0 were calculated as before, giving

$$K_a = 28.0$$

$$\Delta G^0 = -1970 \text{ cal/g equivalent.}$$

The K_a value obtained was greater than that found for the natural phillipsite by a factor of two. A small part of the increase in potassium selectivity may have been due to the presence of the zeolite L impurity, which is known to have a high selectivity for potassium (78).

---

* Reaction mixture 25 g sodium aluminate (commercial)
183 g precipitated silica (B.D.H.)
37 g sodium hydroxide pellets (A.R)
80 g potassium hydroxide pellets (A.R)
860 g water
The gel formed was crystallised in a stirred glass reactor at 100° C for 48 hours.

Figure 7·4: Na–K Exchange in synthetic Phillipsite

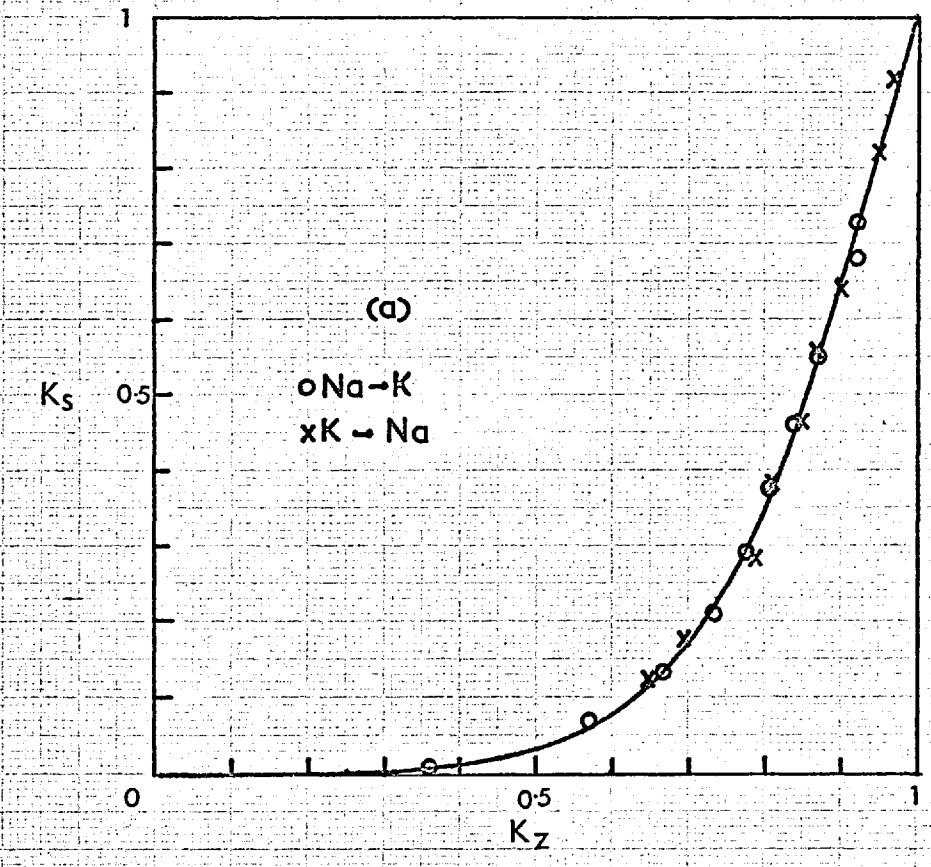

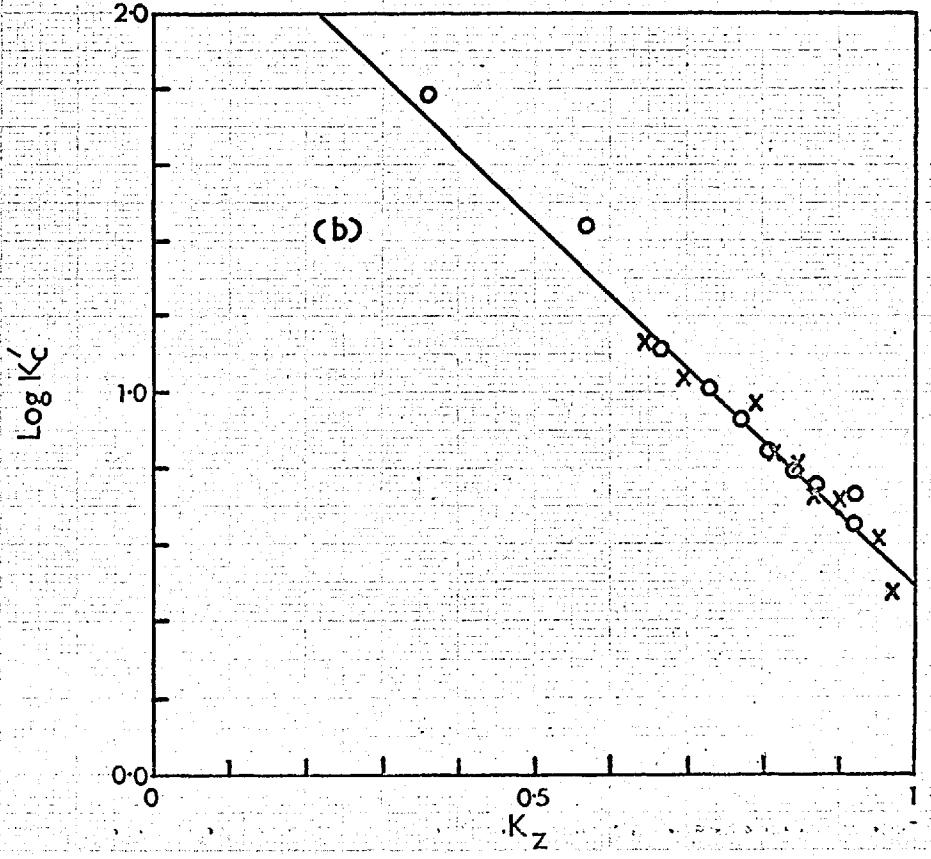

Figure 7·4c

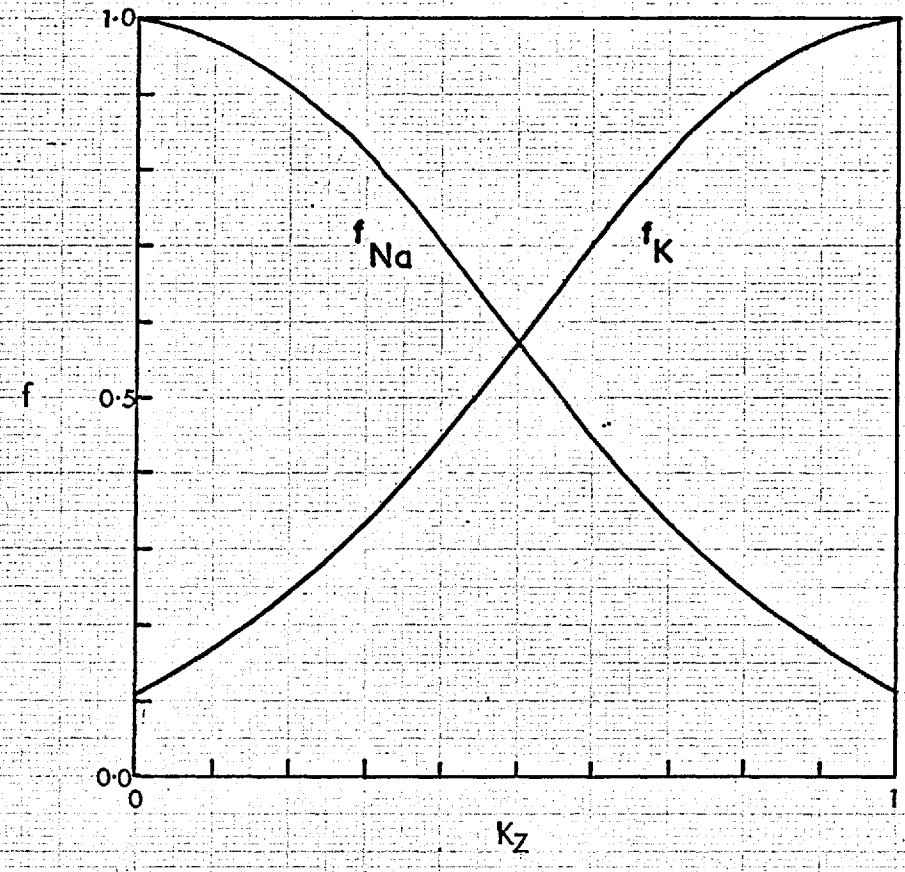

However, quite apart from this, or the effects of different composition or exchange capacity, such differences in K_a values can arise from relatively small errors in the experimental isotherm points.

For an isotherm which obeys Kielland theory, the K_a value is given by the value of K_c' when $K_z = 0.5$. Neglecting solution activity terms, K_a is thus given by

$$K_a = \frac{1-K_s}{K_s} \qquad (K_z = 0.5)$$

For natural phillipsite, $K_z = 0.5$ when $K_s = 0.073$, and $K_a = 12.9$. For the synthetic phillipsite, $K_z = 0.5$ when $K_s = 0.035$, and $K_a = 28.0$. Thus an error of 0.04 in K_s at the mid-point of exchange will account for the difference in K_a values. The effect of this type of error is greater, the higher the selectivity. For a non-selective isotherm ($K_a = 1.0$) an error of 0.04 in A_s when $A_z = 0.5$, produces an error in K_a of approximately 0.16. The actual K_a value found for the Na-K exchange in phillipsite, 12.9, makes phillipsite one of the most selective zeolites for potassium, being only slightly less selective than chabazite ($K_a \approx 16$) (76). On the basis of the measured K_a values for the Na-Li and Na-K exchanges, the lithium form of phillipsite should be extremely selective for potassium.

The presence of substantial amounts of potassium in natural sedimentary phillipsites reflects the preference for potassium shown in the Na-K isotherm. Analysis of samples of bore water in the California/Nevada area, where large sedimentary deposits of phillipsite occur, indicate a potassium fraction in solution of 0.01-0.14. Hay (77) considers that these analyses reflect the probable composition of the saline environment in which the zeolites were deposited. From the observed Na-K isotherm, solution fractions of $K_s = 0.01$-0.14 would give potassium fractions in the phillipsite of 0.06 to 0.30. The natural mineral used in this study had a potassium fraction of 0.21.

The agreement is reasonable, considering the many uncertainties involved in such calculations. Ames (20) has observed a similar correlation between phillipsite and sea-water compositions.

Na-Rb Exchange

The Na-Rb isotherm, shown in Figure 7.5(a) again demonstrated preference for the larger ion. The selectivity coefficient varied linearly with rubidium content, and approached $K_c' = 1$ for maximum rubidium loading. The equation of fit was:-

$$\log K_c' = 2.037 - 2.035\ Rb_z \quad (R = 0.056),$$

giving a Kielland constant C = -1.02.

K_a and ΔG^0 were calculated, giving the values

$$K_a = 10.5$$

and

$$\Delta G^0 = -1400 \text{ cal/g equivalent.}$$

Na-Cs Exchange

The isotherm demonstrated high selectivity for caesium (Figure 7.6(a)). Because of the considerable scatter of the experimental points, the Kielland plot was constructed using values taken off the smoothed experimental isotherm. (See Section 6.) The variation in $\log K_c'$ thus obtained is shown in Figure 7.6(b). The selectivity coefficient increased slightly for caesium loadings up to 0.4 Cs_z, then decreased. This variation was best represented by the cubic equation

$$\log K_c' = 1.436 + 1.024\ Cs_z - 1.023\ Cs_z^2 - 0.890\ Cs_z^3 \quad (R=0.029).$$

Integration gave

$$K_a = 24.2$$

and

$$\Delta G^0 = -1900 \text{ cal/g equivalent.}$$

These results are in good agreement with those obtained by

Figure 7·5: Na–Rb Exchange in Phillipsite

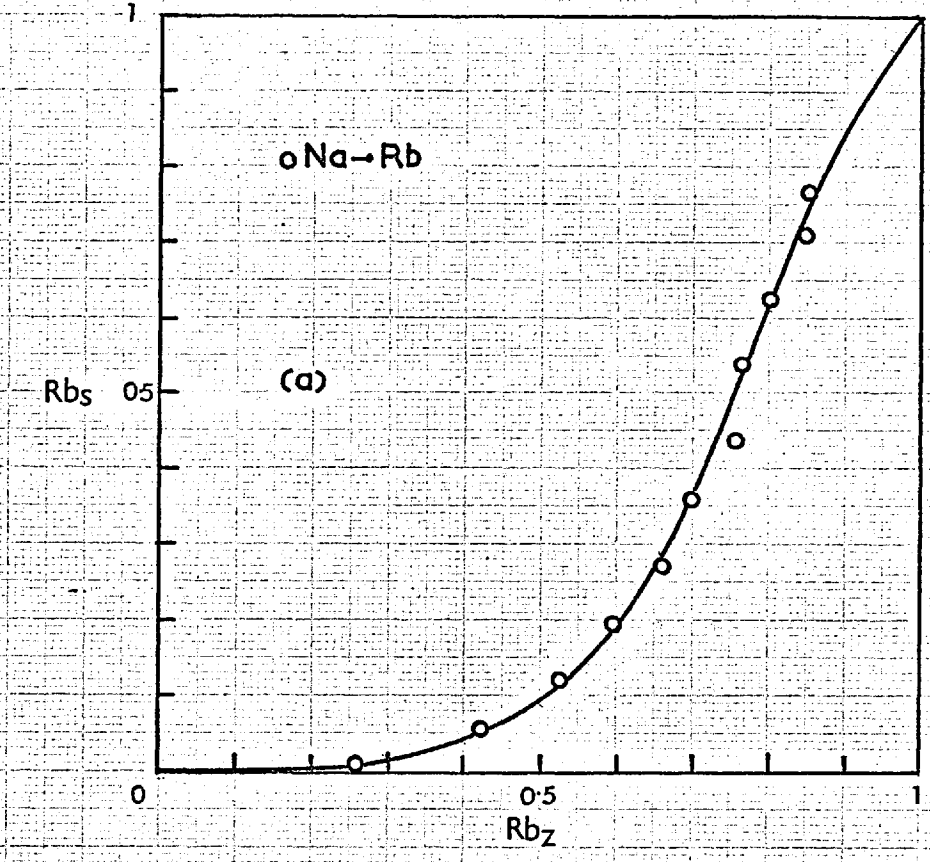

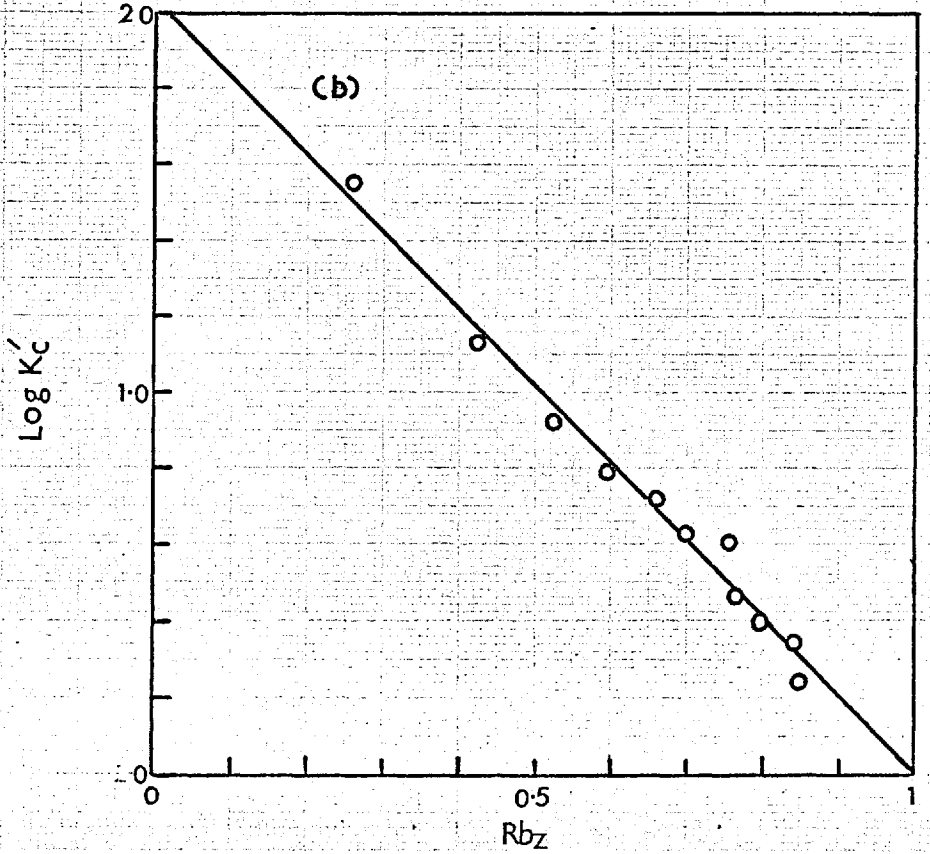

Figure 7·5c

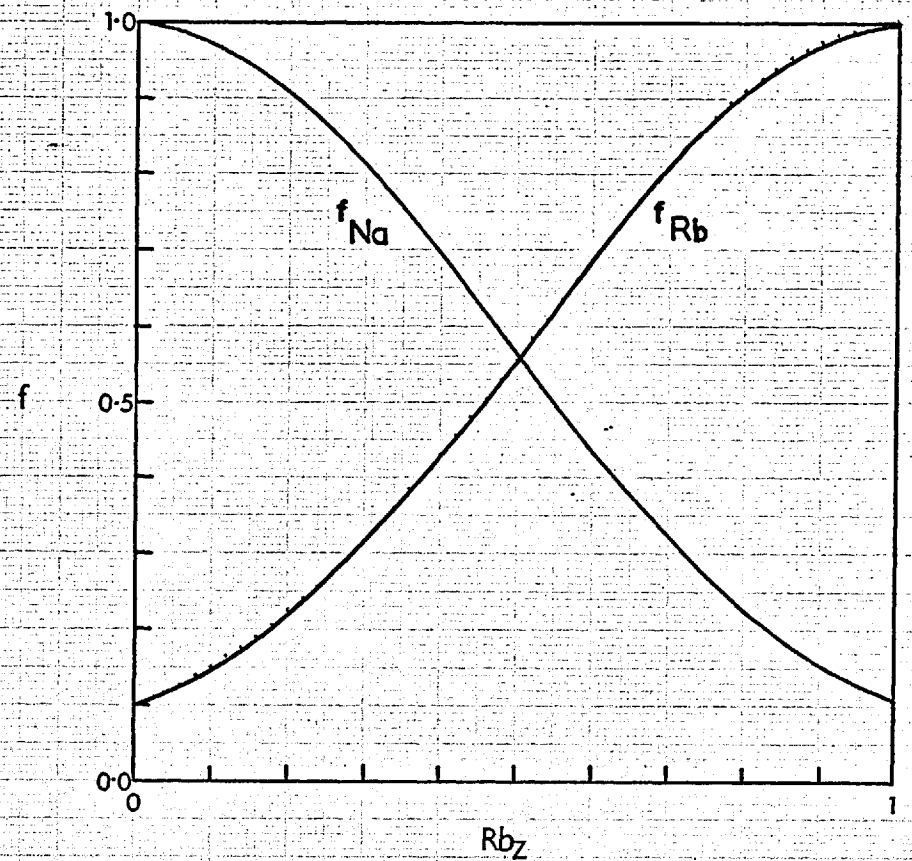

Figure 7·6: Na–Cs Exchange in Phillipsite

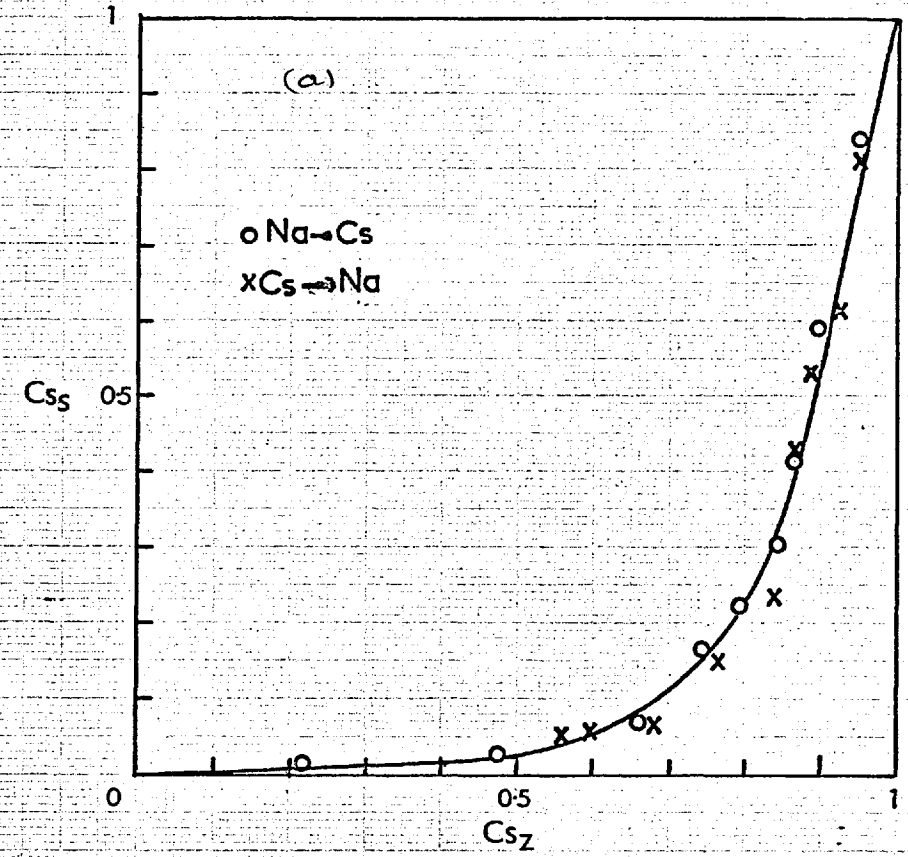

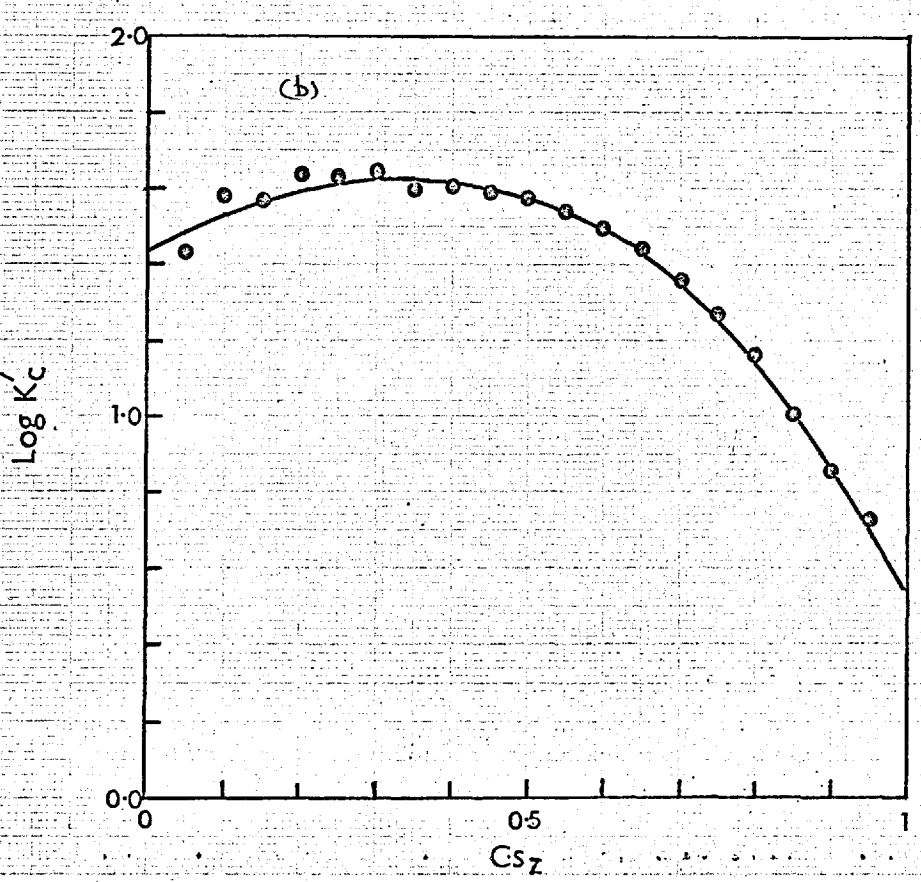

Figure 7·6c

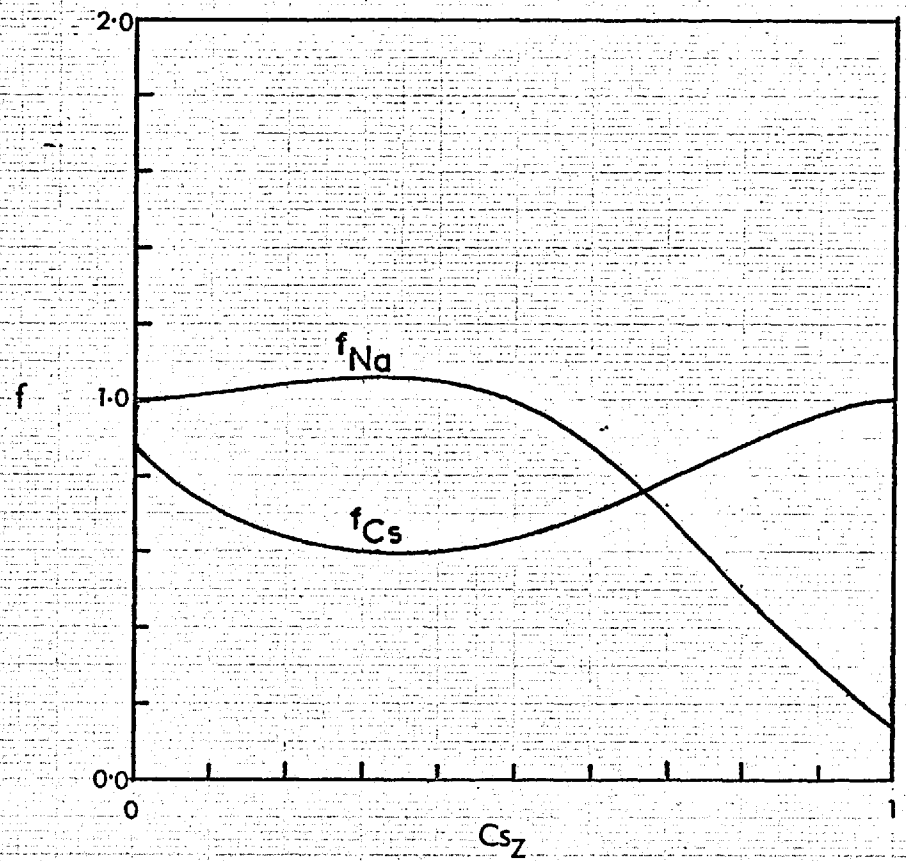

Ames (20) for Nevada phillipsite:-

$$K_a = 26.4$$

$$\Delta G^0 = -1900 \text{ cal/g equivalent.}$$

However, in view of the discrepancies observed for the Na-K exchange, this agreement may be fortuitous.

Summary of Uni-univalent Exchanges

All the uni-univalent exchanges studied were complete and reversible. In all exchanges the ion of larger crystallographic radius was preferred.

The complete exchange observed, and lack of any ion sieve effects, are consistent with the known structure of phillipsite. The main 8-ring channels parallel to the a-axis have an unobstructed diameter of about 4Å, thus allowing access for the largest ion studied, Cs^+, with a diameter of 3.3Å. The main channels are interconnected via rectangular passages (parallel to the b axis) with an unobstructed height of 2.3Å, and width 4Å. Sodium ions could thus diffuse between adjacent main channels, although K, Rb, and Cs ions could not do so without considerable distortion of the lattice. However, the low cation density (4 cations per unit cell), and the possible interchannel diffusion of sodium ions, would be expected to preclude ion sieve effects of the type in which exchange is restricted by the inability of the incoming ion to 'pass" the outgoing ion in the channels.

The ion affinity sequence was approximately the same for all cation loadings, being

$$Rb \sim K \sim Cs > Na \gg Li \quad \text{for} \quad 0 < A_z < 0.2$$

$$Cs > K > Rb > Na \gg Li \quad \text{for} \quad 0.2 < A_z < 1.$$

Eisenman (37) has proposed that selectivity sequences in systems such as zeolites are governed by the anionic field strength in the exchanger. The hydration tendency of the cation involved largely

determines the magnitude of the selectivity. With increasing electric field strength, the least strongly hydrated cation is the first to be desolvated, and most strongly selected by the anionic site. On this basis, Eisenman predicted eleven different affinity series for the alkali metal cations, depending on the anionic field strength. The above affinity series found for phillipsite is approximately Series I of Eisenman, which he predicts for a field strength equivalent to a monovalent anion acting at a distance of about 2.4Å or greater. This correlates roughly with the cation to framework-oxygen distances of about 2.5-3.0Å found by Steinfink.

Such theories of cation selectivities are based on several simplifying assumptions. In actual zeolite systems the cation positions are frequently not known with any great certainty, and may vary with water content, cationic composition, and aluminium distribution. Several types of site may also be involved, each type being associated with a different anionic field strength distribution. More detailed structural investigations and ion exchange data are required before a unified theory of cation selectivity in zeolite systems can be successfully developed.

Na-Ca Exchange

The Na-Ca isotherm is shown in Figure 7.7(a). Sodium was the preferred ion for all cation loadings. The selectivity coefficient varied linearly with calcium ion content (Figure 7.7(b)) and was described by the equation:-

$$\log K'_c = -0.451 - 1.144\ Ca_z \qquad (R = 0.086).$$

Because of the linear variation, a Kielland constant C could be calculated, giving

$$C = -0.57.$$

However, the Kielland theory was developed for uni-univalent exchanges only, and the theoretical interpretation to be placed on the "Kielland

Figure 7·7: Na–Ca Exchange in Phillipsite

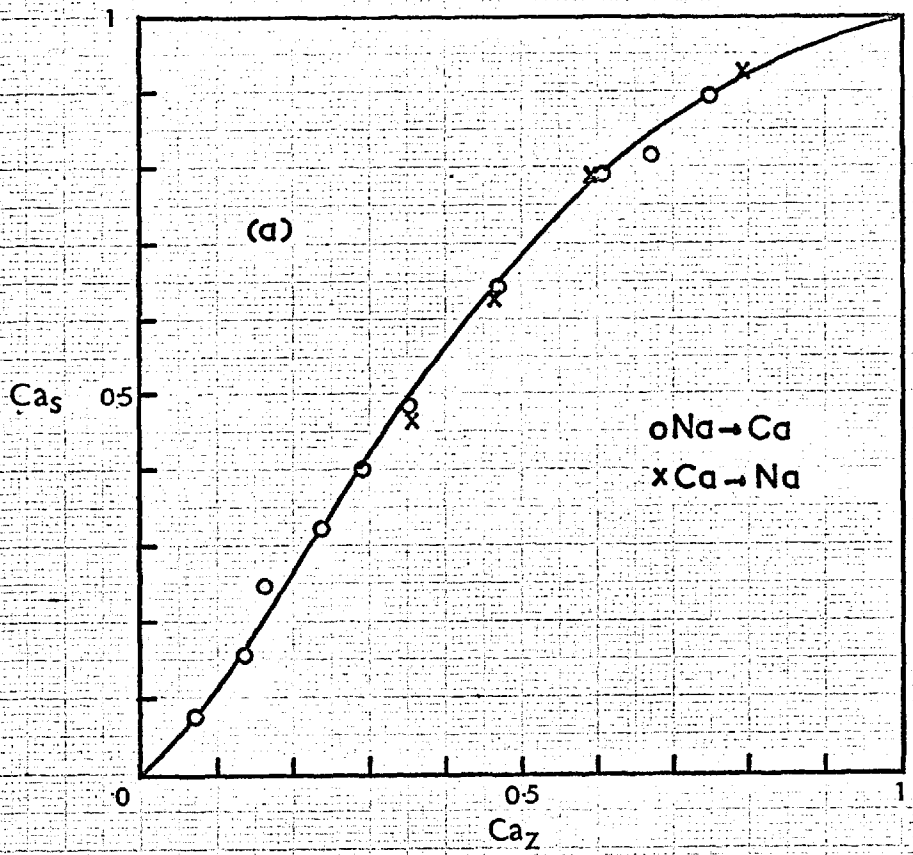

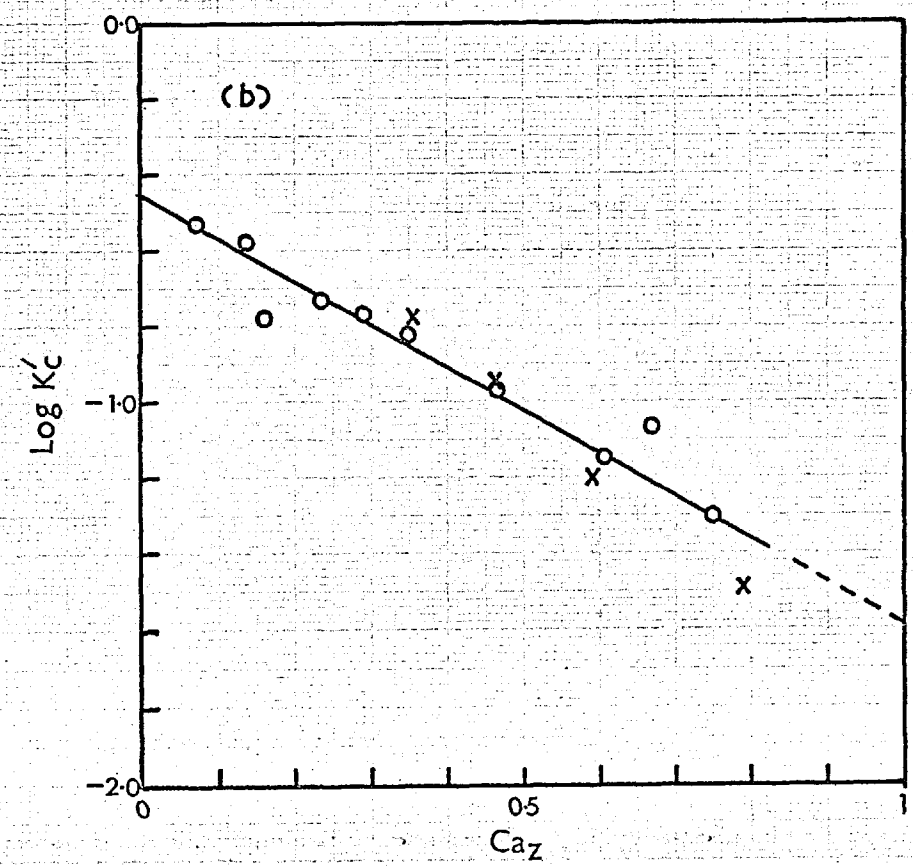

Figure 7·7c

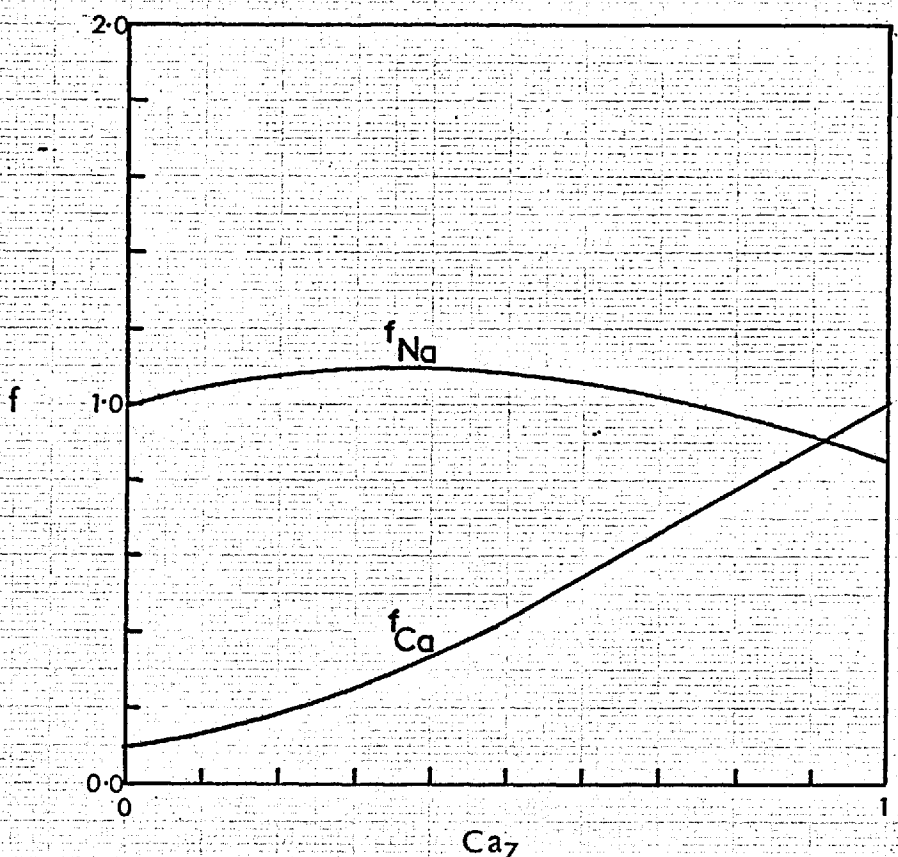

constant" for a uni-divalent exchange is not clear.

The thermodynamic equilibrium constant for the exchange was calculated by Gaines and Thomas theory. For the reaction $2Na^{+}(z) + Ca^{++}(s) \longrightarrow Ca^{++}(z) + 2Na^{+}(s)$, K_a and ΔG^0 were found to be

$$K_a = 0.035$$

$$\Delta G^0 = +990 \text{ cal/g equivalent.}$$

Ames (21) has reported, for the Na-Ca exchange in phillipsite, the following results:

$$K_a = 0.163$$

$$\Delta G^0 = +1100 \text{ cal/g equivalent.}$$

These results cannot be directly compared with those found in the present investigation, as Ames defined K_c' using equivalent ionic fractions for both zeolite and solution concentrations, whereas in this work molalities have been used for solution concentrations. Also, Ames worked at a constant solution concentration of 1.0 N (0.10 N in this work). As discussed by Helferrich (47), an increase in total concentration should, by the Donnan equilibrium theory, decrease the selectivity for the divalent ion in a uni-divalent exchange. A comparison of Figure 7.7(a) with the Na-Ca isotherm given by Ames shows this to be the case.

Na-Sr Exchange

The isotherm, Figure 7.8(a), showed that neither ion was preferred to any great extent. The Kielland plot was again best represented by a linear equation:

$$\log K_c' = -0.486 - 0.522\, Sr_z \qquad (R = 0.081)$$

As for the Na-Ca exchange, a Kielland constant could be calculated:

$$\text{"Kielland constant C"} = -0.26$$

K_a and ΔG^0 were calculated to be

Figure 7·8: Na–Sr Exchange in Phillipsite

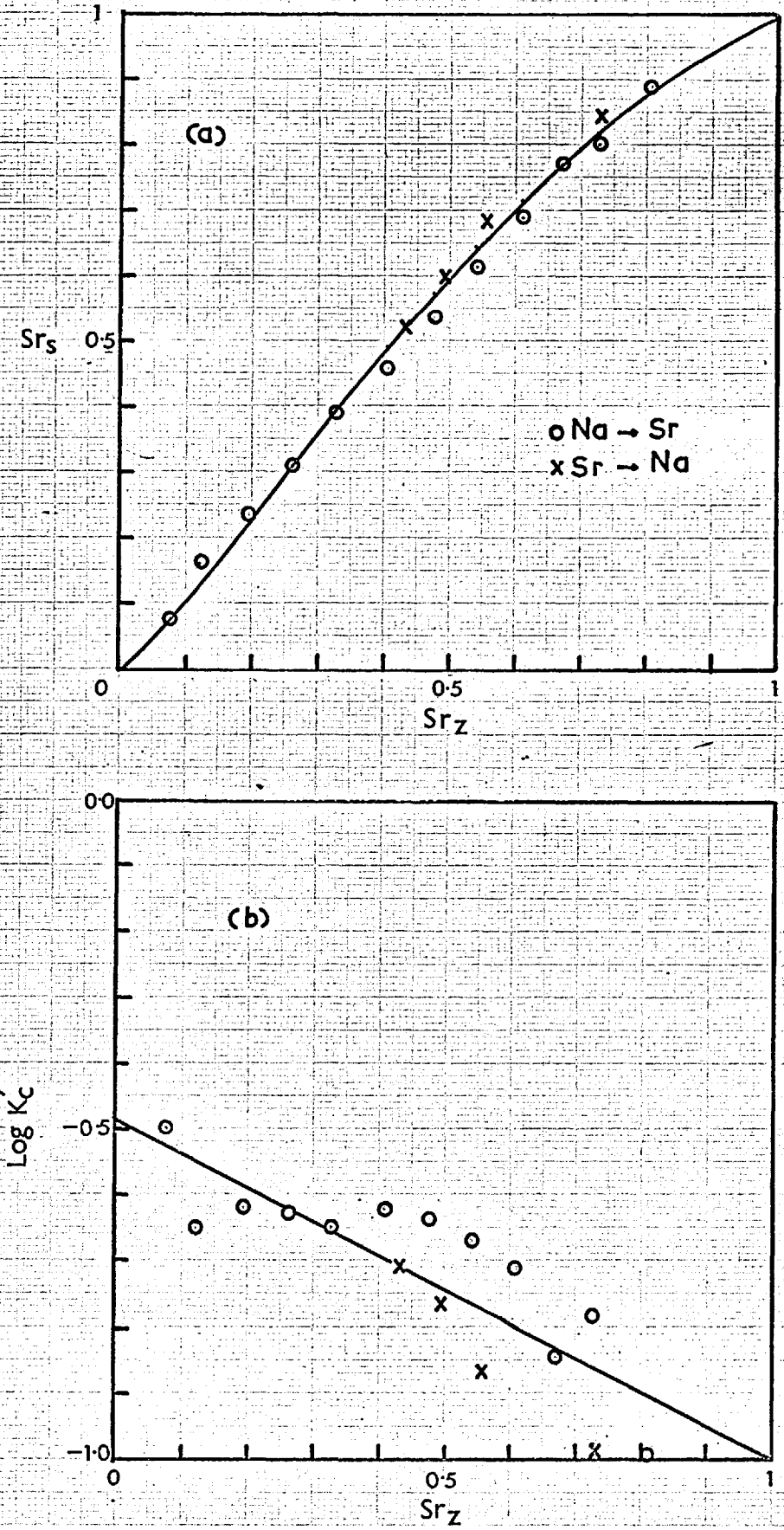

Figure 7·8 c

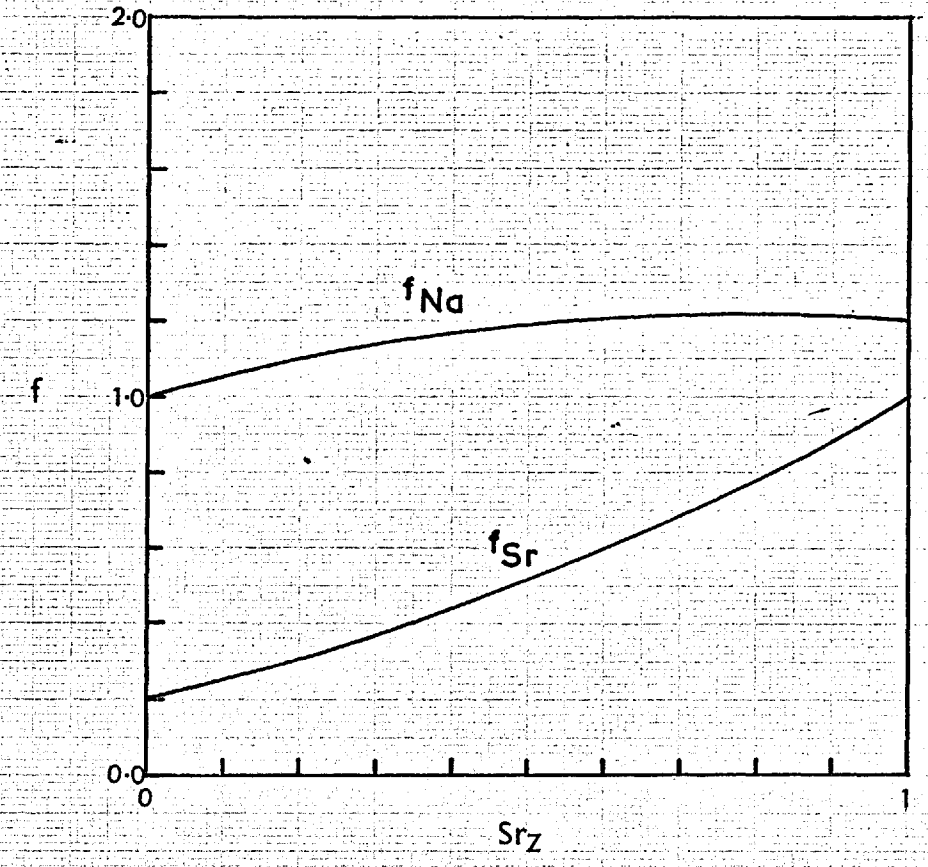

$$K_a = 0.066$$

$$\Delta G^0 = +800 \text{ cal/g equivalent.}$$

Ames (21) found for this exchange

$$K_a = 0.107$$

$$\Delta G^0 = +650 \text{ cal/g equivalent.}$$

For the reasons discussed previously, these results are not directly comparable.

It will be seen that although the isotherm is virtually non-selective, the K_a value is appreciably less than 1. This arises because of the form of the Gaines and Thomas expression for K_a:

$$\log K_a = 0.4343(z_B - z_A) + \int_0^1 \log K_c' \, d A_z$$

The first term involving the valencies of the two ions makes a contribution to $\log K_a$ of -0.4343 for an exchange reaction $B \longrightarrow A$ where A is the divalent ion.

Na-Ba Exchange

The isotherm, Figure 7.9(a), was highly selective for barium, but was irreversible using solutions of 0.10 N. It is probable that the exchange $Ba \longrightarrow Na$ could be effected with stronger solutions.

X-ray photographs of the barium exchanged phillipsite were very similar to those of the natural barium mineral harmotome. This confirms the results of Hoss and Roy (38) and Barrer et al. (39).

Sadanaga (62) has shown that the framework structure of harmotome is essentially the same as that found for phillipsite by Steinfink (61). However, the harmotome unit cell is monoclinic (a = 9.87, b = 14.14, c = 8.72, $\beta = 124^0 50'$), and the distortions of the orthorhombic phillipsite framework which occur to produce the monoclinic cell lead to cavities ideally suited to Ba^{++}, but not to Ca^{++}(62), nor presumably Sr^{++}.

Figure 7·9: Na – Ba Exchange in Phillipsite

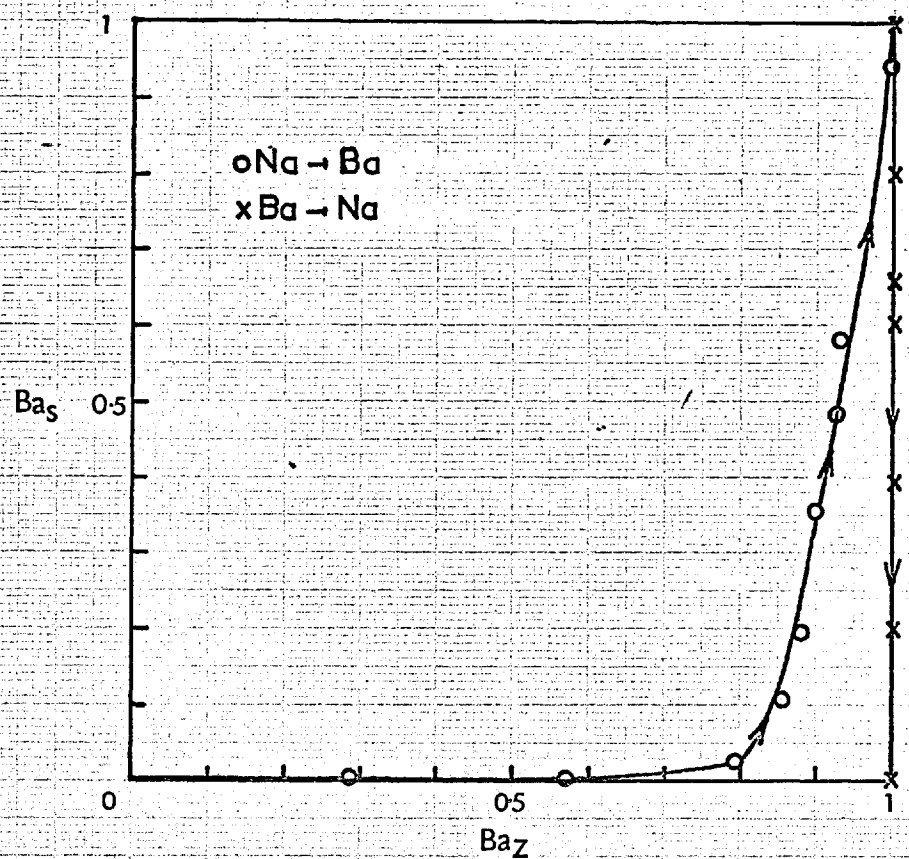

In the particular phillipsite studied here, with a cation density of four monovalent cations per unit cell, exchange for a divalent Ca^{++} or Sr^{++} ions requires only two divalent ions per unit cell. Assuming that the Al distribution is random, this would lead to regions of excess charge in the structure, since the anionic sites must be well separated.

Thus, although most ion exchanges prefer divalent ions (47), in phillipsite the divalent ion preference is reduced by the large site separation.

With Ba^{++} however, the phillipsite cell can transform to the more favourable harmotome configuration. Once in this configuration it is very difficult to reconvert, as evidenced by the very existence of the harmotome mineral in nature. The barium fixation mechanism proposed here may be contrasted with ion fixation in clay minerals. In the latter case fixation of a cation occurs when the electrostatic potential between the cation and the silicate layers is greater than the hydration energy of the cation (79).

The very high selectivity for barium was demonstrated by mixing a sample of Na-phillipsite with 0.1N solutions of $BaCl_2$ (in amounts equivalent to about half the phillipsite capacity). After stirring the mixture for one or two minutes, then filtering, no Ba^{++} could be detected in the filtrate by the usual sulphate ion test. Phillipsite may therefore be useful in applications involving removal of Ba^{++} from neutral or slightly alkaline solution, and for the separation of Ba^{++} from Ca^{++} and Sr^{++}.

7.2 Zeolite Na-P

Analysis

The analysis of Na-P gave the following oxide composition:-

$$0.98Na_2O, Al_2O_3, 3.42SiO_2, 4.0H_2O.$$

X-ray powder photographs showed that the zeolite was the cubic species Na-P_C. On the basis of the known unit cell of Na-P_C, containing 32 oxygen atoms and 16(Al+Si) atoms, the unit cell contents for this sample were calculated to be

$$Na_{5.9}\ Al_{5.9}\ Si_{10.1}\ O_{32}.\ 11.9H_2O$$

This may be compared to the unit cell contents of the sample used by Barrer, Bultitude and Kerr (39) for the structure determination, namely $Na_{5.3}Al_{5.3}Si_{10.7}O_{32}.12.5H_2O$. The sample used by Borer (46) in his structural work had a unit cell content $Na_{6.4}Al_{6.4}Si_{9.6}O_{32}.13H_2O$.

The silica/alumina ratio of the sample, 3.42, lies within the range of 3.3 - 5.3 reported by Barrer et al.(15) for synthetic P zeolites.

The exchange capacities of the various cationic forms of the zeolite were obtained by cation analysis of the exchanged forms. The results, expressed as meq/g hydrated zeolite, are given below:-

Li :	4.51	Cs :	2.78 (see below)
Na :	4.38	Ca :	4.21.
K :	4.40	Sr :	3.87
Rb :	3.54 (calculated)	Ba :	3.58

Analysis of the caesium exchanged form showed a residual non-exchangeable sodium content of 0.50 meq/g. The caesium exchange capacity was calculated from the known water contents of the Cs and Na forms, and the known sodium content of the Na form. The exchange capacity of the Na-P for the Na-Cs exchange was reduced from 4.38 to 4.14 meq/g.

The maximum caesium exchange of 94% is in agreement with the 93% maximum exchange reported for Na-P_T by Taylor and Roy (42).

The water contents of the exchanged forms were measured using a Stanton thermobalance. The results were:-

Li :	17.4%	"Cs" :	8.6%
Na :	15.8%	Ca :	19.2%
K :	10.3%	Sr :	17.1%
Rb :	8.4%	Ba :	14.8%

Crystal Symmetry of P zeolites

Before the results of the ion exchange equilibrium experiments are presented, the short discussion of the phase relationships in the P zeolites given in Section 4 will be extended.

In their original work on the synthesis of the P zeolites, Barrer et al.(15) found three distinct crystal habits, cubic, tetragonal, and orthorhombic. No correlation was found between crystal symmetry and composition. The orthorhombic phase was obtained only rarely, although its synthesis was later confirmed by Regis et al.(63). This species was not encountered in the present work, and therefore will not be discussed.

The unit cell sizes of the cubic and tetragonal species were very similar, the cubic phase having a = 10.0Å, and the tetragonal phase having a = 10.0, c = 9.8. Some variation in the c dimension was found between different preparations. The cubic unit cell was body-centred, but the tetragonal cell appeared to be primitive. The Li, K, Ca and Ba exchanged forms of Na-P_C showed slight changes from cubic symmetry, but were indexed on "pseudocubic" cells with a = 9.8$_9$, 9.8$_5$, 9.9$_5$, 10.03Å respectively. The Ca and Ba forms of the tetragonal phase had X-ray patterns differing from those of the same derivatives of NaP_C . The extent of these differences was not indicated.

Taylor and Roy (42) also prepared both Na-P_C and Na-P_T, and

obtained considerable variation in SiO_2/Al_2O_3 ratio, with no apparent correlation with crystal symmetry. The unit cell of the cubic species agreed with that reported by Barrer et al., a = 10.02Å. A considerable variation was found within the tetragonal species synthesised, the c/a axial ratio varying to a minimum of about 0.975, and both body-centred and primitive tetragonal unit cells occurring in different preparations. The "degree of tetragonality" was measured by Taylor and Roy as the extent of splitting, in units of 2θ, of the strongest (310) line of the powder pattern of the cubic species. Thus

$$\Delta 2\theta(310) = 2\theta(103) - 2\theta(310)$$

Samples with $\Delta 2\theta(310) < 0.70$ appeared to have body-centred tetragonal cells, whereas those with $\Delta 2\theta > 0.70$ had primitive tetragonal cells, indicating a greater departure from cubic symmetry.

The ion-exchanged derivatives of Na-P_T fell into three categories:-

1. Primitive cell, $a \geqslant c$: Li-P_T, Na-P_T
2. Body centred cell, $a > c$: K-P_T, Rb-P_T, Cs-P_T
3. Body centred cell, $c \geqslant a$: Ca-P_T, Sr-P_T, Ba-P_T

Cation exchanged derivatives of Na-P_C were not investigated directly. However, in their investigation of the dehydration behaviour of Na-P_C and Na-P_T, Taylor and Roy (43) found that Na-P_T converted to Na-P_C at $60^0 \pm 3^0$ C. This conversion was rapid and reversible, and occurred without any significant change in unit cell volume. The reaction was considered to be a true first-order phase transition. It is extremely improbable that such a phase transition could involve any breaking of framework atom bonds. Borer reported a small endothermic peak in the D.T.A. curve of Na-P_T at 60^0 C, but considered that this corresponded to loss of loosely bound surface water (46). Borer also found that no "phase changes" occurred during the heating between room temperature and 400^0 C. Taylor and Roy (43) found at least four structural changes in this temperature range. Finally, Borer found that the X-ray powder photograph of Na-P_T could not be explained by a

distorted framework structure of the Na-P_C type. The distortion considered by Borer involved the rotation of one of the basic cubic building units situated at (0, 0, 0). This in turn produced a rotation in the opposite direction of the central cubic unit at $(\frac{1}{2}, \frac{1}{2}, \frac{1}{2})$. It is not known whether any other types of distortion were considered. Borer concluded that the two phases Na-P_T and Na-P_C were separate species because of

(i) different powder patterns at comparable compositions
(ii) different behaviour on heating (TGA, DTA)
(iii) different crystal habits
(iv) different X-ray powder pattern intensities.

The results of the present work support the evidence of Taylor and Roy. X-ray powder patterns of all the monocationic derivatives of Na-P_C prepared agreed with those reported by Taylor and Roy for the corresponding derivatives of Na-P_T. The Na-P_C $\longleftrightarrow$ Na-P_T phase transition was also confirmed.

When the Na-P_C was originally synthesised, it gave a cubic Na-P pattern, together with faint muscovite lines (arising from the muscovite impurity in the kaolinite used for synthesis). This muscovite was removed by repeated sedimentation, as described in Section 4. After the final decantation, the zeolite was filtered, washed first with water, then with 70% aqueous alcohol, and finally acetone. The product was then dried at 80° C overnight. The next day a small sample was taken for an X-ray photograph. The photograph showed the pattern of pure Na-P_T. (d-spacings for both Na-P_C and Na-P_T are given in Appendix 1.) The following day, a further sample was taken from the bottle of zeolite, which had been stored, after drying, at room temperature. This photograph showed Na-P_C, with only very faint traces of Na-P_T. The bulk sample was then split into two portions, one of which was stored in a desiccator over saturated ammonium chloride, the other in the original bottle (sealed). After another day, both samples had reverted to pure Na-P_C.

Two years later, an X-ray of the sample stored in the bottle showed a mixture of Na-P_C and Na-P_T. The sample equilibrated over ammonium chloride was still pure Na-P_C. The mixture reverted to Na-P_C when it was stored over ammonium chloride for a week.

The cubic-tetragonal transition thus appears to depend on both temperature and water-vapour pressure.

As these observations support the evidence of Taylor and Roy, the exchange behaviour of Na-P_C to be discussed can be validly compared with the exchange behaviour of Na-P_T.

Na-Li Exchange

The isotherm is shown in Figure 7.10(a). The exchange was apparently reversible within the limits of experimental error, and was highly selective for sodium. Because of this high selectivity, it was not possible to obtain experimental values for Li_z greater than about 0.5, using 0.1N solutions.

The variation of the selectivity coefficient with lithium loading is shown in Figure 7.10(b). Log K_c' increased rapidly for Li_z up to about 0.15, then decreased with increasing Li_z. The best equation of fit found using the CALCIS program was:-

$$\log K_c' = -1.521 + 1.921\ Li_z - 5.498\ Li_z^2 \qquad (R = 0.083)$$

Integration gave $K_a = 0.004$.

Although the error of fit was relatively low for such a selective isotherm, this equation was not very satisfactory outside the range of the experimental data, giving a log K_c' value of -5.1 and $Li_z = 1.0$. This could not be overcome by taking points from the smoothed isotherm, since these could not be reliably estimated. The fit in the low Li_z region also consistently over-estimated log K_c', although only by small amounts. The procedure finally adopted was to draw a smooth curve through the log K_c' versus Li_z points up to $Li_z \approx 0.2$, and assume a

Figure 7.10: Na–Li Exchange in P

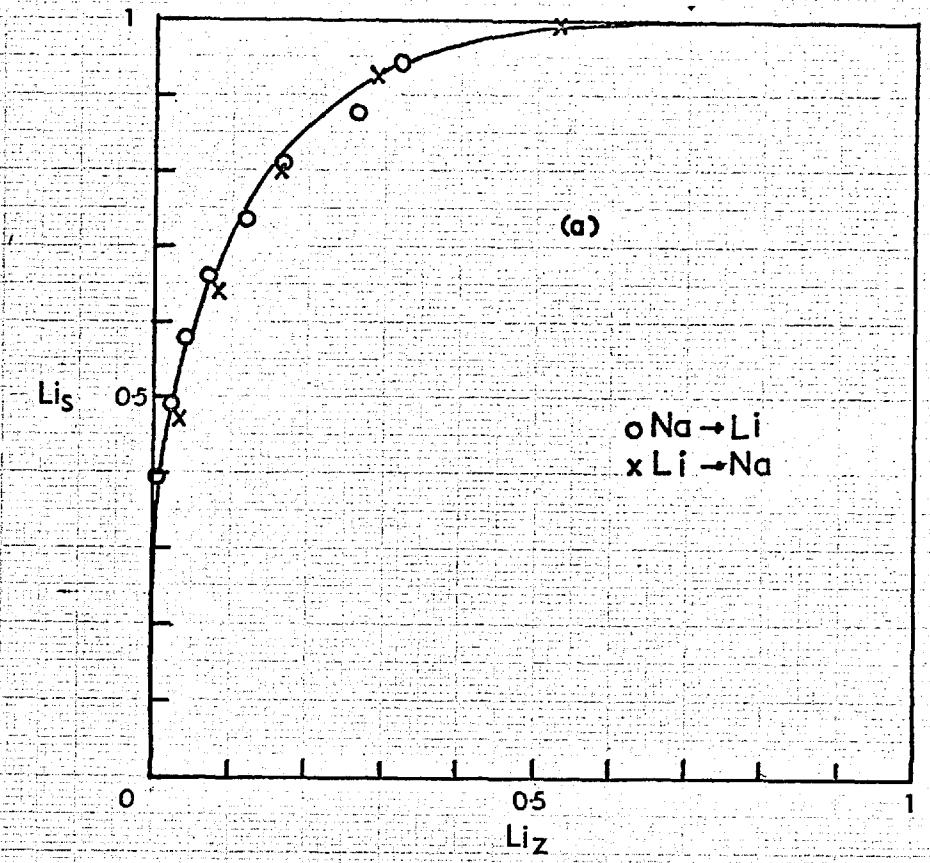

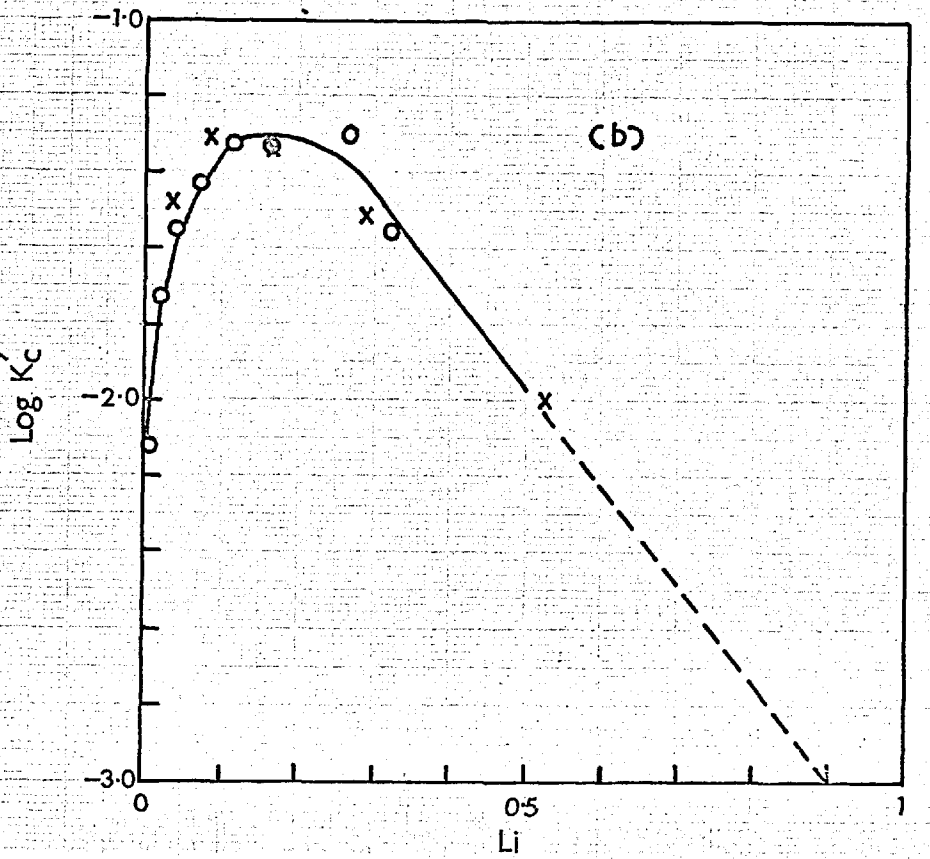

Figure 7·10c

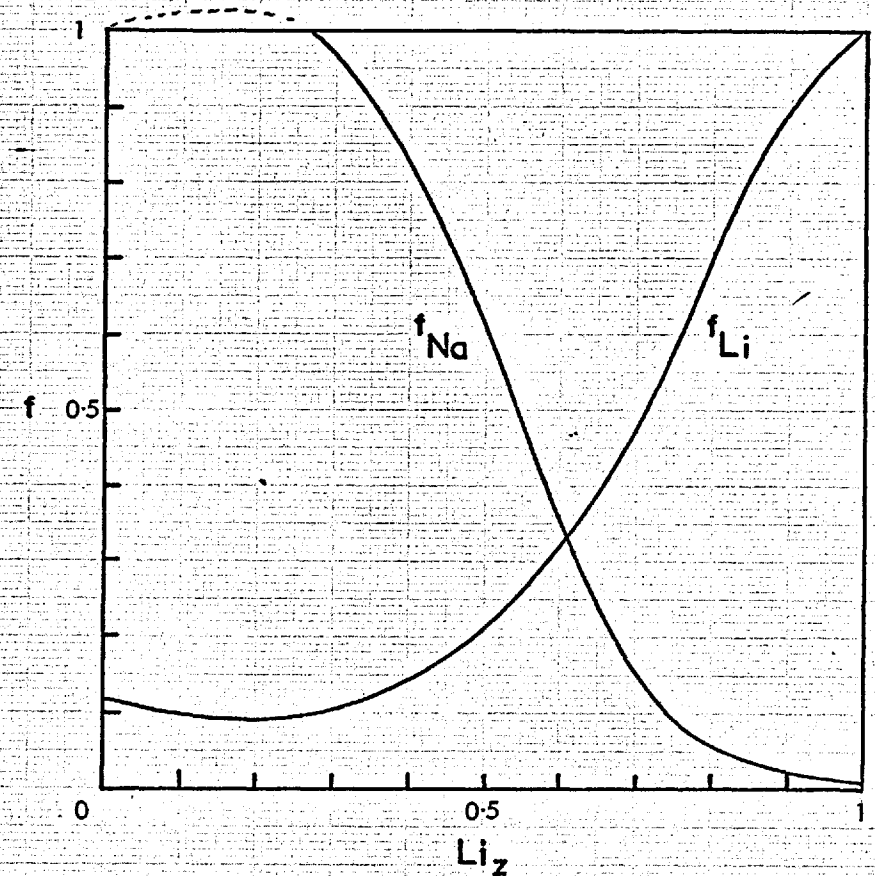

linear relationship between log K_c' and Li_z for Li_z greater than 0.2. K_a was then determined by graphical integration, gaving values of K_a and ΔG^0 :-

$$K_a \approx 0.009$$

$$\Delta G^0 \approx +2800 \text{ cal/g equivalent}$$

The conversion of Na-P to Li-P involves a change from a body-centred cubic lattice to a primitive tetragonal lattice. X-ray powder photographs of some of the partially exchanged samples clearly showed how this change was accomplished and also provided a possible explanation for the shape of the Kielland plot.

Sample composition	Phases present
$Li_z = 0.005$	Na-P_c + some Na-P_T
$Li_z = 0.07$	Na-P_T + some Na-P_c
$Li_z = 0.17$	Na-P_T + trace Na-P_c
$Li_z > 0.17$	Single tetragonal phase, changing smoothly from Na-P_T to Li-P_T with increasing Li_z.

In the region $0 < Li_z < \sim 0.2$, both cubic and tetragonal Na-P were present, showing the limited solid solubility of these two phases under the experimental conditions. The slope of the Kielland plot in this region is high and positive, and equivalent to a Kielland constant greater than that for which phase separation would be expected to commence.

Taylor and Roy (42) did not report any evidence of limited solid solubility in the Na-Li exchange of Na-P_T. This is consistent with the present results, since no change from Na-P_c to Na-P_T was involved.

Na-K Exchange

The Na-K isotherm is shown in Figure 7.11(a). The unusual shape of this isotherm was similar to that expected for an exchange obeying Kielland theory, with a Kielland coefficient positive and close to the critical value (+0.87). Inspection of the plot of log K_c' versus K_z (Figure 7.11(b)) showed that log K_c' did vary approximately linearly with K_z. The best linear fit found using the CALCIS program (omitting points with K_z less than 0.1 and greater than 0.9, as these, because of their scatter, contributed a disproportionately high weight in the least-squares procedure) was

$$\log K_c' = -0.061 + 1.254\ K_z \quad (R = 0.034)$$

The Kielland constant C was positive, and equal to +0.63. It is believed that this is the first case yet reported of a consistent positive Kielland constant, for an exchange isotherm in a zeolite.

For the purpose of calculating K_a, however, the best representation of the Kielland plot was given by the quadratic equation:-

$$\log K_c' = -0.137 + 1.673\ K_z - 0.419\ K_z^2 \quad (R = 0.025)$$

K_a and ΔG^0 were calculated from this equation, giving

$$K_a = 3.63$$

and

$$\Delta G^0 = -760 \text{ cal/g equivalent.}$$

The linear fit gave a K_a value of 3.68.

The solid isotherm curve shown in Figure 7.11(a) was calculated from the quadratic equation of fit. The solid phase activity coefficients shown in Figure 7.11(c) were also calculated from this equation.

This exchange involves the conversion of body-centred cubic Na-P ($a \approx 10.0$Å) to the body-centred tetragonal K-P ($a \approx 9.91$, $c \approx 9.62$). This change requires a volume contraction of about 60Å^3 per unit cell, and a contraction in the c-direction of about 4%, even though the sodium

Figure 7·11: Na–K Exchange in P

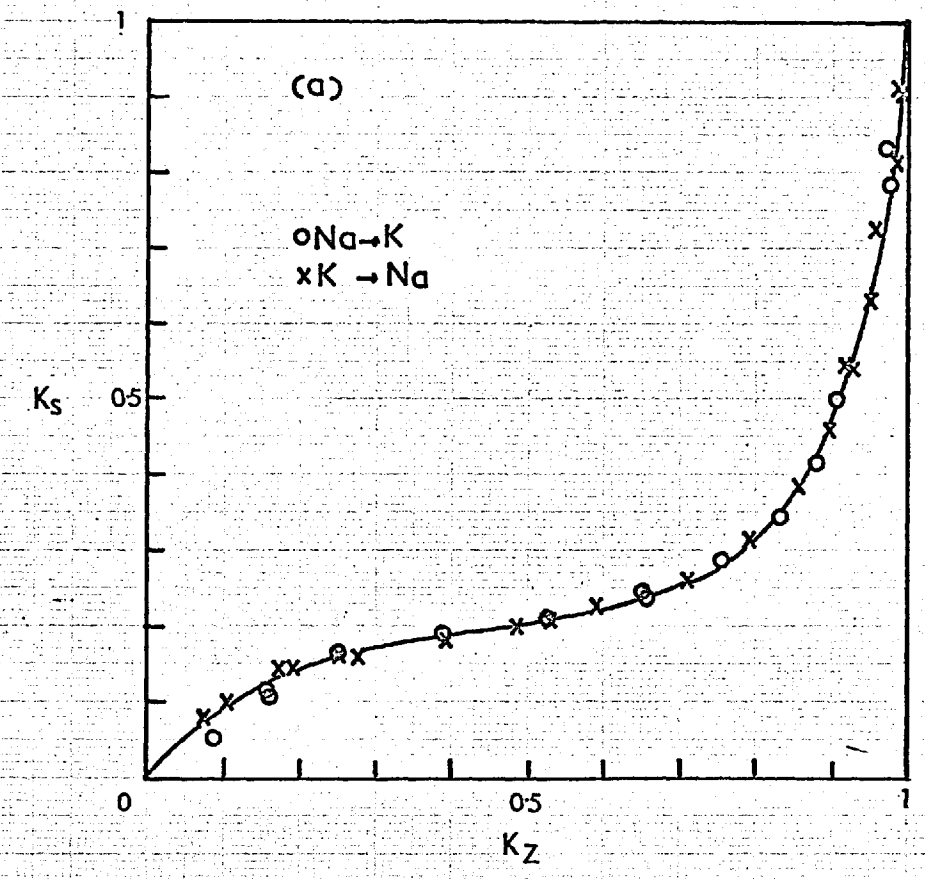

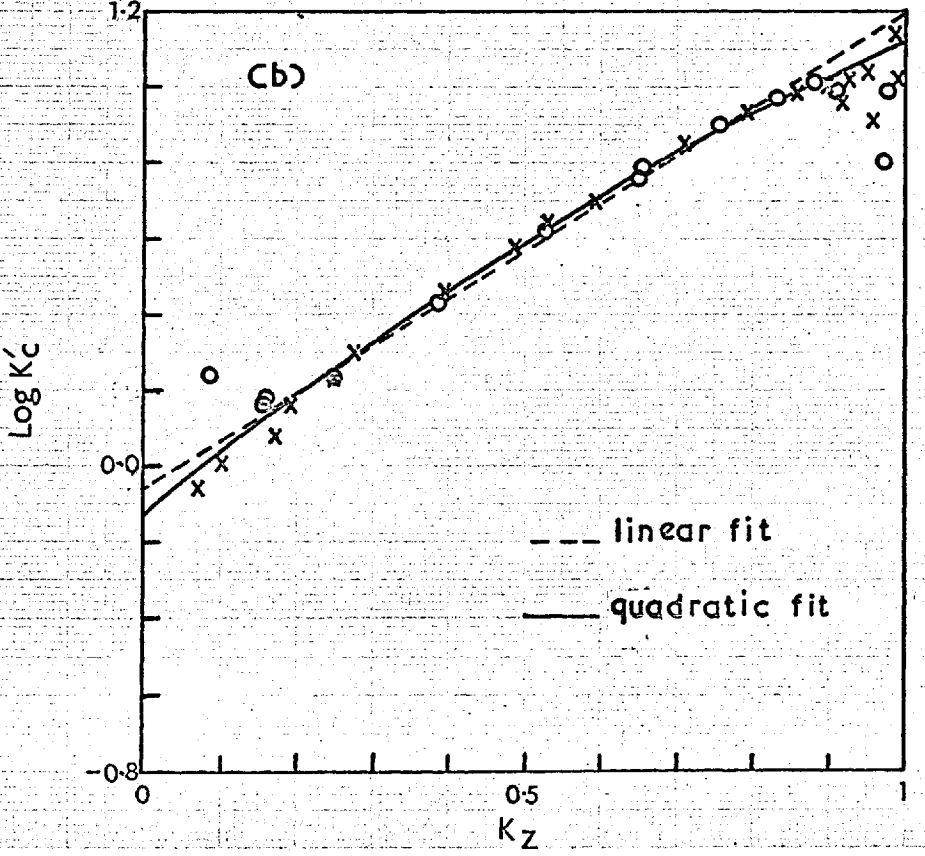

Figure 7·11c

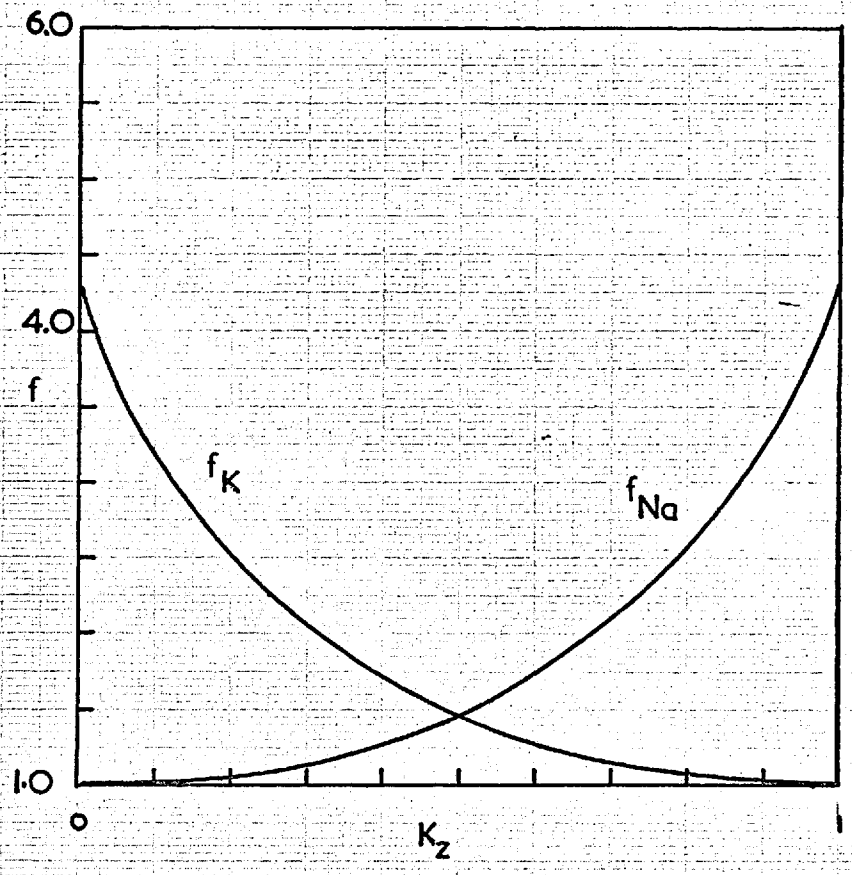

cations are being replaced by potassium ions. The additional space required by the potassium ions is evidently found at the expense of water molecules. The water content of K-P, 10.3%, corresponds to about $8H_2O$ per unit cell, compared with $12H_2O$ for Na-P_c.

X-ray powder photographs were obtained for several exchange samples of varying potassium content. The (310) and (103) lines were measured and from these approximate values of a and c were calculated. These measurements were not corrected for film shrinkage, and the absolute values of a and c obtained are therefore only approximate. The relative changes in a and c only were required.

The results obtained are shown in Figure 7.12, in which unit cell dimensions are plotted against K_z.

All the samples X-rayed consisted of a single phase. For K_z between 0.0 and 0.1 the unit cell remained cubic. The next sample available, with $K_z = 0.195$, showed a single body-centred tetragonal phase with $a \approx 9.96$ and $c \approx 9.88$. All other samples had body-centred tetragonal cells, with a changing from 10.0Å for Na-P_c to 9.9 for K-P_T. The change in c was more rapid for K_z between 0.2 and 0.5 than for K_z greater than 0.5. The region of most interest is, of course, between $K_z = 0.1$ and $K_z = 0.2$, for which no samples were available. Extrapolation of the c curve would appear to indicate that the change from a cubic cell to a tetragonal cell occurred at a specific composition of the zeolite, probably near $K_z = 0.1$.

The positive Kielland coefficient found for this exchange indicates that occupation of adjacent sites in the Na rich lattice by two K^+ ions is more favourable than occupation by one Na^+ and one K^+ ion. This is a direct result of the Barrer and Falconer interpretation of Kielland's equation discussed in Section 3. On this basis the structural changes can be qualitatively interpreted as follows. For small potassium loadings, adjacent sites may be occupied by K^+ ions without causing noticeable deviations from cubic symmetry. However, at a particular critical potassium loading, possibly at $K_z \approx 0.1$, occupation of adjacent

Figure 7·12

Unit cell changes for

Na – K Exchange in P

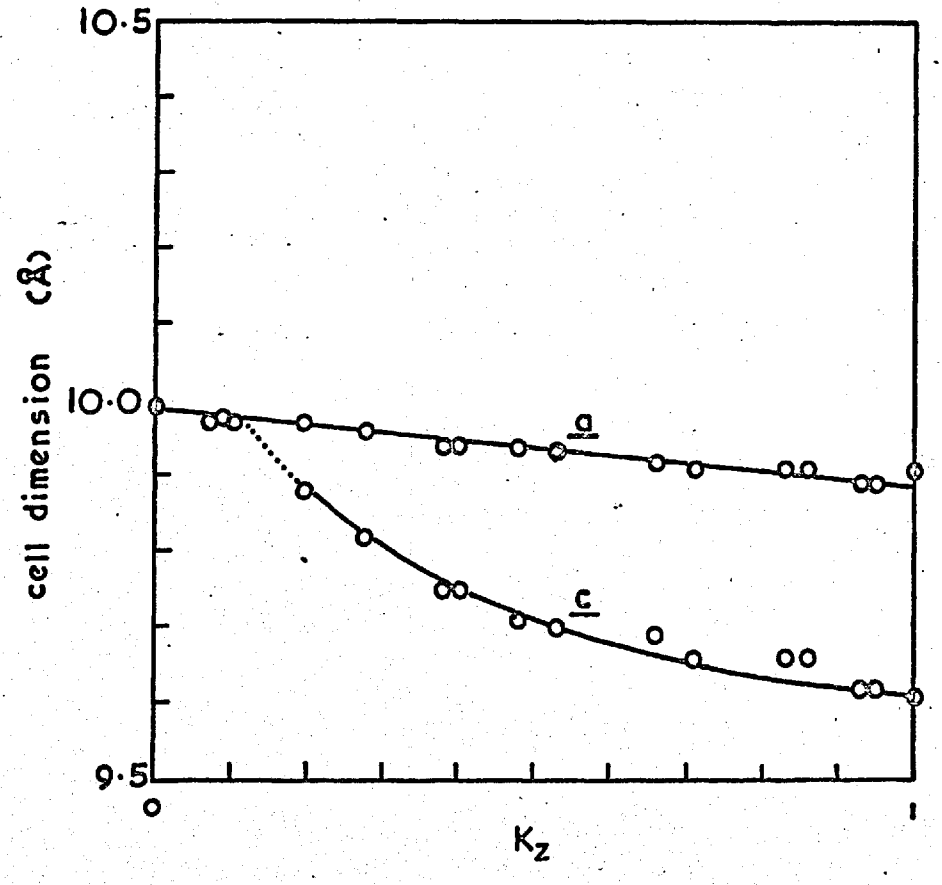

sites requires a slight distortion of the cubic lattice to a tetragonal lattice. The amount of distortion increases with increasing potassium loading. On the evidence available, phase separation does not occur, presumably because the necessary cation movement and water loss can be accomplished without nucleating a separate potassium-rich phase.

The Na-K exchange for Na-P_T does, however, lead to phase separation. Taylor and Roy (42) report a two-phase region extending from $K_z \approx 0.15$ to $K_z \approx 0.4$. For K_z less than 0.15, the primitive tetragonal cell contracted slightly in both a and c with increasing potassium loading. For K_z greater than 0.4, the body-centred tetragonal cell changed in a similar way to Figure 7.12 over the same region.

Na-Rb Exchange

The Na-Rb isotherm is shown in Figure 7.13(a). Rubidium was the preferred ion. The Kielland plot, shown in Figure 7.13(b) was best described by the cubic equation

$$\log K_c' = 0.743 - 0.730\ Rb_z + 3.448\ Rb_z^2 - 3.863\ Rb_z^3 \quad (R=0.065)$$

Integration of $\log K_c'$ between the limits $Rb_z = 0$ and $Rb_z = 1$ gave

$$K_a = 3.64$$

and the free energy of exchange ΔG^0 was therefore calculated to be

$$\Delta G^0 = -760 \text{ cal/g equivalent.}$$

The K_a value for this exchange was very similar to that found for the Na $\longrightarrow$ K exchange.

X-ray photographs of the limited number of exchange samples available showed that the unit cell changes were also similar to those found in the Na-K exchange.

The results are shown in Figure 7.14. For Rb_z less than 0.13, a pure cubic phase was present. For $Rb_z \geqslant 0.38$, a body-centred tetragonal phase was found.

Figure 7·13: Na–Rb Exchange in P

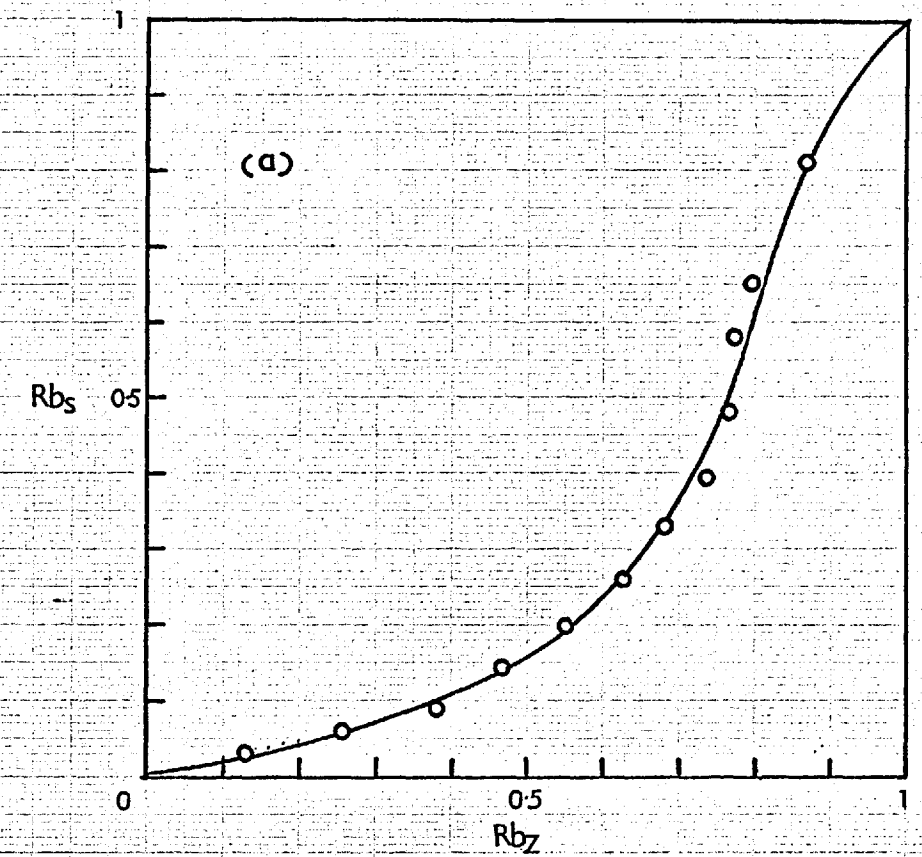

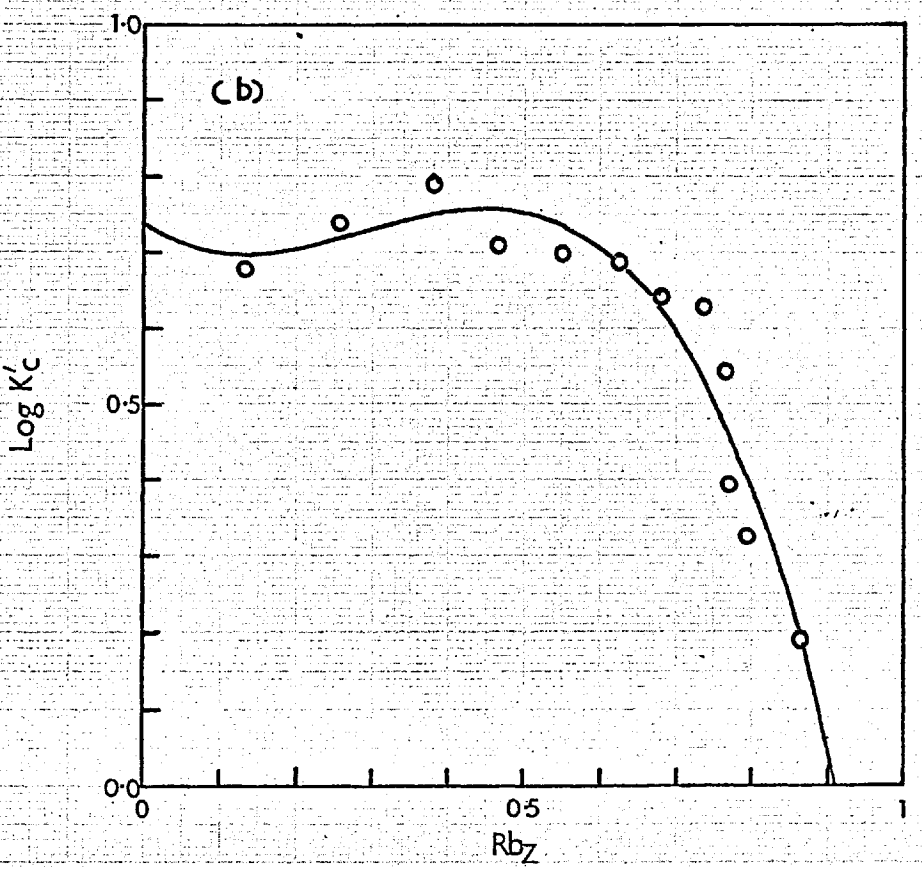

Figure 7.13 c

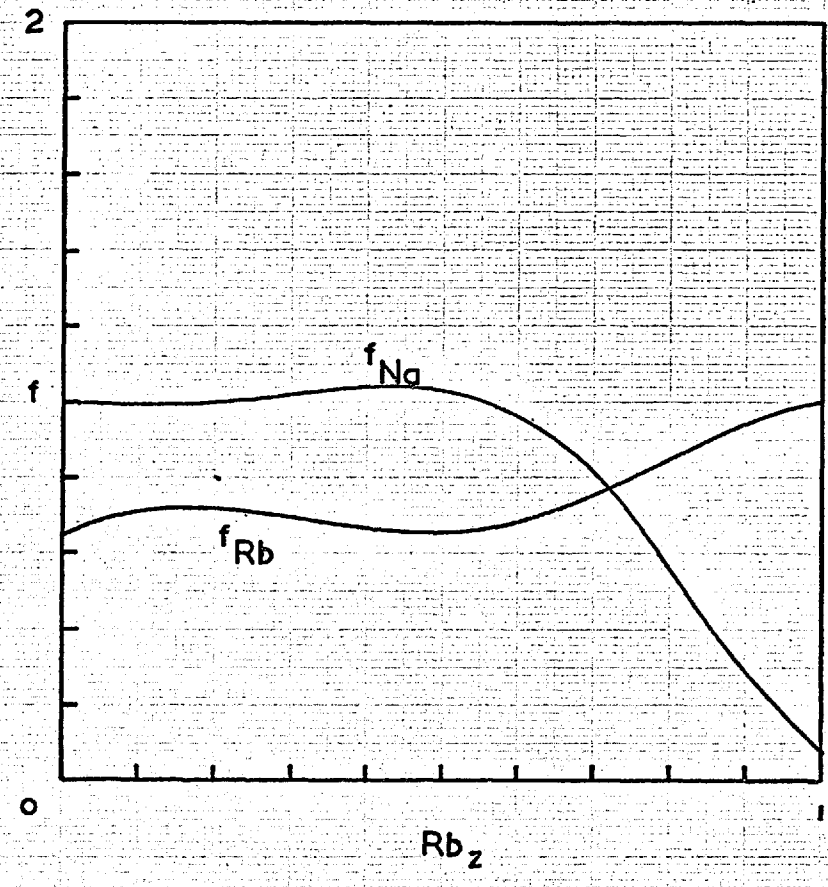

Figure 7·14

Unit cell changes for

Na – Rb Exchange in P

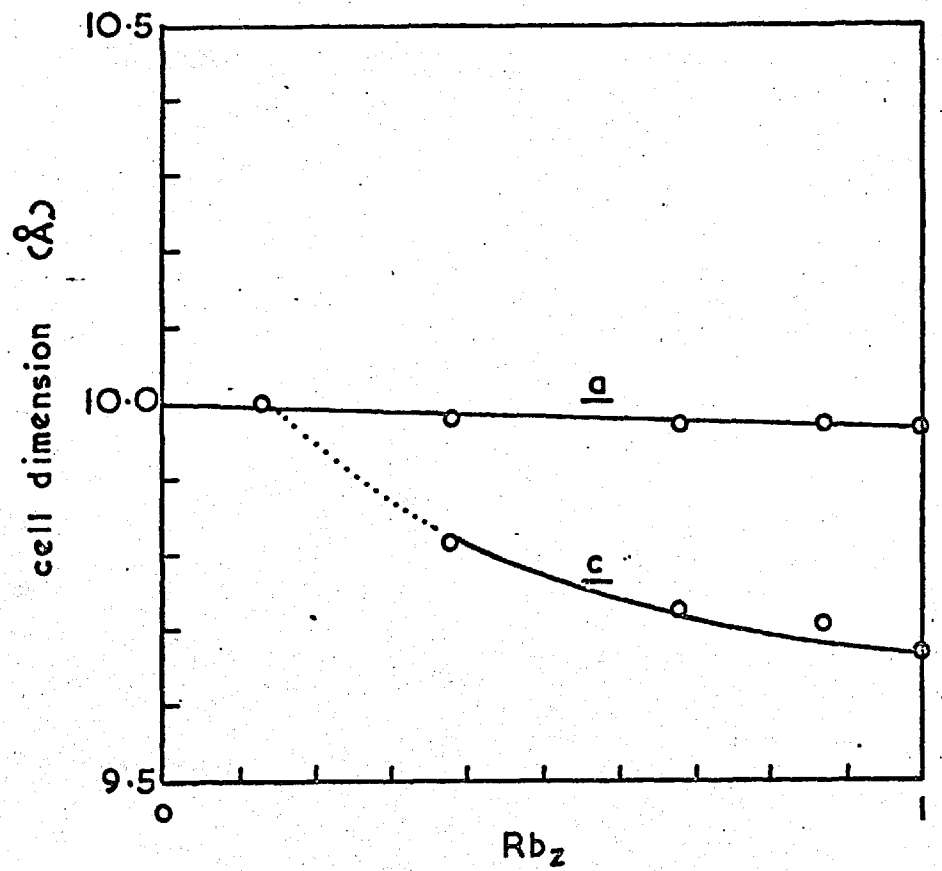

Na-Cs Exchange

The experimental isotherm and Kielland plot are shown in Figures 7.15(a) and 7.15(b) respectively. The isotherm points showed a great deal of scatter, which in turn gave a poor least-squares fit for the Kielland plot, indicated by the high R value of 0.149.

The best equation of fit found was

$$\log K_c' = 1.927 - 6.586\ Cs_z + 13.212\ Cs_z^2 - 9.996\ Cs_z^3$$

The K_a value calculated from this equation was 3.46, giving a free energy of exchange ΔG^0 of 730 cal/g equivalent. This K_a value is again similar to those found for the Na-K and Na-Rb exchanges.

No X-ray photographs were taken for samples representing the isotherm points. However, the final unit cell of Cs-P, which as discussed earlier still contains 0.5 meq Na^+/g, is similar to those of K-P and Rb-P, namely a body-centred tetragonal cell. Taylor and Roy give the dimensions of the Cs-P cell as $a \approx 10.1$, $c \approx 9.8$. It is likely that the cell changes for the reaction $Na\text{-}P_C$ to $Cs\text{-}P_T$ are basically similar to those found for the Na-K and Na-Rb exchanges. However a must increase from 10.0Å to 10.1Å, instead of decreasing slightly as in the other two cases.

Na-Sr Exchange

This exchange was also measured at a constant solution concentration of 0.1 equivalents/litre. The ion strength of the solution varied from 0.10 to 0.15. The Na-Sr isotherm, Figure 7.16(a), showed a considerably greater preference for Sr than had been shown for the alkali metal cations studied. Because of the high selectivity, accurate measurements were not obtained below $Sr_z = 0.4$.

The Kielland plot, Figure 7.16(b) was therefore constructed using points taken off the smoothed experimental isotherm. The resulting plot was best represented by a linear equation,

$$\log K_c' = 0.900 + 0.215\ Sr_z \qquad (R = 0.041)$$

Figure 7·15: Na–Cs Exchange in P

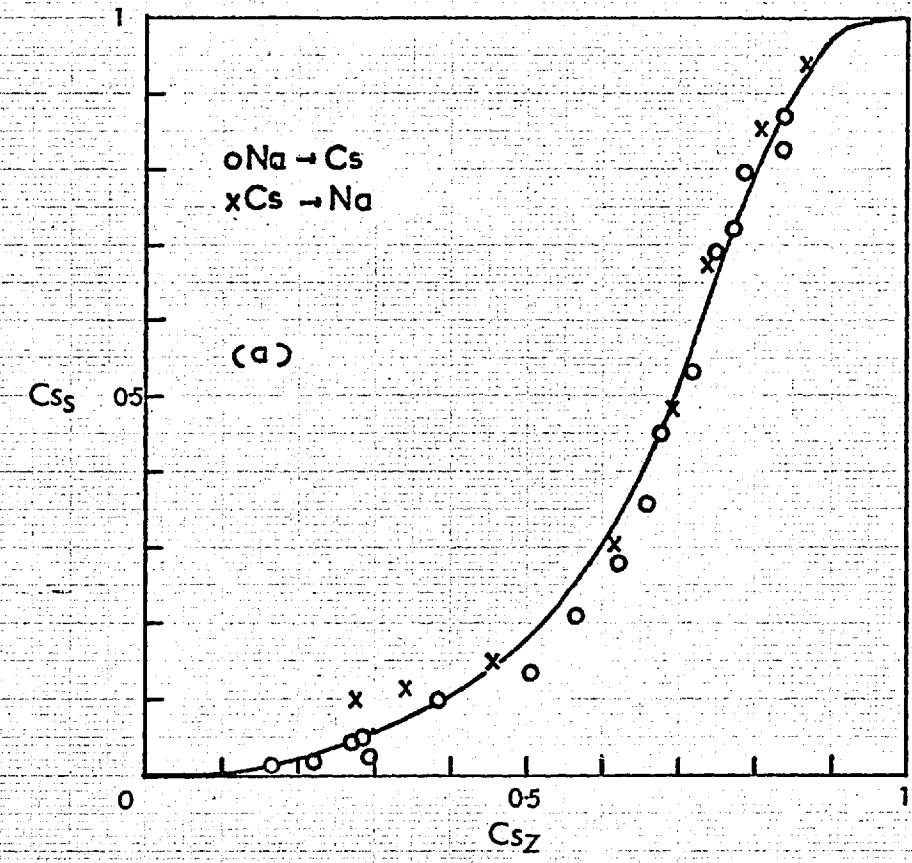

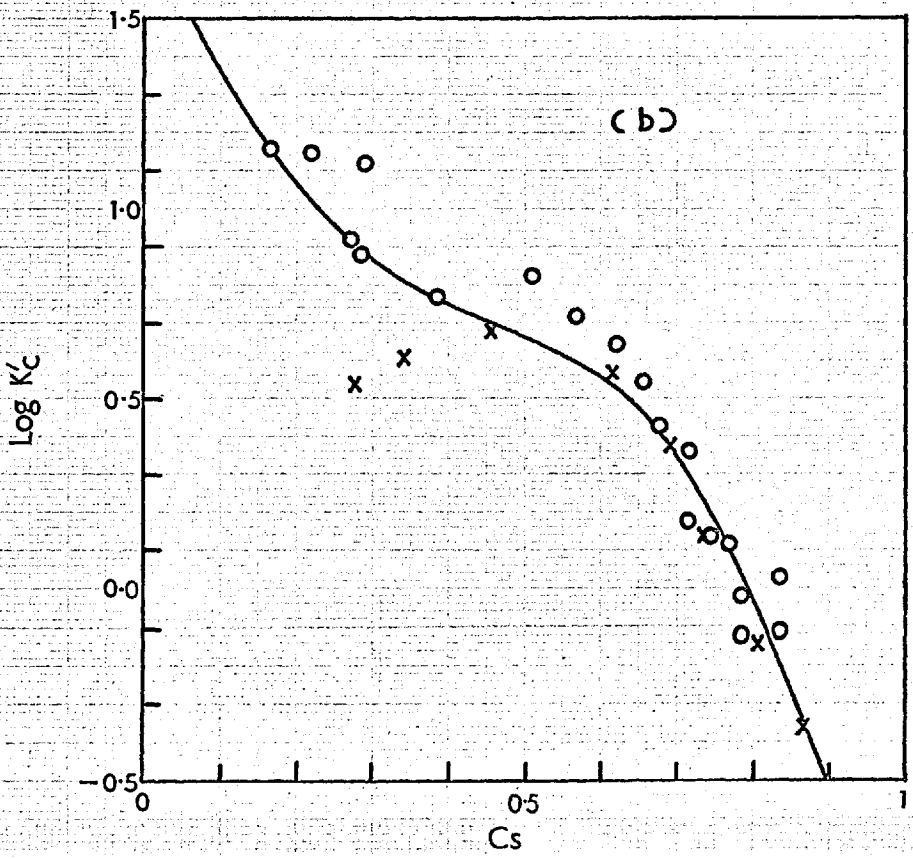

Figure 7-15c

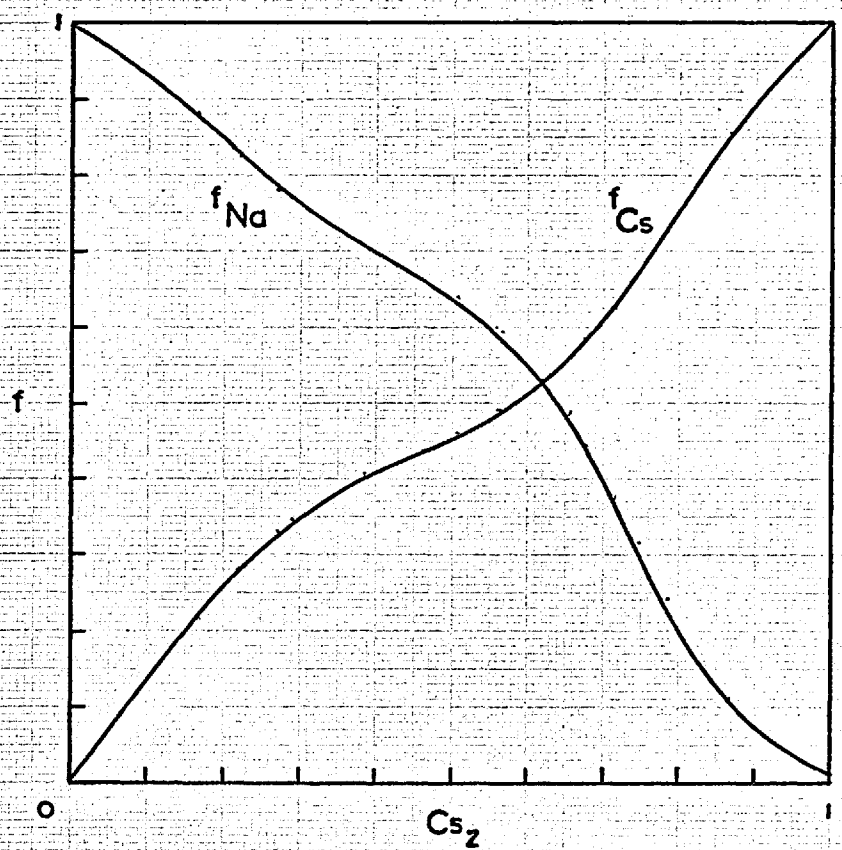

Figure 7·16: Na–Sr Exchange in P

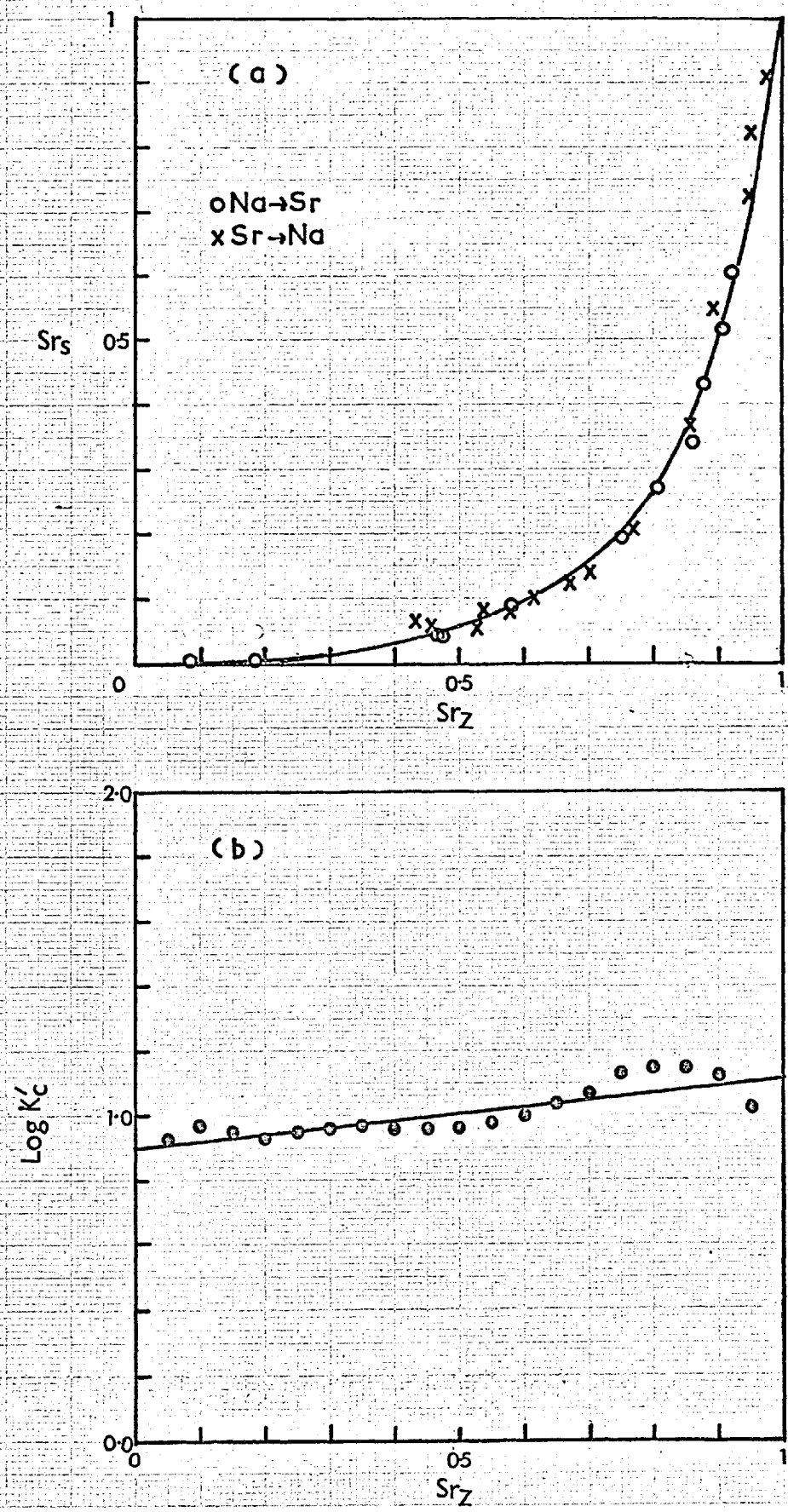

Figure 7·16c

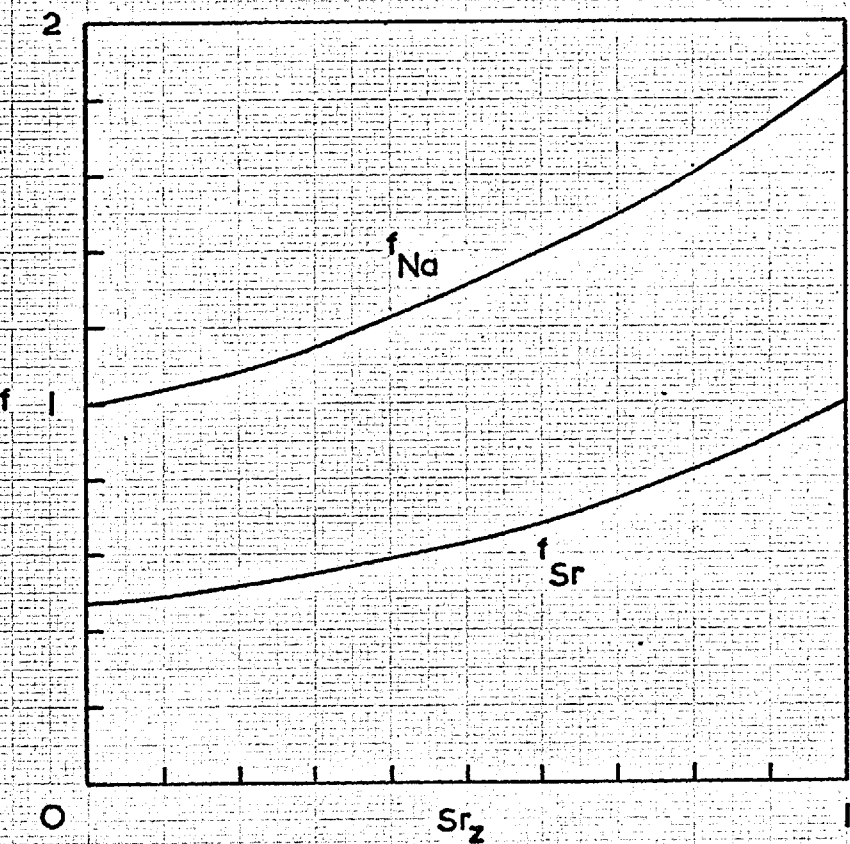

K_a was calculated to be 3.75, for the reaction

$$2Na^{+}_{(z)} + Sr^{++}_{(s)} \longrightarrow Sr^{++}_{(z)} + 2Na^{+}_{(s)}$$

The effect of the $(z_B - z_A)$ term in the Gaines and Thomas expression for K_a was again apparent from the magnitude of the K_a obtained.

The standard free energy of exchange was evaluated from the expression

$$\Delta G^0 = \frac{-RT \ln K_a}{z_A \, z_B}$$

$$= -390 \text{ cal/g equivalent.}$$

No X-ray investigation was undertaken for this exchange. Taylor and Roy found that the Ca, Sr, and Ba derivatives of Na-P_T all had body-centred tetragonal cells with $c > a$. (Group (3) of Taylor and Roy.) The Ca and Ba forms of Na-P_c prepared in this work had X-ray patterns agreeing with those quoted by Taylor and Roy for the Na-P_T derivatives, and it is likely that the Sr form of Na-P_c was also the same as the Sr form of Na-P_T.

Na-Ba Exchange

The sodium-barium exchange was highly selective for barium, as shown in Figure 7.17(a). As with the Na-Ba exchange in Nevada phillipsite, almost quantitative removal of barium from solution was observed for barium loadings up to 0.5 Unlike that in phillipsite, the exchange was reversible. Thus Na-P_c may prove to be very useful for removal of barium from aqueous solutions. Separation of barium and strontium does not however appear to be feasible using this zeolite.

The Kielland plot for the Na-Ba exchange is shown in Figure 7.17(b). The effect of moderate scatter in the experimental isotherm points for such a selective isotherm is apparent. No reliable equation of fit could be found for the Kielland plot. The "best" fit obtained was the linear equation

Figure 7·17: Na – Ba Exchange in P

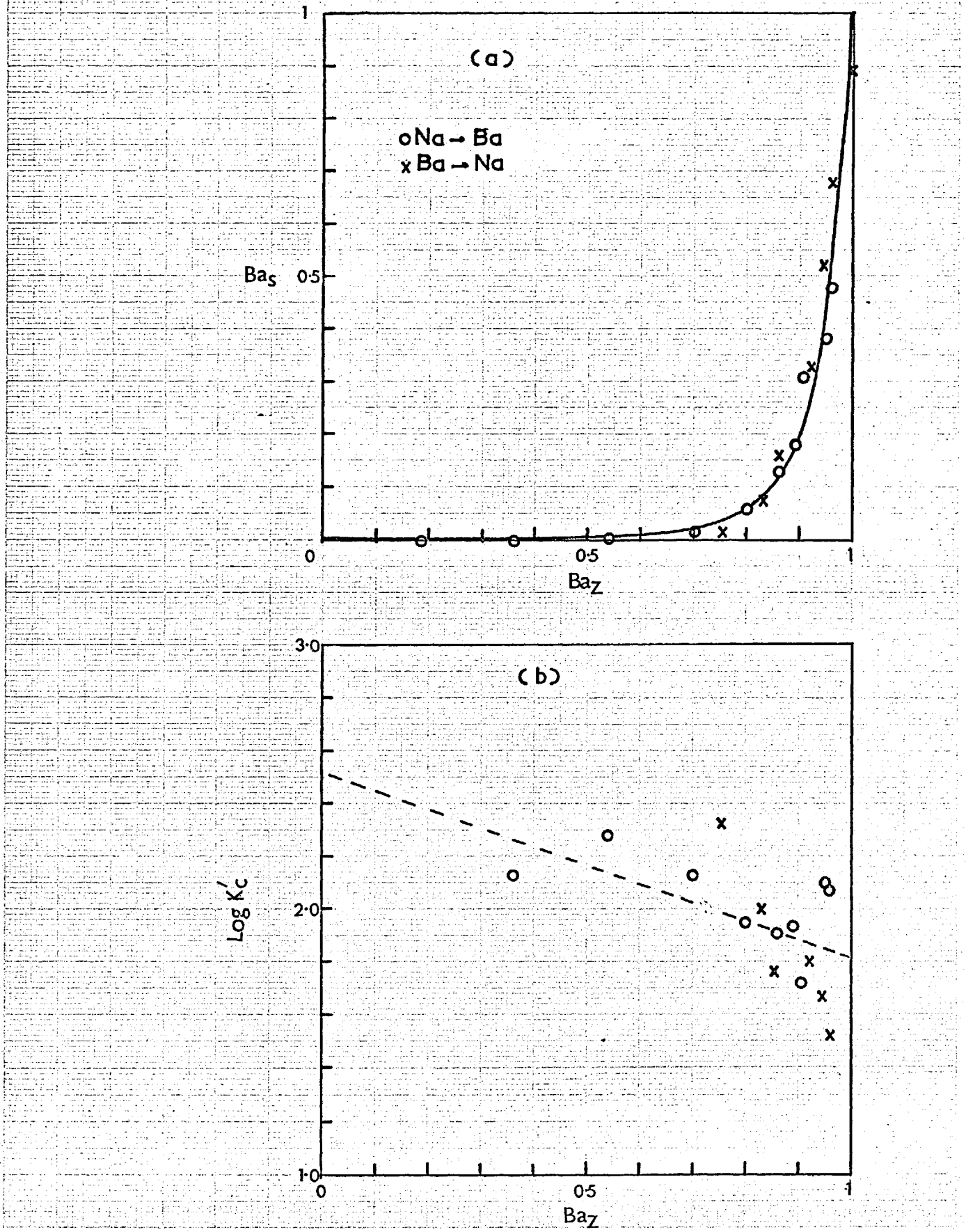

$$\log K_c' = 2.517 - 0.692\ Ba_z.$$

This equation obviously gives a poor representation of the Kielland plot, and no reliable estimate of K_a could be obtained. (The above equation gave a value of 55.)

X-ray photographs of samples with $Ba_z = 0.18$ and 0.36 showed the presence of two phases. One phase appeared to be tetragonal, but the other could not be positively identified as either Na-P_c or Na-P_T. Other samples showed a single tetragonal phase, progressively changing to the pattern of Ba-P with increasing Ba_z. Taylor and Roy reported a two-phase region for the exchange Na-P_T ⟶ Ba-P_T, and also for the Na⟶Ca exchange (not studied here). It is likely that the Na-Sr exchange also had a two-phase region. However the scatter of the experimental points was too great to enable any possible hysteresis loop associated with this region to be detected, and no X-ray evidence was available.

Summary

The exchange behaviour of Na-P_c has been shown to involve considerable alterations in the symmetry of the P structure. Most of the theories which have been developed for ion exchange in zeolites, assuming rigid frameworks and regular cation sites in the lattice, are clearly not applicable in this case. In the Na-K exchange, the Kielland theory nevertheless provided a possible qualitative interpretation of the exchange behaviour.

In the Na-K, Na-Rb, and Na-Cs exchanges, the cation of larger radius was prepared, but K_a values for these three exchanges were approximately the same. There was some evidence that the change from the cubic body-centred lattice of Na-P_c to the body-centred tetragonal lattices of K-P, Rb-P and Cs-P occurred, not via a two phase region, but at a specific crystal composition.

The Na-Sr and Na-Ba exchanges, which involved changes to Sr and Ba tetragonal cells with c > a, did appear to have two-phase regions,

although no definite evidence of these appeared in the exchange isotherms.

The high selectivity for barium observed in the Na-Ba exchange indicated that Na-P may be of practical importance for the removal of barium from neutral or alkaline aqueous solutions.

7.3. Zeolites K-F and K-F(Cl)

Analysis of K-F

The original preparation of K-F contained some muscovite impurity from the kaolinite used in the synthesis. Because of the very small particle size of the zeolite, sedimentation was not effective in removing this impurity. Analysis of the sample gave an apparent oxide formula of

$$0.99K_2O, Al_2O_3, 2.3SiO_2, 2.5H_2O.$$

Other samples of K-F, prepared towards the end of this work from kaolinite which did not contain any muscovite, had silica/alumina ratios of 2:1, as reported for K-F by Barrer and Baynham (14), Barrer, Cole and Sticher (44), Ovsepyan and Zhdanov (65), and Borer (46).

The original sample was, however, used for the ion-exchange experiments, as at that time the purer kaolinite was not available. The presence of the muscovite (about 7%) is not considered to have had any significant effect on the results obtained. The cation exchanged derivatives of the K-F contained less muscovite impurity than the parent zeolite, as some separation occurred during the preparation of these derivatives.

The monocationic forms were analysed for cation capacity and water content. The results were:-

Cation	Exchange Capacity meq/g	Water w/w %
Li	5.61	20.3
Na	5.00	19.0
K	5.06	11.5
Cs	3.42(calc)	7.0
Ca	5.14	18.2
Sr	4.54	14.0
Ba	4.00	12.5

K-F(Cl) Synthesis

Part of Sticher's work (44) on the synthesis of species K-F(Cl) was repeated. Reaction mixtures of kaolinite, potassium hydroxide and potassium chloride were crystallised at 80° C. Two base concentrations were used, 4M and 10M. In his work Sticher had used 4 Molal KOH. The higher base concentration was selected because it was more representative of the conditions used for the synthesis of K-F.

The results are shown in Figure 7.18 and 7.19. At a base concentration of 4 Molal, the results were in good agreement with those of Sticher. The maximum amount of salt intercalated was 5.6%.

For salt concentrations below 0.6 Molal, X-ray photographs showed that the product was not K-F(Cl) but a mixture of K-F(Cl) and zeolite K-I (44). This result was not unexpected, since the crystallisation fields of potassium zeolites synthesised from kaolinite and potassium hydroxide indicate that K-I is the most usual product at a base concentration of 4 Molal (44). Samples synthesised from mixtures containing more than 0.6 M KCl were all pure K-F(Cl), indicating that at these salt concentrations, the formation of K-I is hindered and K-F(Cl) favoured. A similar directing influence of a salt present during synthesis was reported by Barrer, Cole and Sticher in the koalinite + NaOH system. The presence of very small amounts of sodium nitrate was found to promote the synthesis of cancrinite, under conditions in which sodalite would normally be formed (44).

At a base concentration of 10 Molal (Figure 7.19) all products were K-F(Cl). The amount of salt imbibed increased very rapidly, reaching 2% by weight at the lowest salt concentration studied, 0.02 Molal. The maximum amount of salt incorporated was 6.6% at salt concentrations above 1.5 Molal. This increase in the maximum % KCl incorporated with increasing base concentration was previously observed by Sticher, and the present results agree well with those reported by him.

Figure 7-18

Synthesis of K–F(Cl)

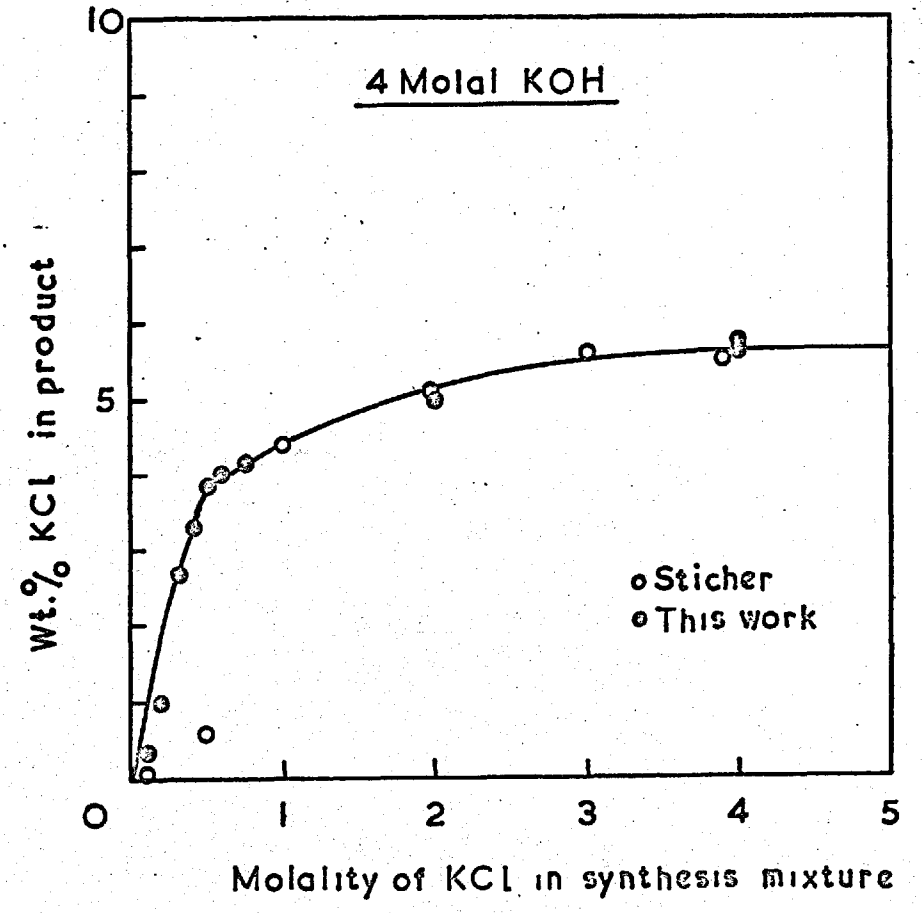

Figure 7·19

Synthesis of K-F(Cl)

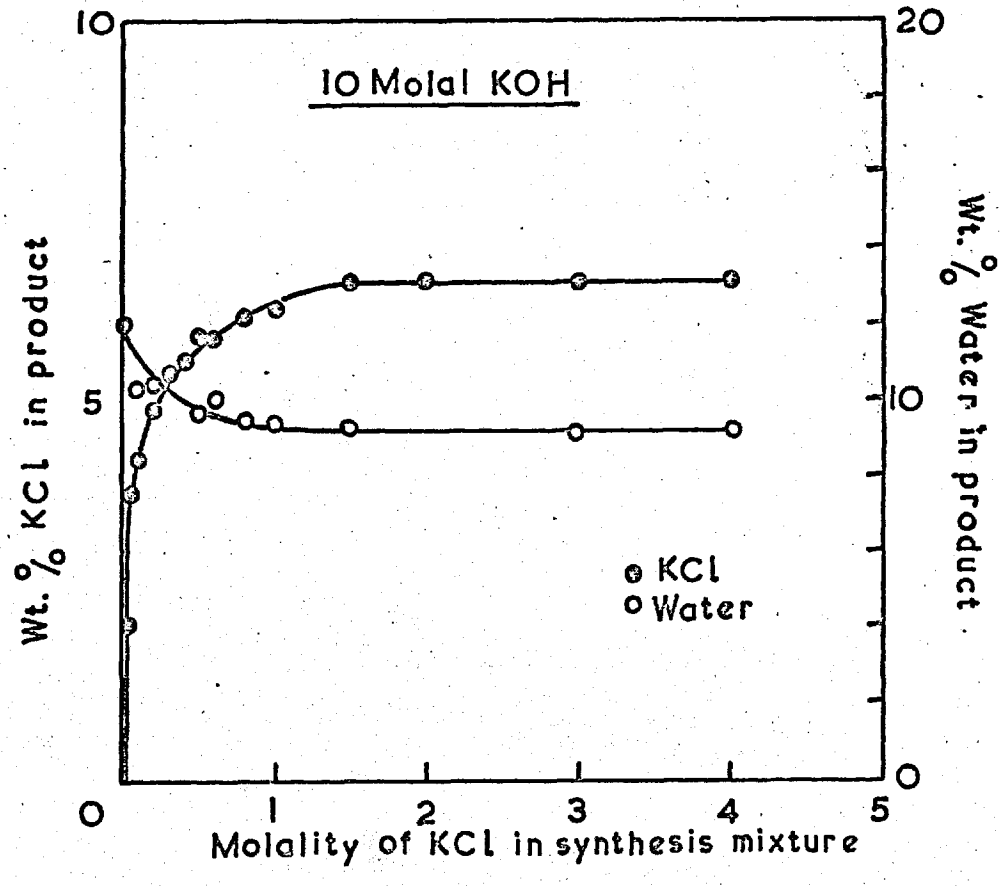

The water contents of the samples decreased with increasing salt loading, as shown in Figure 7.19. At maximum salt loading, the water content was 9.1%, compared with 12.0% for K-F synthesised under identical conditions, but in the absence of potassium chloride.

Analysis of a sample of K-F(Cl) containing 6.58% KCl gave the following oxide formula:-

$$0.97K_2O, Al_2O_3, 2.04SiO_2, 0.34KCl, 1.9H_2O.$$

In this analysis the K_2O content was calculated from the total potassium and potassium chloride contents. The apparent cation deficiency in the above formula is thought to be a result of experimental errors in this difference method of calculation.

Na-K isotherms were measured using three samples of K-F(Cl), with potassium chloride contents of 2.1%, 4.2% and 5.8%. The exchange capacities of these samples were 5.13, 5.31, and 5.70 meq/g, calculated from the total potassium contents.

K-Li and K-Ba exchanges were studied using a sample containing 6.56% KCl, and a total potassium content of 5.97 meq/g.

X-ray Powder Patterns

X-ray photographs of the various cationic forms of zeolite F showed several differences in the number, position, and intensity of diffraction lines. This confirms the observations of Barrer, Cole, and Sticher (44). A list of d-values and qualitative intensities for the sodium and potassium exchanged forms of the zeolite are given in Appendix 1. All attempts to index these patterns were unsuccessful.

As an example of the changes in line positions observed, the positions of the four strongest lines of K-F (at d-values of 6.9, 3.08, 2.97 and 2.82) are shown in Figure 7.20, together with the positions of what appear to be the corresponding lines in the patterns of the other cationic forms. Distances are shown in units of 4θ,

Figure 7·20

Relative positions of some strong X-ray lines of zeolite F derivatives.

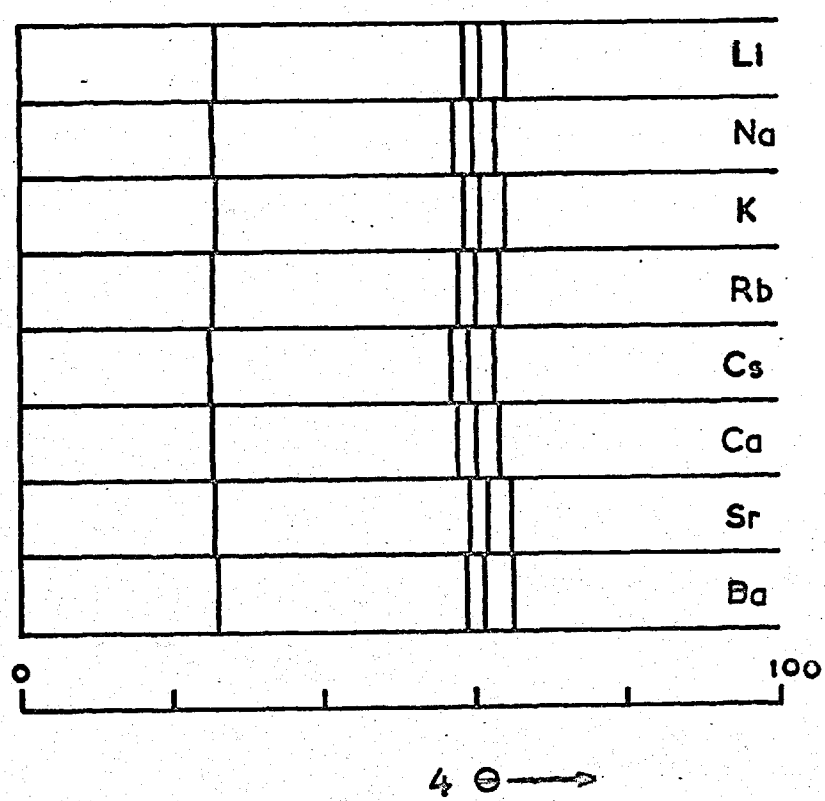

where θ is the Bragg diffraction angle. These units correspond to distances in millimetres on photographs taken with the Guinier-de Wolff camera.

If the relative positions of the lines are assumed to reflect the relative unit cell sizes, then the Li and K forms had unit cells of approximately equal size, but smaller than the unit cells of the Na and Cs forms. The Rb form and the Ca form had cells intermediate in size between those of, for example, Na-F and K-F. The cells of the Sr and Ba derivatives were apparently even more contracted than those of the K and Li forms. No correlation between cell size and cation radius was apparent.

The powder pattern of K-F(Cl) was very similar to that of the parent zeolite K-F.

Exchange Isotherms

All the exchange isotherms were measured at 25° C, using solutions of constant total concentration, 0.1 equivalent/litre. The common anion in solution was chloride, except in the Na-K and K-Li exchanges with K-F(Cl), for which nitrates were used.

Because of the nature of the isotherms obtained, the CALCIS program was of limited use in calculating the results.

Na-Cs Exchange in zeolite F

The sodium-caesium exchange isotherm is shown in Figure 7.21(a). Exchange was complete and reversible, but a marked selectivity reversal occurred at a caesium loading of 0.64. The Kielland plot for this isotherm is given in Figure 7.21(b).

The shape of the isotherm was similar to that reported by Barrer and Meier (24) for the sodium-silver exchange in zeolite A, in which exchange occurred on two types of site. Barrer and Meier had shown that the observed Na-Ag isotherm could be resolved into two "ideal"

Figure 7·21 : Na-Cs Exchange in F

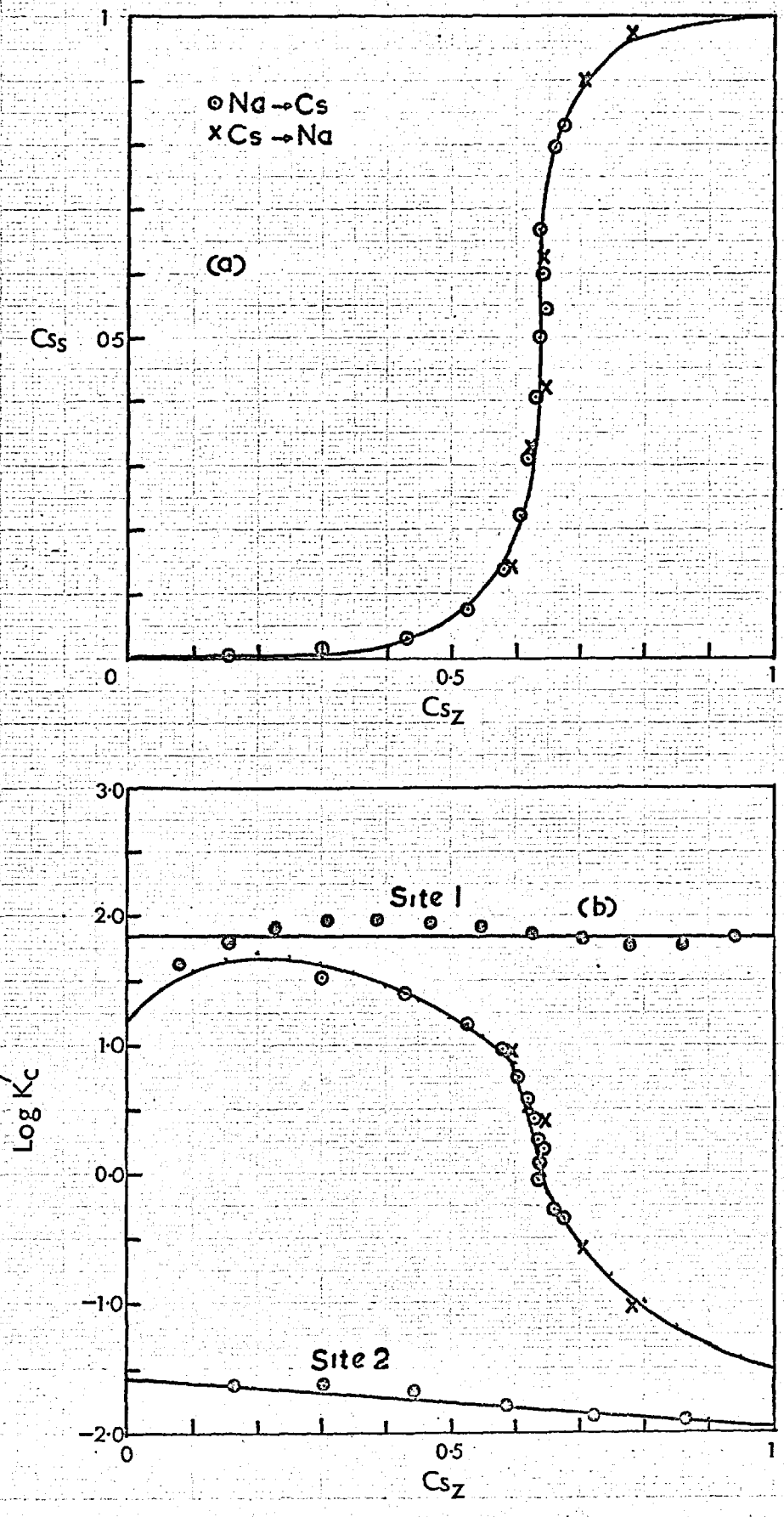

isotherms, for each of which log K'_c was constant.

In the present case, it was considered unlikely that, if two types of exchange site were present in zeolite F, they would each exhibit ideal behaviour. Other exchanges studied did not exhibit ideal behaviour, and it was therefore thought that the isotherm may possibly have been explained by two types of exchange site , each obeying Kielland's equations. The resolution of the isotherm into two Kielland constituents was attempted as follows:-

Consider a general uni-univalent exchange between the cations A and B in a zeolite in which there are N types of exchange site .

Let f_i = fraction of sites of type i ($\sum_i f_i = 1$)

A_i = equivalent fraction of ion A on sites of type i in the zeolite

$\overline{A}$ = overall equivalent fraction of ion A in the zeolite

$K'_{c(i)}$ = corrected selectivity coefficient for sitesof type i

$\overline{K'_c}$ = overall corrected selectivity coefficient.

Then

$$\overline{A} = \sum_{i=1}^{N} f_i A_i \qquad \text{Equation 7.1}$$

$$\overline{K'_c} = \frac{\overline{A}}{1-\overline{A}} \cdot \frac{B_s}{A_s} \cdot \Gamma \quad (\Gamma = \text{ratio of solution activity coefficients})$$

$$= \frac{\overline{A}}{1-\overline{A}} \cdot S \quad \text{where } S = \frac{B_s}{A_s} \cdot \Gamma \qquad \text{Equation 7.2}$$

$$K'_{c(i)} = \frac{A_i}{1-A_i} \cdot S \qquad \text{Equation 7.3}$$

From equation 7.1,

$$A_i = \left(\overline{A} - \sum_{j \neq i}^{N} f_j A_j \right) / f_i$$

Substitution in equation 7.3 gives

$$K'_{c(i)} = \frac{\overline{A} - \sum_{j \neq i}^{N} f_j A_j}{f_i - \overline{A} + \sum_{j \neq i}^{N} f_j A_j} \cdot S$$

From equation 7.2,

$$S = \frac{1-\overline{A}}{\overline{A}} \cdot \overline{K}'_c$$

Therefore

$$K'_{c(i)} = \frac{\overline{A} - \sum_{j \neq i}^{N} f_j A_j}{f_i - \overline{A} + \sum_{j \neq i} f_j A_j} \cdot \frac{1-\overline{A}}{\overline{A}} \cdot \overline{K}'_c \qquad \text{Equation 7.4}$$

In general, $\overline{A}$ and $\overline{K}'_c$ are known, or can be calculated from the experimental data. However f_i and A_i are generally unknown.

For two types of site equations 7.1 and 7.4 become

$$\overline{A} = f_1 A_1 + f_2 A_2$$

$$K'_{c_1} = \frac{(\overline{A} - f_2 A_2)}{(f_1 - \overline{A} + f_2 A_2)} \cdot \frac{(1-\overline{A})}{\overline{A}} \cdot \overline{K}'_c$$

$$K'_{c_2} = \frac{(\overline{A} - f_1 A_1)}{(f_2 - \overline{A} + f_1 A_1)} \cdot \frac{(1-\overline{A})}{\overline{A}} \cdot \overline{K}'_c$$

Although f_1, f_2, A_1 and A_2 are not known, for the Na-Cs isotherm in zeolite F these quantities may be estimated if

(i) it is assumed that the selectivity reversal occurs at the point where $Cs_Z = f_1$,

(ii) it is assumed that the two sites are exchanged consecutively, that is, negligible exchange occurs on sites of type 2 until all sites of type 1 are filled.

With these assumptions we have:-

for sites (1)

$$\overline{A} = f_1 A_1 \qquad (A_2 = 0) \qquad \text{Equation 7.5}$$

$$\therefore K'_{c(1)} = \frac{(1-\overline{A})}{(f_1 - \overline{A})} \cdot \overline{K}'_c \qquad \text{Equation 7.6}$$

for sites (2)

$$\overline{A} = f_1 + f_2 A_2 \qquad (A_1 = 1) \qquad \text{Equation 7.7}$$

$$K'_{c(2)} = \frac{(\overline{A} - f_1)}{\overline{A}} \cdot \overline{K}'_c \qquad \text{Equation 7.8}$$

On the first assumption above, for the Na-Cs exchange,

$$f_1 = 0.64$$

$$f_2 = 0.36$$

Therefore A_1, A_2, $K'_{c(1)}$, $K'_{c(2)}$ can be calculated from equations 7.5 to 7.8.

These calculations were performed, using points taken off the smoothed Na-Cs isotherm. The Kielland plots obtained for the two types of sites are shown in Figure 7.21(b). Each Kielland plot was approximately linear, and individual site Kielland constants and K_a values were calculated, giving

for sites (1),

$$K_{a(1)} = 69.2$$

$$C_{(1)} \approx 0.$$

and for sites (2),

$$K_{a(2)} = 0.017$$

$$C_{(2)} \approx -0.19.$$

The two individual site isotherms calculated from these results,

and the resultant calculated isotherm, are shown in Figure 7.22. The resultant isotherm was a very good approximation to the observed isotherm.

The overall thermodynamic equilibrium constant for the exchange was calculated in two ways:

(i) by graphical integration of the observed Kielland plot (Figure 7.21(b)) between the limits $Cs_z = 0$ and $Cs_z = 1$. This gave

$$\overline{K}_a = 3.42$$

(ii) from the individual K_a values, calculated for each type of site, according to the equation:-

$$\log \overline{K}_a = f_1 \log K_{a(1)} + f_2 \log K_{a(2)}.$$

This gave

$$\overline{K}_a = 3.47.$$

It is considered that the agreement between these two values justifies the assumptions on which the calculated values were based.

From the K_a value obtained from the experimental data, the standard free energy ΔG^0 for the overall exchange was calculated to be

$$\Delta G^0 = -730 \text{ cal/g equivalent.}$$

Na-K Exchange

The experimental isotherm is shown in Figure 7.23 (a). There was a well-defined hysteresis loop covering the region $0.6 < K_z < 0.95$. The K⟶Na isotherm agrees well with that reported by Sticher (44).

X-ray photographs of samples corresponding to the hysteresis loop region of the isotherm showed that two phases were present. Densitometer traces of the four strongest lines in these photographs are shown in Figure 7.24. The presence of the two phases, one characteristic of

Figure 7·22

Calculated Na–Cs Isotherms for F

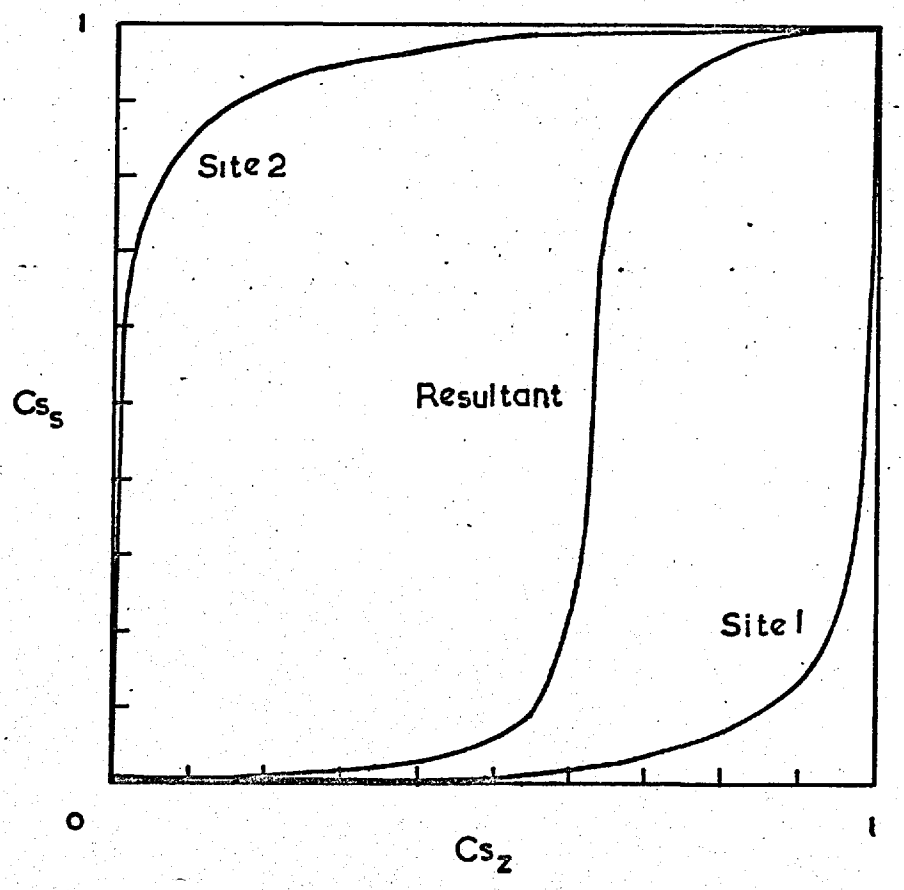

Figure 7·23: Na–K Exchange in F

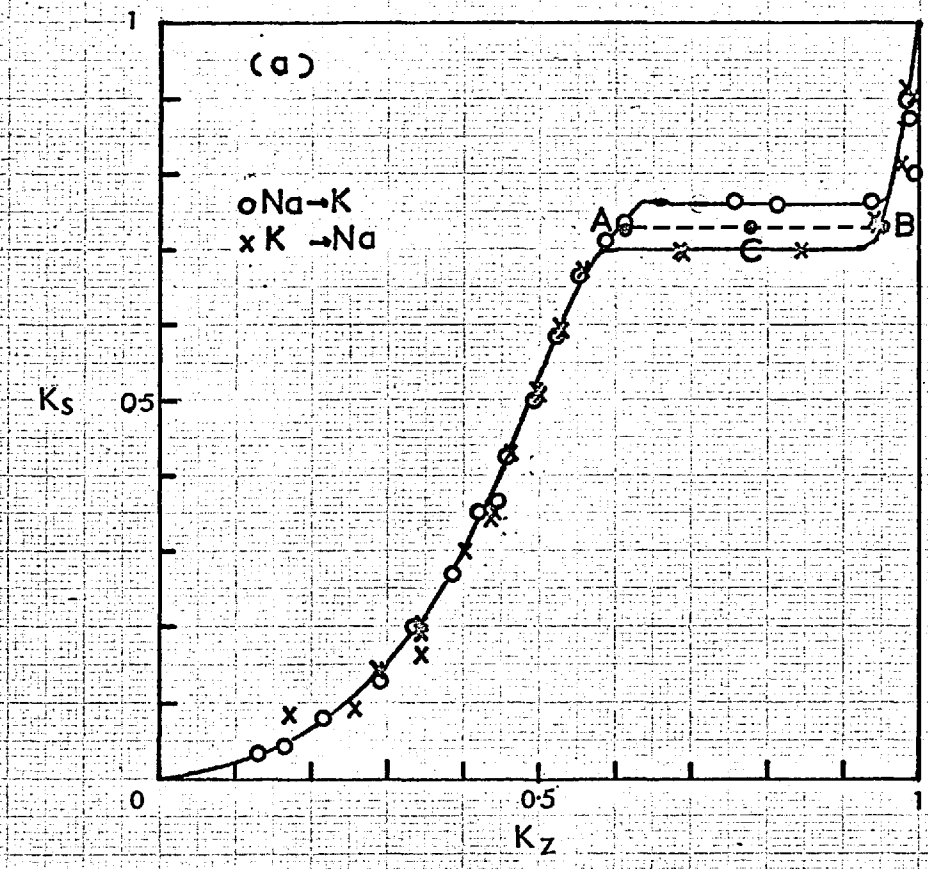

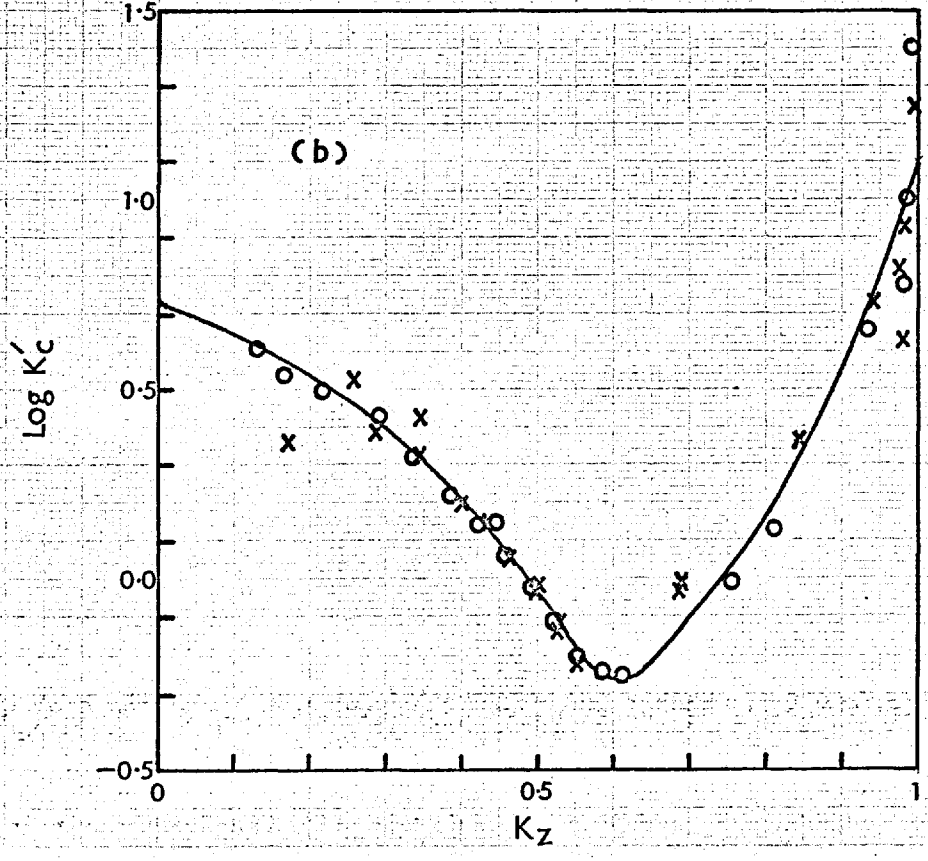

Figure 7·24

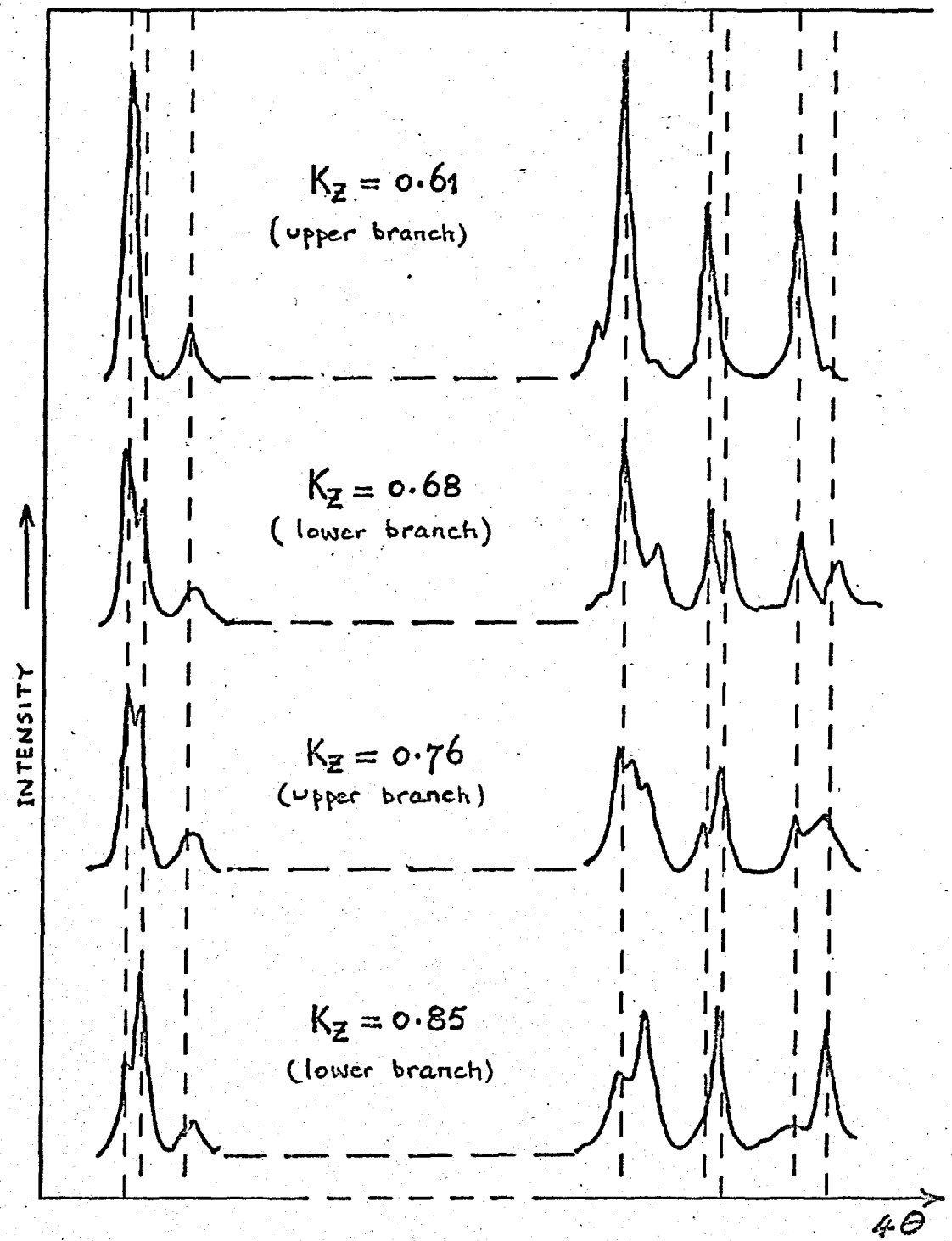

Smoothed Densitometer Traces of X-Ray Powder Photographs of (Na,K)F samples in the hysteresis loop region of the sodium-potassium isotherm.

Na-F, the other of K-F, can be clearly seen. The proportions of the two phases varied with potassium loading.

The Kielland plot for the exchange is shown in Figure 7.23(b). ~~There was a slight rise in log K_c' at low K_z values, then~~ log K_c' fell to a minimum at $K_z \approx 0.6$. The log K_c' values for points on the two branches of the hysteresis loop increased rapidly with increasing K_z. The slope of the curve in this hysteresis region was positive, and greater than the critical slope on Kielland's theory.

Although the theories of reversible thermodynamics are not strictly applicable to such an isotherm, an attempt was made to explain the exchange behaviour in terms of two Kielland types of exchange site. The following assumptions were made.

(i) Two types of site were present, in the same ratio as that found for the Na-Cs exchange (i.e., $f_1 = 0.64$, $f_2 = 0.36$).

(ii) The hysteresis loop was assumed to be symmetrical about the line $K_s = 0.73$. The centre point of the loop (point C in Figure 7.23(a)) then had the co-ordinates $K_z = 0.773$, $K_s = 0.730$.

(iii) The extra free energy terms associated with the nucleation of the second phase were assumed to be of the same magnitude in the forward and reverse directions. The observed horizontal branches of the hysteresis loop were thus assumed to be equidistant, in K_s, from the theoretical path ACB that the isotherm would have followed if these free energy terms were zero.

(iv) Both types of site were assumed to exhibit Kielland behaviour. The Kielland constant for the first site was assumed to be less than the critical value +0.87.

Consider the points A, B, and C, each having the same K_s co-ordinate. By assumption (IV), the isotherm for site 1, A_s = function (A_1, K_{a_1}, C_1), is single-valued for $0 < A_1 < 1$. (A here refers to potassium). Therefore points A, B, and C have the same

A_1 contribution to the overall equivalent ion fraction $\overline{A}$ in the zeolite.

Because the hysteresis loop was assumed to be symmetrical, the centre point C must, by Kielland's theory, correspond to a cation fraction for site 2 of 0.5.

As for the Na-Cs exchange treatment,

$$\overline{A} = f_1 A_1 + f_2 A_2 .$$

At point C therefore, $A_1 = 0.5$, and $\overline{A} = 0.773$, which gives

$$0.773 = f_1 A_1 + 0.36 \times 0.5$$

$$\therefore f_1 A = 0.593$$

$$A_1 = 0.927 \quad (f_1 = 0.64).$$

This value of A_1 also applies at points A and B. Therefore at point A, where $\overline{A} = 0.605$,

$$0.605 = 0.593 + 0.36\ A_{2\,(A)}$$

$$\therefore A_{2\,(A)} = 0.033.$$

At point B, $\overline{A} = 0.940$,

$$0.940 = 0.593 + 0.36\ A_{2\,(B)}$$

$$A_{2\,(B)} = 0.964.$$

Because site 2 is assumed to follow a Kielland isotherm,

$$\log K_{a(2)} = \log K'_{c(2)} + C_{(2)}(1-2\ A_{(2)}) \qquad \text{Equation 7.9}$$

This equation must be satisfied at each of the points A, B, and C.

At point C, $A_{(2)} = 0.5$

$$K_{a(2)} = \frac{1-A_s}{A_s} \cdot \Gamma \qquad (A_s = 0.730)$$

$$= 0.374$$

$$\log K_{a(2)} = -0.427$$

At point A therefore, substituting in equation 7.9,

$$-0.427 = \log \frac{A_2(A)}{(1-A_2(A))} \cdot \frac{(1-A_s)}{A_s} \cdot \Gamma + C_{(2)}(1-2A_2(A))$$

whence

$$C_{(2)} = +1.57.$$

As expected, the Kielland constant for site 2 was positive, and greater than the critical value +0.87 at which phase separation would be expected to occur.

Application of equation 7.9 to point B gave

$$C_{(2)} = +1.54.$$

Taking the mean of these values, the site 2 isotherm is therefore defined by the constants $K_{a(2)}$ and $C_{(2)}$:-

$$K_{a(2)} = 0.374$$

$$C_{(2)} = +1.56.$$

The Kielland plot and isotherm for site 1 were calculated from the smoothed experimental data and the calculated site 2 results, by difference. The results for the site 1 Kielland plot are shown in Figure 7.25(b) together with the calculated Kielland plot for site 2. From the Kielland plot, $K_{a(1)}$ and $C_{(1)}$ were calculated to be

$$K_{a(1)} = 4.57$$

$$C_{(1)} = -0.33.$$

The isotherms for sites 1 and 2 are shown in Figure 7.25(a), and the resultant isotherm for the overall exchange is given in Figure 7.26. This isotherm did not, of course, give a hysteresis loop, but had a maximum and minimum in the region of the observed hysteresis. Such behaviour would not be valid, and the expected isotherm path in this region would be the horizontal line shown. The calculated isotherm thus gave a reasonable representation of the observed Na-K exchange behaviours of zeolite F, despite the various assumptions made.

Figure 7·25: Calculated Na–K isotherms for F

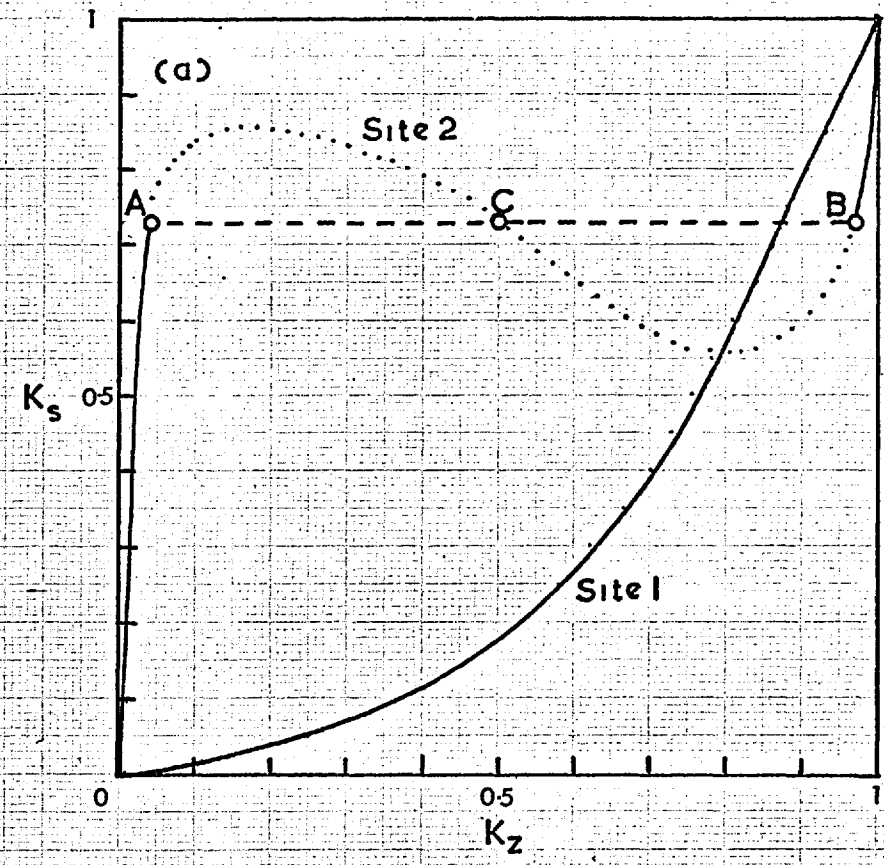

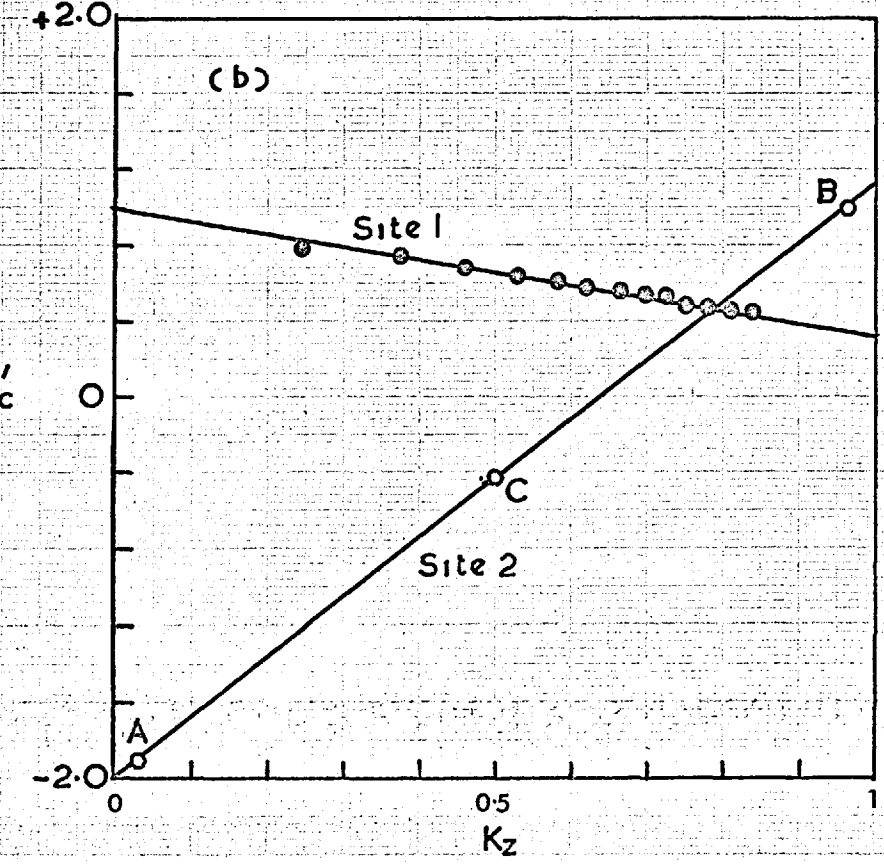

Figure 7·26: Calculated Na–K Isotherm for zeolite K–F

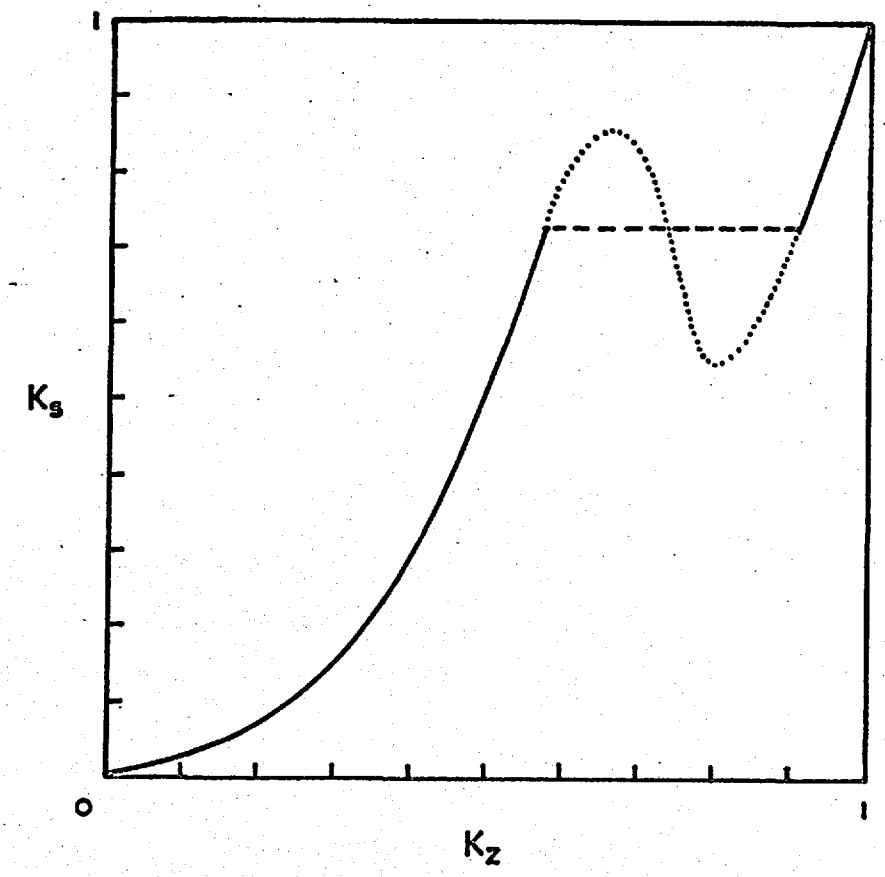

An estimate of the overall K_a value for the Na-K exchange was obtained by graphical integration of the observed Kielland plot. In doing this, mean values of log K_c' were used in the hysteresis-loop region. The result was

$$\overline{K}_a = 1.96$$

This value agreed well with that calculated from the individual site isotherms, according to the equation

$$\log \overline{K}_a = f_1 \log K_{a(1)} + f_2 \log K_{a(2)}$$

$$= 0.64 \log 4.57 + 0.36 \log 0.374$$

whence

$$\overline{K}_a = 1.86.$$

Na-K Exchange in zeolite K-F(Cl)

Potassium to sodium isotherms were determined for three samples of K-F(Cl), having potassium chloride contents of 5.8%, 4.2% and 2.1%. Alkali metal nitrate solutions were used in these exchanges.

The results are shown in Figure 7.27. The reverse isotherms, Na ⟶ K, do not exist for K-F(Cl), since the potassium chloride was found to be lost during the K ⟶ Na exchange, and the species Na-F(Cl) did not contain any chloride. The loss of chloride is shown for the K ⟶ Na exchange in the sample containing 5.6% KCl in Figure 7.28, where the fraction of chloride remaining in the zeolite, Cl_z, is plotted against the potassium loading.

The shape of the K ⟶ Na isotherm for the sample containing 5.6% KCl is different from that found for K-F. Potassium selectivity was much greater in the salt-bearing zeolite, and there was no apparent behaviour which indicated the presence of two exchange sites. This may indicate that the presence of the salt tended to lessen the energetic heterogeneity of the sites assumed to be present in K-F,

Figure 7·27: K–Na Exchange in K–F(Cl)

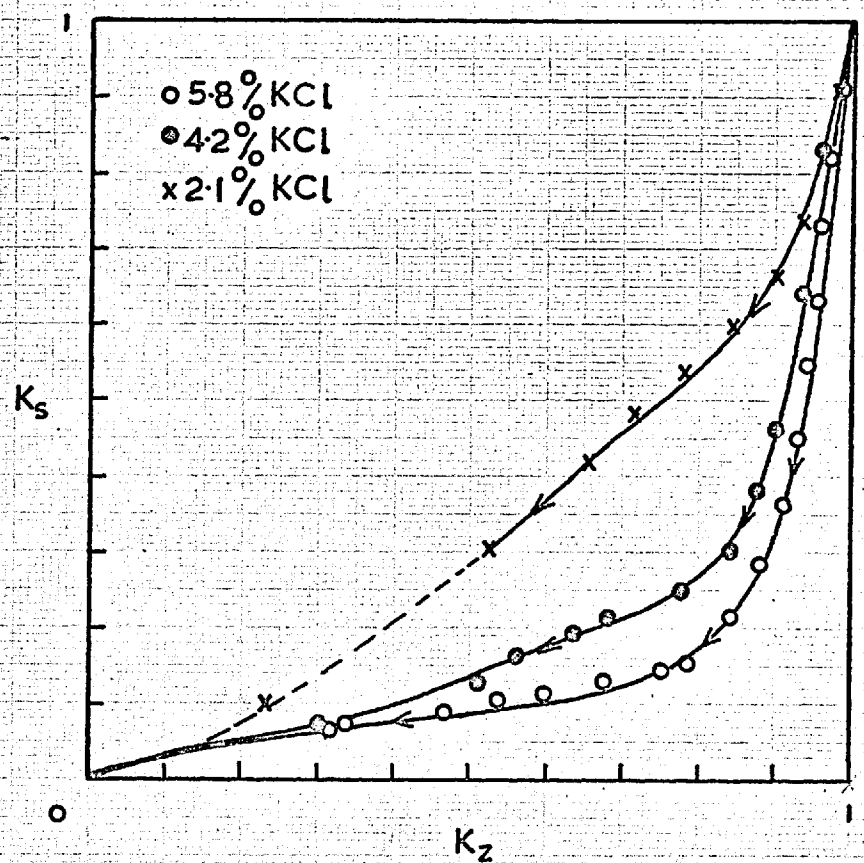

Figure 7·28: Chloride ion loss during K–Na Exchange in K–F(Cl)

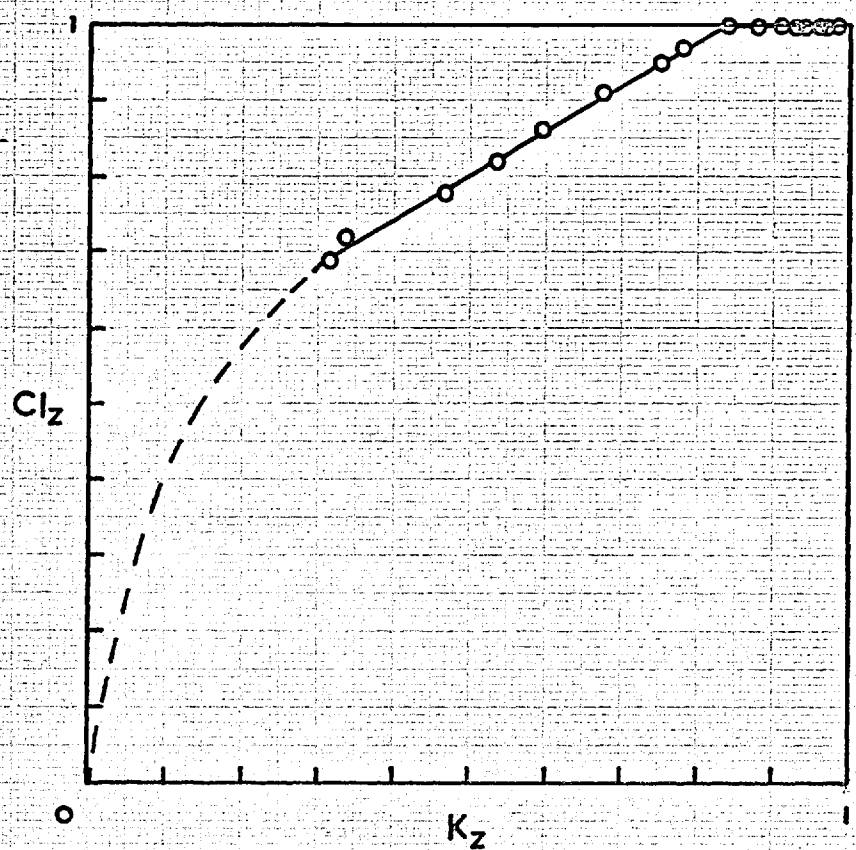

and that the gradual release of the occluded salt as exchange progressed allowed the K-F to Na-F structural changes to occur without an intermediate two-phase region. The actual explanation of the difference in exchange behaviour could perhaps be found from a detailed crystallographic study of the cation and salt positions in the K-F structure. At the present time however, the framework structure of K-F is not known.

Na-Li Exchange in zeolite F

The Na-Li exchange isotherm for zeolite F is shown in Figure 7.29(a). The Kielland plot is shown in Figure 7.29(b).

As was observed in the Na-K exchange, there was a well-defined hysteresis loop in the isotherm. X-ray photographs of samples corresponding to the hysteresis region again revealed in the presence of two phases along both horizontal portions of the hysteresis loop.

The isotherm was resolved into two Kielland isotherms using the procedures described for the Na-K exchange. The same assumptions were made. The site 1 isotherm was again calculated by difference.

The results of this treatment were as follows:-

Site 1

$$K_{a(1)} = 1.114$$

$$C_{(1)} = 0$$

Site 2

$$K_{a(2)} = 0.891$$

$$C_{(2)} = +1.268$$

The Kielland constant for site 2 was positive and greater than the critical value at which phase separation would be expected to occur.

The calculated isotherms for the two sites, and the resultant isotherm, are shown in Figure 7.30. The calculated resultant isotherm

Figure 7·29: Na–Li Exchange in F

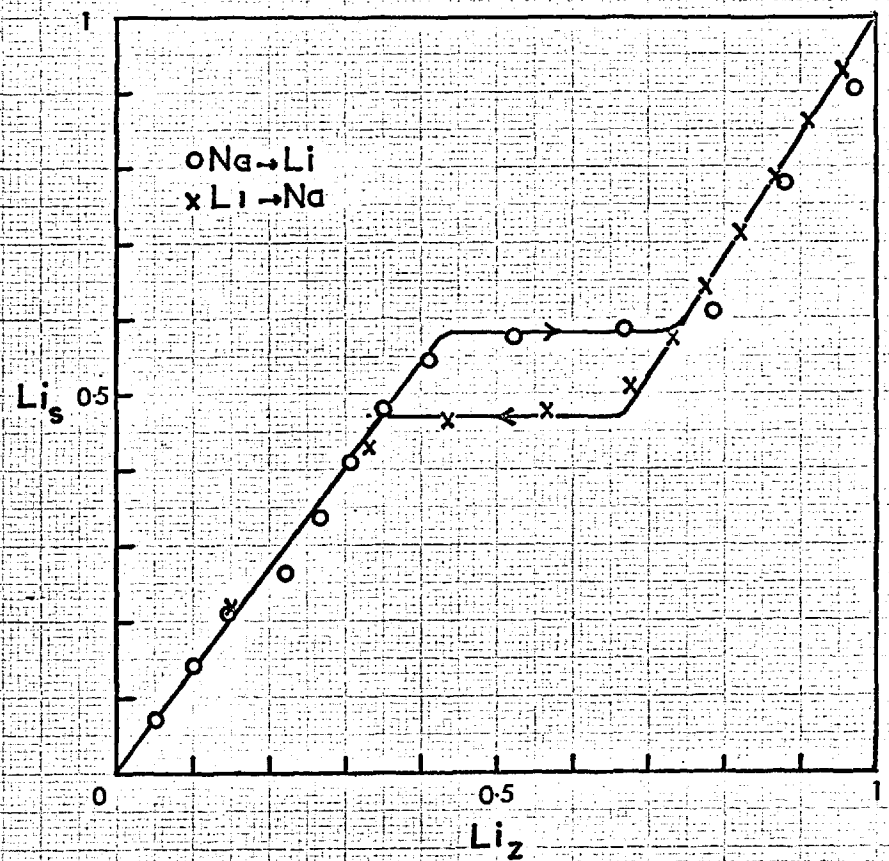

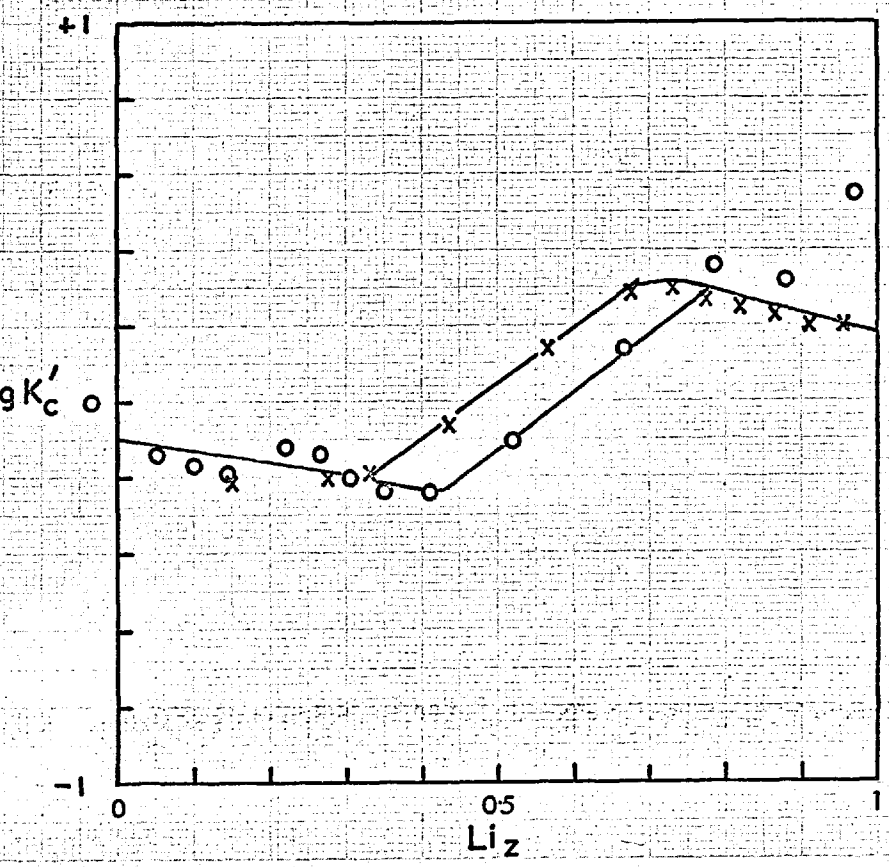

Figure 7·30

Calculated Na–Li Isotherms for zeolite F

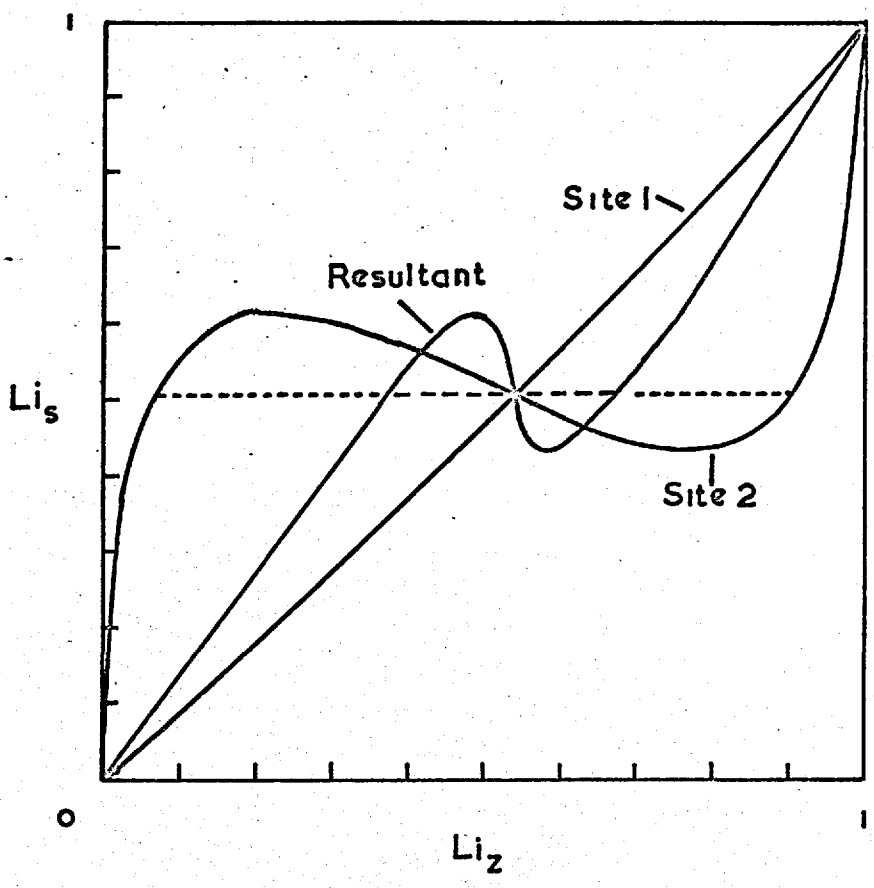

gave a very good approximation to the observed isotherm.

The overall thermodynamic equilibrium constant was estimated by graphical integration of the observed Kielland plot, giving the result

$$\overline{K}_a = 1.01$$

The $\overline{K}_a$ value calculated from the individual K_a values of the two Kielland site isotherms was 1.03. The agreement between these two values is good considering the assumptions made in the isotherm resolution procedure.

K-Li Exchange in zeolite F

This exchange was found to be completely reversible. The isotherm and Kielland plot are shown in Figure 7.31. There was a selectivity reversal at $Li_z \approx 0.3$, which tends to support the presence of two types of exchange site. The sites considered as type 1 in the Na-K and Na-Li exchanges presumably correspond to the potassium-selective region of the K-Li isotherm. The selectivity reversal in the K-Li isotherm was not sufficiently sharp to enable the method of resolution used for the Na-Cs isotherm (consecutive occupancy of sites) to be applied here.

This isotherm therefore was not resolved into two constituent Kielland isotherms. The thermodynamic equilibrium constant was calculated by graphical integration of the Kielland plot, giving

$$K_a = 0.51.$$

The standard free energy of exchange ΔG^0 was calculated to be +400 cal/g equiv. for the K⟶Li exchange. The $\overline{K}_a$ values found for the Na ⟶ K and Na ⟶ Li exchanges were 1.01 and 1.96. These results are not strictly valid, since both these isotherms had hysteresis loops, and were not therefore reversible in the thermodynamic sense. However, neglecting this objection, a thermodynamic equilibrium constant may be predicted for the K⟶Li exchange from the values of K_a found for

Figure 7·31: K–Li Exchange in F

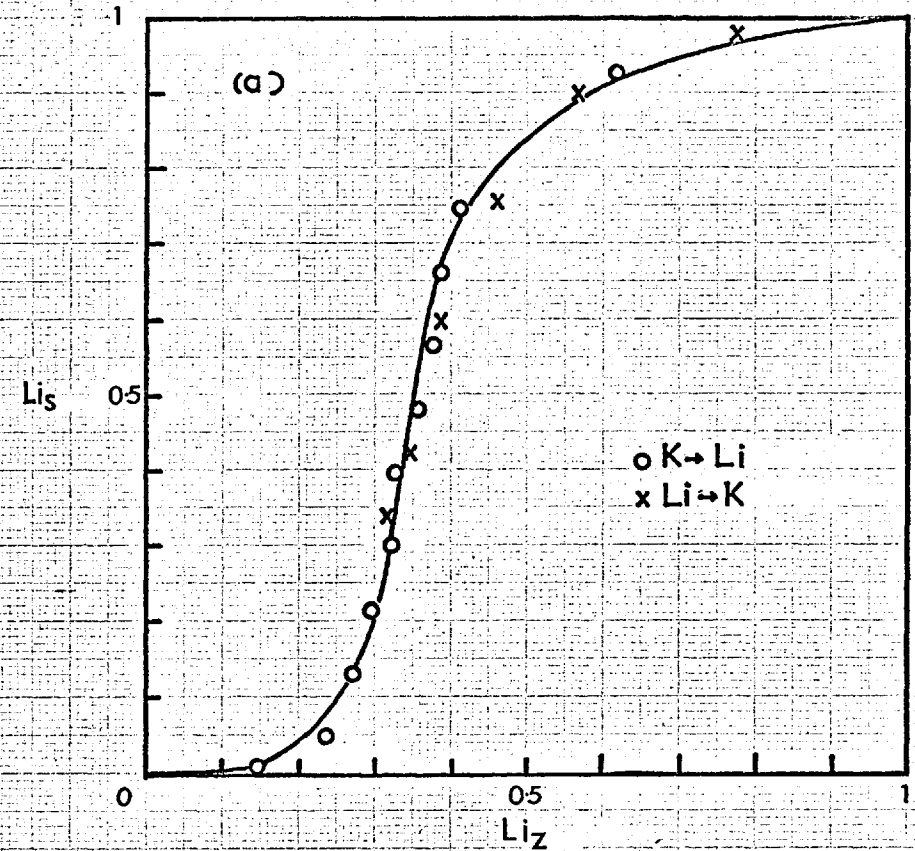

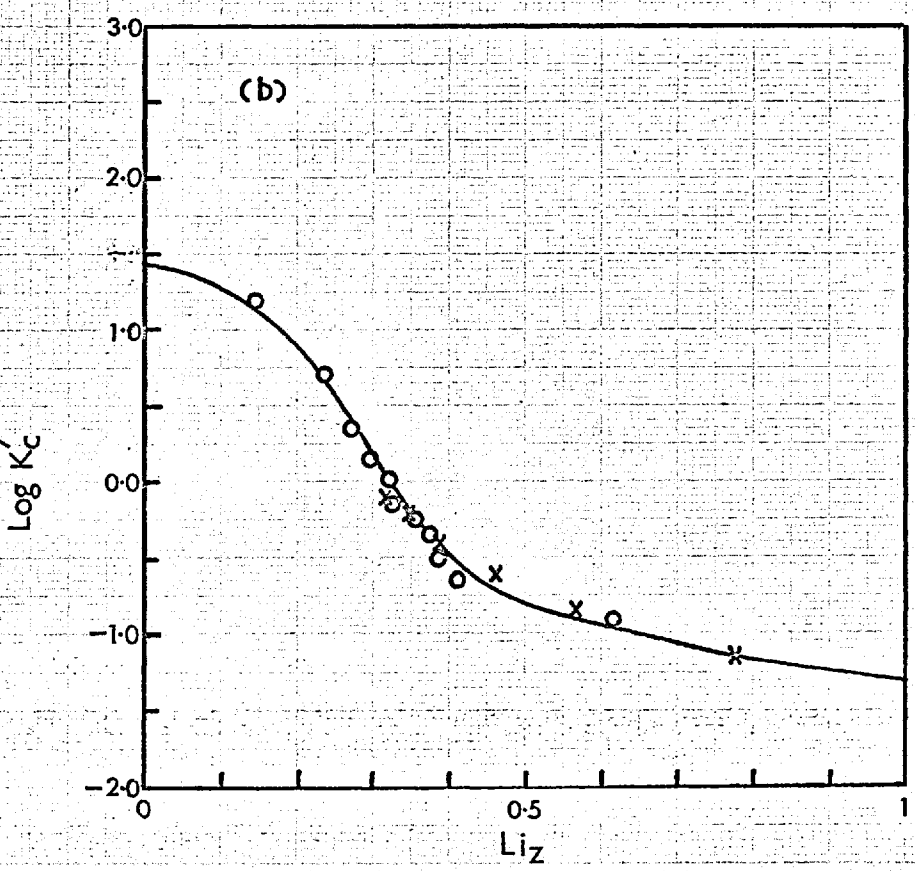

the Na⟶K and Na⟶Li exchanges.

Thus

$$\log K_{a\ K\rightarrow Li} = \log K_{a\ Na\rightarrow Li} - \log K_{a\ Na\rightarrow K}$$

$$= \log 1.01 - \log 1.96$$

$$= -0.288 .$$

$$\therefore K_{a\ K\rightarrow Li} = 0.515$$

This value is in good agreement with that found experimentally, 0.51.

K-Li Exchange in K-F(Cl)

This exchange was investigated using a sample of K-F(Cl) containing 6.56% potassium chloride. The isotherm, which was measured using solutions of potassium and lithium nitrates of constant total concentration 0.1 equivalent/litre, is shown in Figure 7.32.

The initial selectivity for lithium observed in the K-Li exchange of zeolite K-F did not appear. As in the case of the K⟶Na exchanges in K-F and K-F(Cl) the presence of the occluded salt seems to have removed the heterogeneity of the two types of exchange site believed to be present in K-F.

The fully-exchanged Li form of K-F(Cl) was analysed and found to contain no potassium chloride. The Li⟶K isotherm for K-F(Cl) does not therefore exist.

K-Cs Exchange in zeolite K-F

The K-Cs exchange isotherm is shown in Figure 7.33. A hysteresis loop existed over the entire isotherm. X-ray photographs of samples representing the K⟶Cs branch of the hysteresis loop showed that the change from the K-F structure to the Cs-F structure proceeded via an intermediate unit cell, similar to that of Rb-F in size.

Figure 7·32 : K–Li Exchange in K–FCCD

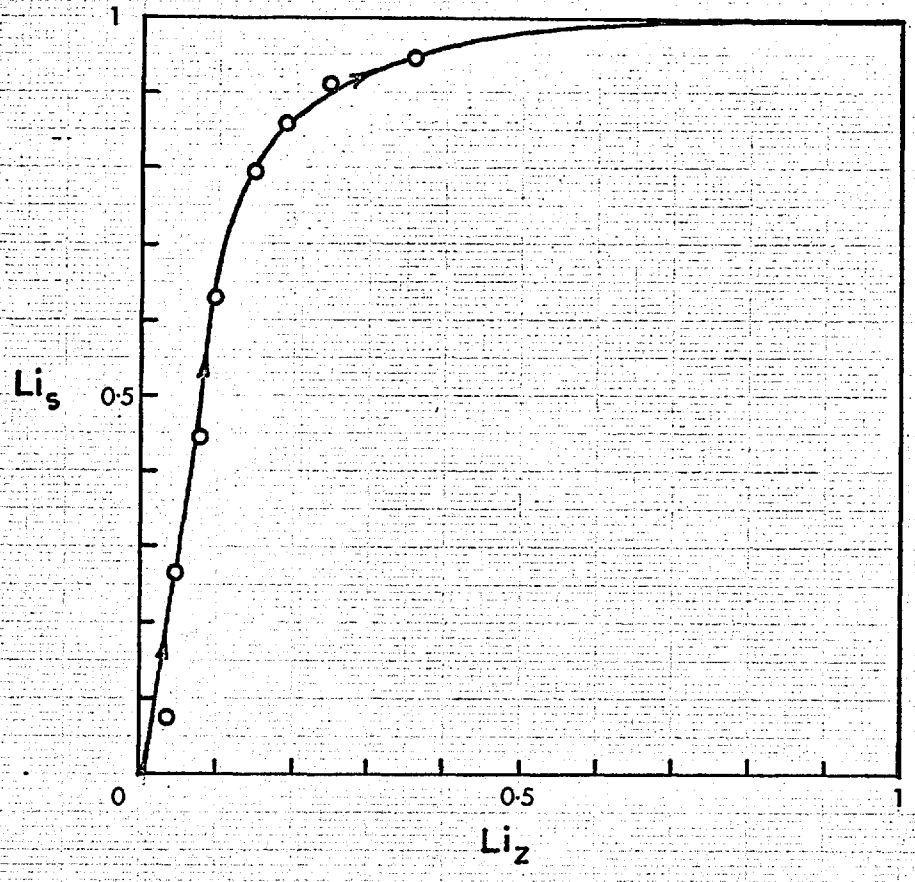

Figure 7·33: K–Cs Exchange in K–F

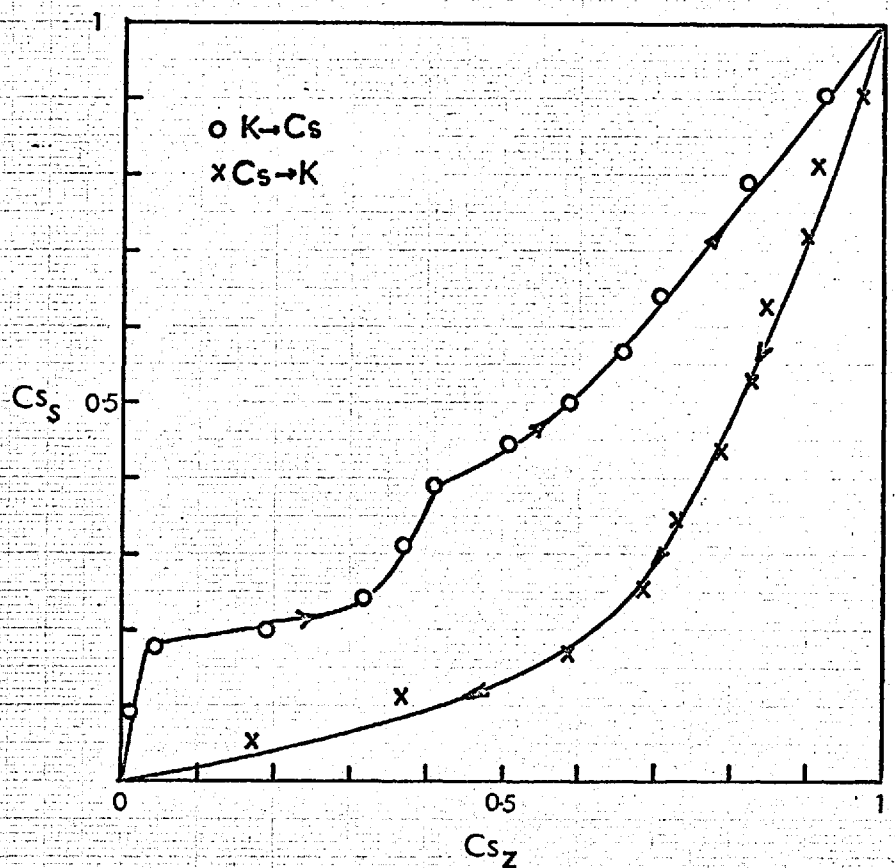

This change in structure with changing caesium loading occurred approximately as shown below:-

Cs_z	Phases Present
0.01	K-F
0.05	K-F + some intermediate phase
0.19	K-F + intermediate phase
0.32, 0.37, 0.41	Intermediate phase
0.50, 0.59, 0.66	Intermediate phase
0.71, 0.82, 0.92	Cs-F

Samples from the Cs ⟶ K branch of the exchange isotherm changed from the Cs-F structure to the K-F structure without going through an intermediate phase. Samples with Cs_z less than 0.59 appeared to consist of the two phases Cs-F and K-F.

No attempt was made to analyse this complex isotherm in terms of two types of exchange site.

Uni-divalent exchanges in zeolite F

The Na-Ca, Na-Sr and Na-Ba exchange isotherms are shown in Figure 7.34, 7.35 and 7.36 respectively.

Marked hysteresis was observed in the Na-Ca exchange. In the Na-Sr exchange only 10% of the strontium present in Sr-F could be replaced by sodium using 0.1N solutions. Both these exchanges showed a high selectivity for the divalent ion up to loadings of about 0.5, but a reversal of selectivity occurred with higher loadings of the divalent ion.

Figure 7·34: Na–Ca Exchange in F

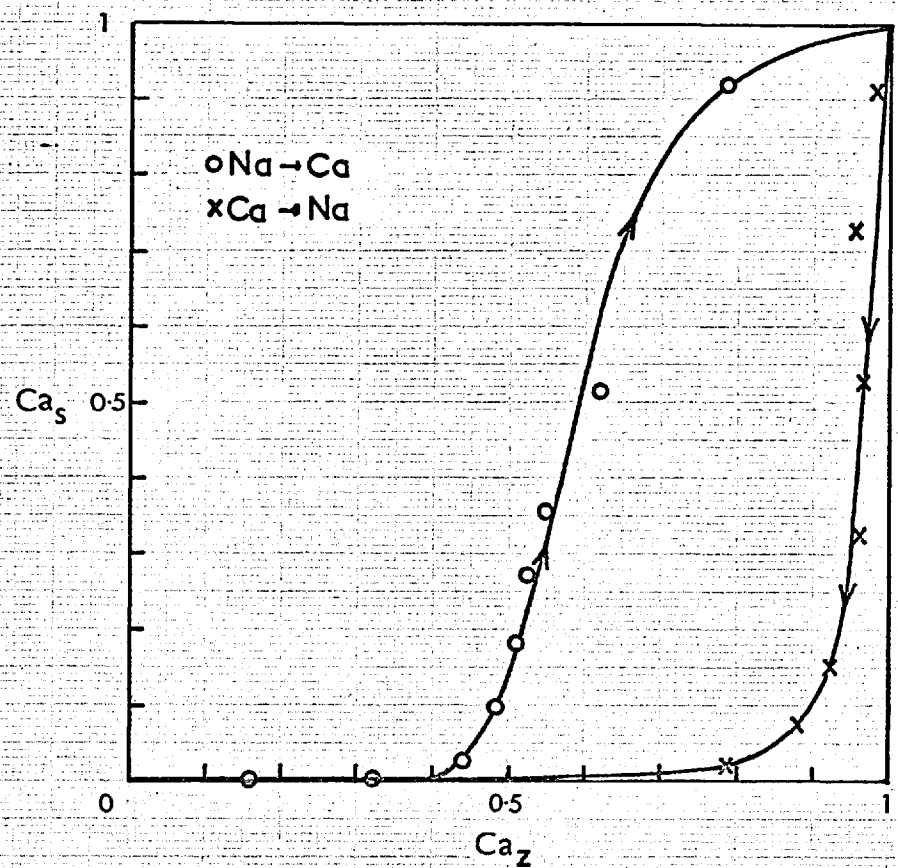

Figure 7·35: Na–Sr Exchange in F

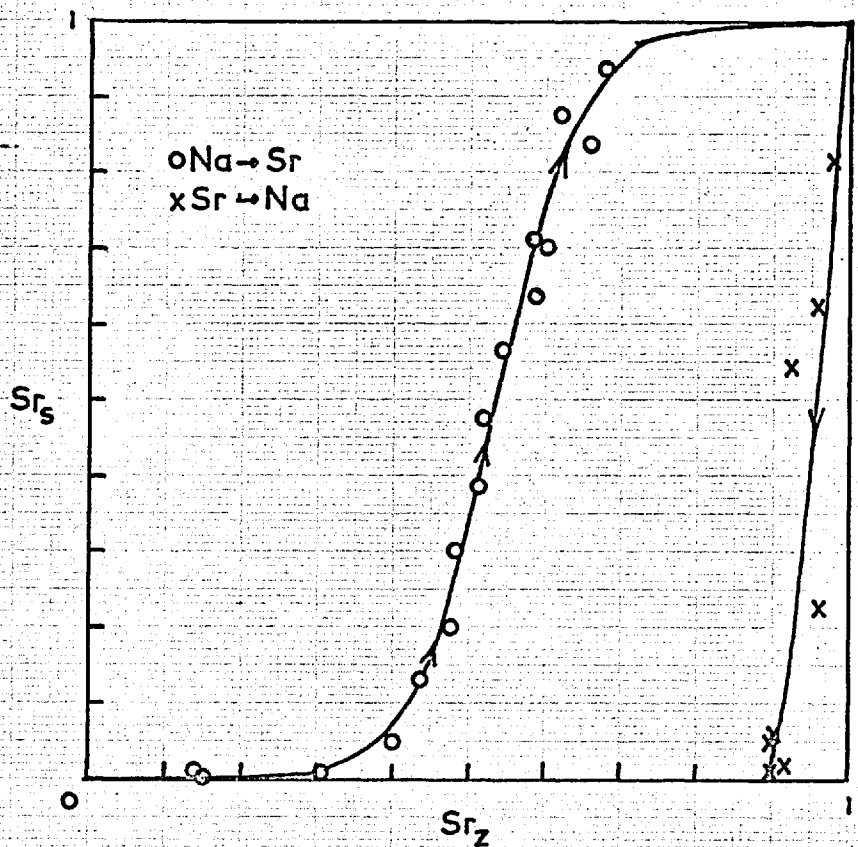

Figure 7·36: Na–Ba Exchange in F

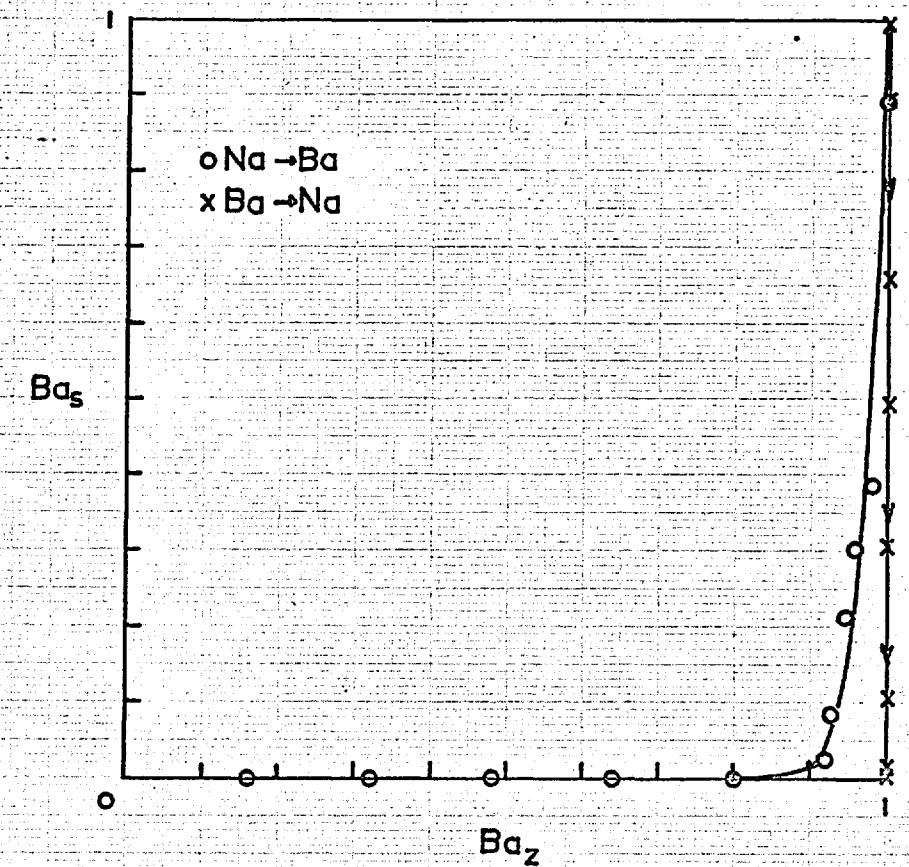

The Na-Ba exchange was completely irreversible, even when saturated sodium chloride solutions were used in an attempt to effect exchange to sodium. The selectivity for barium was extremely high, and quantitative removal of barium from solution was obtained for barium loadings of up to 0.8. Thus Na-F should prove to be a very satisfactory material for removing barium ions from neutral or alkaline solution. Separation of barium from the alkali metal ions could probably be effected, although separation from other alkaline earth cations is likely to be less effective.

The K-Ba exchange isotherm is shown in Figure 7.37. Quantitative removal of barium from solution was again obtained, but only for barium loadings up to 0.5, at which point the selectivity reversed sharply. Although complete exchange to the barium form was not obtained using 0.1N solutions, fully-exchanged Ba-F was prepared from K-F using more concentrated barium chloride solution. Reconversion of Ba-F to K-F was impossible to achieve.

K-Ba Exchange in K-F(Cl)

The K-Ba exchange isotherm for a sample of K-F(Cl) containing 6.56% KCl is shown in Figure 7.38.

Exchange did not occur past the point $Ba_Z = 0.2$ which approximately corresponds to the amount of potassium associated with the occluded chloride ions. No chloride ion loss was detected.

General Discussion

A qualitative explanation of part of the unusual ion-exchange behaviour of zeolite F may be provided by changes in the structure of this material in its various cationic forms.

The X-ray powder patterns for these forms of F, shown in Figure 7.20, may be classified in three main classes:

I Na-F and Cs-F

II K-F, Li-F, and (probably) Ca-F

III Sr-F and Ba-F.

Figure 7·37: K – Ba Exchange in F

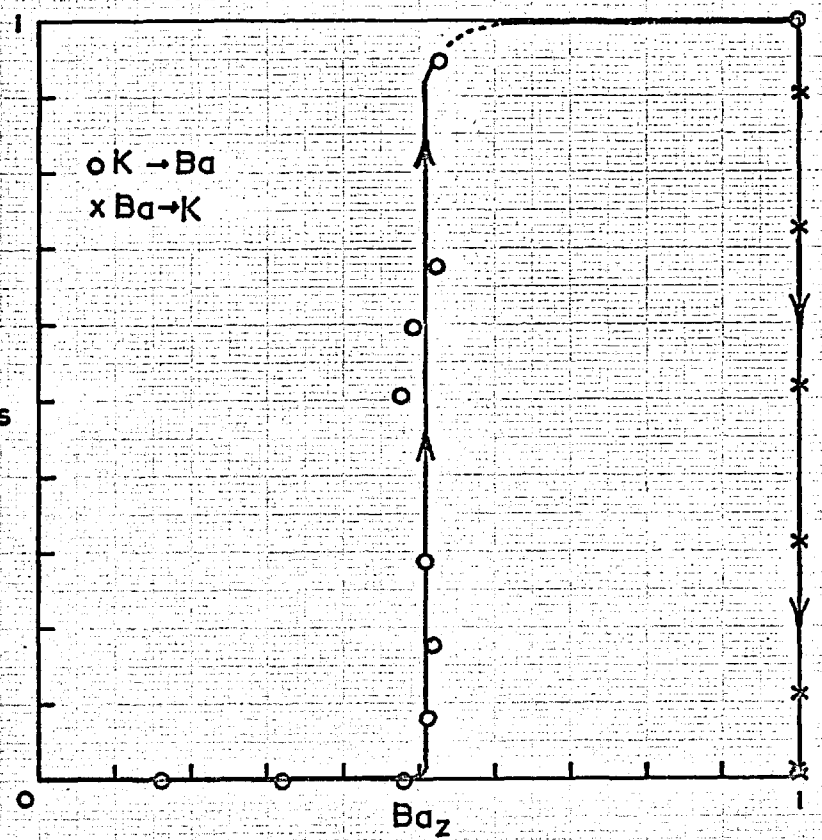

Figure 7·38: K–Ba Exchange in K–F(Cl)

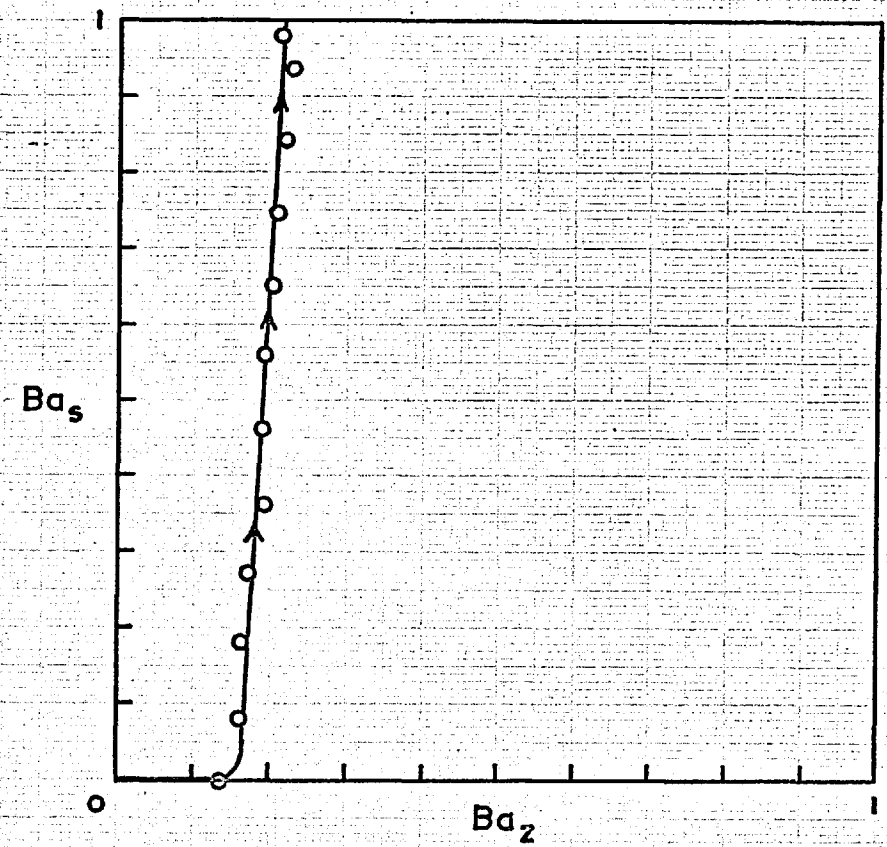

Within each class, the unit cells appear to be of approximately the same size. Between classes, the unit cell sizes appear to decrease in the order I > II > III.

Completely reversible exchanges occurred only between ions of the same class (Na-Cs, and K-Li). Exchanges involving ions of classes I and II were reversible, but with hysteresis (Na-K, Na-Li, K-Cs, Na-Cs). Uni-divalent exchanges between ions of groups I or II, and group III (Na-Ba, Na-Sr, K-Ba) were essentially irreversible.

Most of the uni-univalent exchanges were successfully interpreted in terms of two types of exchange site. The selectivity sequence found for site 1, comprising 64% of all available sites, was

$$Cs > K > Li > Na.$$

The sequence for site 2 was the reverse:

$$Na > Li > K > Cs.$$

These two sequences correspond to Series X and I respectively on Eisenman's model of cation selectivity (37). On this model, the sequence observed for Site 2 should indicate a higher anionic field strength at those sites than at site 1. Since the Si:Al ratio in zeolite F is 1:1, this cannot arise from variations in aluminium distribution throughout the framework structure. A difference in anionic field strength might arise, however, if site 2 was associated with relatively small cavities or structural sub-units, whereas site 1 was associated with larger units or channels.

This possibility is supported by some characteristics of the species K-F(Cl). Potassium chloride can only be incorporated in the K-F structure during synthesis, and is very difficult to remove once formed. Sticher (44) found that extraction with hot water under reflux for several hours failed to remove the occluded salt. K-F(Cl) is also extremely thermostable, collapsing only at 1095° C with release of the salt (44). These observations suggest that the chloride ions may be entrapped in cavities in the F structure.

Release of KCl did occur when K-F(Cl) was exchanged with a small ion, Li^+, and also with Na^+. In the latter case there is evidence of cell expansion during the exchange. In all exchanges studied for K-F(Cl), the presence of the trapped salt clearly affected the behaviour of type 2 sites, reversing the selectivity of these sites in many cases.

The Structure of Zeolite F

As stated previously, the crystal structure of zeolite F has not been determined, nor indeed has the X-ray diffraction pattern of K-F been indexed. The following comments may be of value to any investigator who may attempt the structure determination in the future.

D.E. Mainwaring, in these laboratories, has recently prepared the rubidium form of zeolite F ("Rb-D" of Barrer, Cole, and Sticher (44)) by synthesis from kaolinite. The X-ray powder pattern of this material has since been tentatively indexed as a tetragonal unit cell with the dimensions

$$a = b = 9.98_3 \text{ Å}$$

$$c = 13.23 \text{ Å} .$$

The agreement between observed and calculated d-values was good. Systematic absences in the powder pattern indicated that the unit cell was apparently body-centred. If this indexing is provisionally accepted as correct, then the four strongest lines in the Rb-F pattern (shown in Figure 7.20) become the (110), (222), (114) and (312) reflections respectively. The analysis and density of this sample of Rb-F have not as yet been determined.

Borer, however, has reported an analysis and density for a mixed (Na, Li) form of zeolite F (46). The analysis was given as

$$0.20Na_2O, 0.75Li_2O, Al_2O_3, 2SiO_2, 3.2H_2O$$

and the density reported to be 2.05 g/cm^3 .

The above formula indicates a small cation deficiency. If this is corrected by assuming a similar distribution of sodium and lithium cations as found by analysis, the oxide formula becomes

$$0.21Na_2O, 0.79Li_2O, Al_2O_3, 2SiO_2, 3.2H_2O$$

for which the formula weight is 316.3 g. The density is assumed to be unchanged by this adjustment.

The four strongest lines in the powder pattern of this zeolite are at d-values of 6.91, 3.05, 2.94, and 2.79. Using the indices found for the corresponding lines in Rb-F, the unit cell dimensions, and hence the unit cell volume of the (Na, Li)F may be calculated.

Thus
$$Q_{110} = \frac{1}{d^2_{110}} = 0.0209$$

$$a = 9.78\text{Å}$$

$$Q_{312} - Q_{222} = \frac{2}{a^2}$$

$$a = 9.76$$

$$\text{Mean } a = \underline{9.77\text{Å}}$$

$$Q_{114} - Q_{110} = \frac{16}{c^2}$$

$$c = \underline{12.997\text{Å}}$$

Hence the unit-cell volume V, is given by

$$V = a^2 c$$

$$= 1241\ \text{Å}^3.$$

If there are Z formula units per unit cell, then Z is given by

$$Z = \frac{\rho \times N_0 \times V}{W}$$

where ρ = density

N_0 = Avogadro's number

V = unit cell volume

W = formula weight.

Application of this formula gives

$$Z = 4.85$$
$$\approx 5 .$$

The unit cell formula for Li-F would therefore become

$$Li_{10}Al_{10}Si_{10}O_{40} . 16H_2O.$$

Thus there are 20(Si+Al) atoms in the unit cell of approximate dimensions 10 x 10 x 13 Å.

One possible framework structure containing 20 Si or Al tetrahedra per unit cell, and with the approximate tetragonal cell dimensions quoted above is shown in Figure 7.39. This may provide a basis for a detailed structure determination of zeolite F. The structure shown does not however exhibit body-centred symmetry.

Figure 7·39

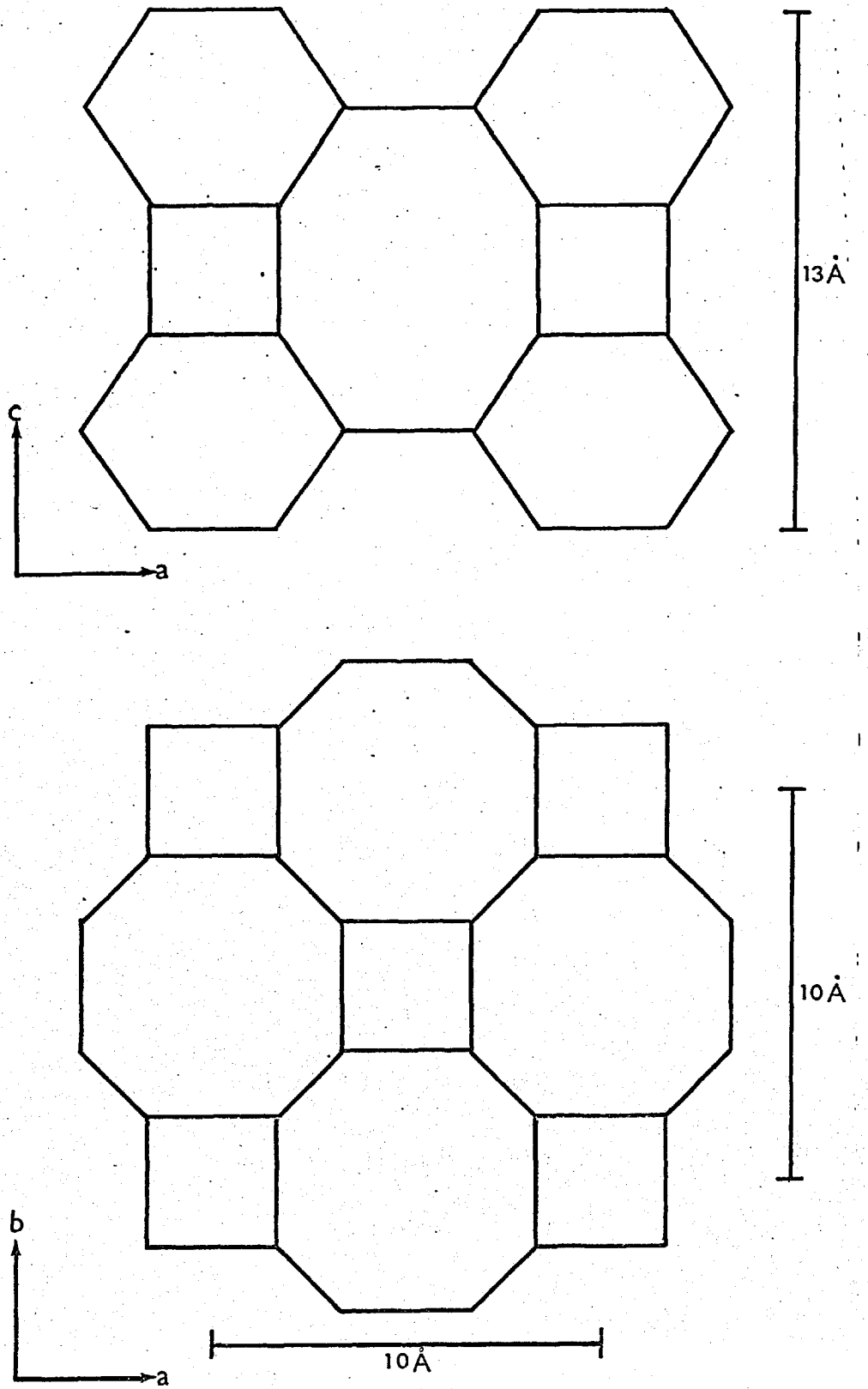

HYPOTHETICAL TETRAGONAL STRUCTURE

8. Appendices

8.1. X-ray data for Na-P_C, Na-P_T, Na-F and K-F.

8.2. Listing of CALCIS and SVAS.

8.3. Tabulation of experimental ion-exchange isotherm results.

8.11 Indexed d-spacings and intensities for zeolite Na-P (cubic)

$a = 9.992\text{Å}$ Space Group I $4/m\bar{3}\ 2/m$

hkl	d (observed)	d (calculated)	Intensity
110	7.07	7.06	s
200	4.99_0	4.99_6	m
211	4.08_1	4.07_9	s
220	3.530	3.532	vw
310	3.157	3.159	vs
222	2.885	2.884	mw
321	2.668	2.670	s
400	2.501	2.498	w
330 411	2.353	2.355	mw
420	2.245	2.234	w
332	2.127	2.130	vw
422	2.041	2.039	mw
510 431	1.961	1.959	m
521	1.823	1.824	mw
440	1.766	1.766	m
530 433	1.714	1.713	m
600 442	1.664	1.665	m
532 611	1.620	1.621	mw
620	1.581	1.580	w
541	1.540	1.542	w
622	1.507	1.506	w

8.12 Indexed d-spacings and intensities for zeolite Na-P (tetragonal)

a = 10.090 ; c = 9.803

hkl	d obs.	d calc.	I
110	7.15	7.13	s
101	7.05	7.03	s
111	5.77	5.77	w
200	5.05	5.04	s
002	4.90	4.90	s
201	4.49_5	4.48_6	vw
102	4.41_2	4.40_9	w
211	4.10_5	4.09_9	vs
112	4.04_4	4.04_0	mw
202	3.517	3.515	w
212	3.320	3.320	m
301 or 310	3.186	3.191 3.181	vs
103	3.110	3.109	s
311	3.033	3.034	mw
113	2.969	2.971	w
302	2.769	2.773	vw
203	2.743	2.743	vw
321	2.690	2.691	ms
312	2.673	2.674	vw
213	2.646	2.647	ms
400	2.525	2.522	mw
410	2.447	2.447	vw
322	2.428	2.430	mw
104	2.381	2.381	w
303	2.341	2.344	vw
331	2.314	2.311	vw
420	2.253	2.256	vw
421	2.200	2.199	m
214	2.152	2.154	m
323	2.125	2.125	vw
422	2.049	2.049	w
403	1.997	1.997	vw
501, 431	1.977	1.977	w
005	1.961	1.961	vw
511	1.941	1.940	vw
333	1.923	1.923	vw
502, 432	1.866	1.866	vw
423	1.853	1.857	vw
521	1.839	1.840	vw

N.B. Also v. weak lines at d-values of 6.84, 6.57, 5.65, 4.19, 3.88, 3.01, 2.94 which could not be indexed on the above tetragonal cell.

8.13 d-spacings and intensities for Na-F and K-F

Na-F		K-F	
d(Å)	Intensity	d(Å)	Intensity
7.10	s	7.87	w
6.66	m	6.94	s
4.89	m	6.52	w
4.47	vw	4.78	vw
4.27	vw	4.18	vw
4.03	w	3.48	m
3.57	mw	3.22	w
3.35	w	3.20	vw
3.19	w	3.11	w
3.15	vs	3.08	ms
3.03	ms	2.97	s
2.88	ms	2.82	ms
2.56	vw	2.74	vw
2.52	mw	2.69	vw
2.44	mw	2.58	vw
2.31	mw	2.56	vw
2.25	w	2.46	vw
2.24	w	2.32	vw
2.14	vw	2.26	w
2.13	vw	2.19	vw
2.01	w	1.86	vw
1.89	mw	1.74	w
1.87	w		
1.83	vw		
1.78	m		
1.73	mw		
1.72	vw		

```
$JOB  10014021    B.M.MUNDAY  IBJOB    3.0    3000
$EXECUTE        IBJOB
$IBJOB          FIOCS
$IBFTC CALCIS
C
C THIS PROGRAM CALCULATES SOLID PHASE ACTIVITY COEFFICIENTS,SOLUTION
C PHASE ACTIVITY COEFFICIENTS,RATIONAL SELECTIVITY COEFFICIENTS (KC)
C (CORRECTED FOR SOLUTION ACTIVITIES),AND THE RATIONAL THERMODYNAMIC
C EQUILIBRIUM CONSTANT KA FOR THE ION-EXCHANGE REACTION
C            ZB.A(S) + ZA.B(Z) = ZB.A(Z) + ZA.B(S)
C   WHERE (S) REFERS TO SOLUTION PHASE,(Z) REFERS TO SOLID PHASE
C  ZA=VALENCY OF ION A, ZB OF ION B. IT IS ASSUMED THAT 1) THERE IS A
C COMMON ANION X OF VALENCY ZX ,2) THAT SALT INCLUSION AND SOLVENT
C UPTAKE ARE NEGLIGIBLE (I.E. WATER CONTENTS OF A(Z) AND B(Z) ARE SAME.
C  DATA REQUIRED ARE AS FOLLOWS-
C      ZA,ZB,ZX, AZ,AS (EQUIVALENT FRACTIONS OF ION A IN ZEOLITE AND
C SOLUTION FOR ALL POINTS MEASURED),TN (CONSTANT (N.B.**) CONCN.OF
C EXCHANGE SOLUTION (EQUIVALENTS PER LITRE),AGAM,BGAM (MEAN IONIC
C ACTIVITY COEFFICIENTS OF SALTS AX AND BX AT MOLALITY EQUIVALENT
C TO NORMALITY TN ),GRADA,GRADB (SIGNED FACTORS OR GRADIENTS OF LINES
C          AGAM(I) = AGAM(I(TN)) + GRADA*(I-I(TN))
C  WHERE I=IONIC STRENGTH  )
C  THIS PROGRAM HAS A TWO-CARD TITLE
C  THE MAXIMUM NUMBER OF DATA POINTS PER JOB IS 50
      DIMENSION AZ(50),AS(50),TITLE(24),ID(50),Y(50),F(4,50),A(4,4),B(4)
     1,D(5),C(3,4),FA(3,50),FB(3,50),CL(3,50),GTKA(3),AZC(49),ASC(3,49),
     1AA(5,4,4),R(3),SSS(3,50)
      COMMON TITLE,ZA,ZB,ZX,TN,NJ,N,AZ,AS,AGAM,BGAM,GRADA,GRADB,Y,C,FA,
     1FB,CL,GTKA,IND,R,CKIEL,NNN,SSS
      READ(5,100)NJOB
  100 FORMAT(40X,I5)
      DO 9000 NJ=1,NJOB
      CALL INPUT
      CALL GLUECK($5000)
      CALL LEAST
      CALL ZACT
 5000 CALL OUTPUT($9000)
C FOR UNI-UNIVALENT REACTIONS CALCULATE THE ISOTHERM ITSELF
      IF((IFIX(ZA).EQ.1).AND.(IFIX(ZB).EQ.1))CALL REVERS
 9000 CONTINUE
      STOP
      END
```

Contd.

```
$IBFTC SUB1
      SUBROUTINE INPUT
C THIS ROUTINE READS IN THE DATA. NOTE THAT TITLE USES TWO CARDS.
      DIMENSION AZ(50),AS(50),TITLE(24),ID(50),Y(50),F(4,50),A(4,4),B(4)
     1,D(5),C(3,4),FA(3,50),FB(3,50),CL(3,50),GTKA(3),AZC(49),ASC(3,49),
     1AA(5,4,4),R(3),SSS(3,50)
      COMMON TITLE,ZA,ZB,ZX,TN,NJ,N,AZ,AS,AGAM,BGAM,GRADA,GRADB,Y,C,FA,
     1FB,CL,GTKA,IND,R,CKIEL,NNN,SSS
      READ(5,101)(TITLE(J),J=1,24)
      READ(5,102)ZA,ZB,ZX,TN,AGAM,GRADA,BGAM,GRADB
      I=0
    1 I=I+1
      IF(I-50)2,2,10
    2 READ(5,103)AZ(I),AS(I),ID(I)
      IF(ID(I))1,1,10
   10 N=I-1
      IND=ID(I)
      RETURN
  101 FORMAT(12A6/12A6)
  102 FORMAT(F3.1,1X,F3.1,1X,F3.1,1X,F4.2,1X,F5.3,1X,F6.3,1X,F5.3,1X,F6.
     13)
  103 FORMAT(F5.3,1X,F5.3,29X,I5)
      END
```

Contd.

```
$IBFTC SUB2
      SUBROUTINE GLUECK(*)
C THIS ROUTINE COMPUTES SOLUTION ION-ACTIVITIES BY GLUECKAUFS EQUATION
      DIMENSION AZ(50),AS(50),TITLE(24),ID(50),Y(50),F(4,50),A(4,4),B(4)
     1,D(5),C(3,4),FA(3,50),FB(3,50),CL(3,50),GTKA(3),AZC(49),ASC(3,49),
     1AA(5,4,4),R(3),SSS(3,50)
      COMMON TITLE,ZA,ZB,ZX,TN,NJ,N,AZ,AS,AGAM,BGAM,GRADA,GRADB,Y,C,FA,
     1FB,CL,GTKA,IND,R,CKIEL,NNN,SSS
C  IF UNI-UNIVALENT REACTION,COMPUTE KCDASH DIRECTLY SINCE G IS CONSTANT
C  AND EQUAL TO BGAM/AGAM FOR ALL IONIC STRENGTHS SI.
      IF((ZA.EQ.1.).AND.(ZB.EQ.1.))GO TO 201
      GO TO 202
  201 DO 203 I=1,N
      CK=((AZ(I)*(1.-AS(I)))/((1.-AZ(I))*AS(I)))*BGAM/AGAM
      Y(I)=ALOG10(CK)
  203 CONTINUE
      IF(IND.EQ.11111)RETURN1
      RETURN
  202 CONTINUE
      GK1A=ZB*((2.*ZB)-ZA+ZX)
      GK2A=ZA*(ZB+ZX)*(ZB+ZX)/(ZA+ZX)
      GK3A=0.5*ZA*ZB*ZX*(ZA-ZB)*(ZA-ZB)/(ZA+ZX)
      GK1B=ZA*((2.*ZA)-ZB+ZX)
      GK2B=ZB*(ZA+ZX)*(ZA+ZX)/(ZB+ZX)
      GK3B=0.5*ZB*ZA*ZX*(ZB-ZA)*(ZB-ZA)/(ZB+ZX)
      SIA=0.5*TN*ZX*(ZX+ZA)
      SIB=0.5*TN*ZX*(ZX+ZB)
      DO 210 I=1,N
      SI=0.5*TN*ZX*(ZX+ZB+(AS(I)*(ZA-ZB)))
      FI=1.+1./SQRT(SI)
      AM=TN*AS(I)/ZA
      BM=TN*(1.-AS(I))/ZB
      GA=AGAM+GRADA*(SI-SIA)
      GB=BGAM+GRADB*(SI-SIB)
      GLA=ALOG10(GA)
      GLB=ALOG10(GB)
      UA=GK1A*GLA-GK2A*GLB-GK3A/FI
      UB=GK1B*GLB-GK2B*GLA-GK3B/FI
      GLAX=GLA-((BM/(4.*SI))*UA)
      GLBX=GLB-((AM/(4.*SI))*UB)
      GL=(ZA*(ZB+ZX)/ZX)*GLBX-(ZB*(ZA+ZX)/ZX)*GLAX
      G=EXP(2.303*GL)
      BZ=1.-AZ(I)
      CK=((AZ(I)/AM)**ZB)*((BM/BZ)**ZA)*G
      Y(I)=ALOG10(CK)
  210 CONTINUE
      IF(IND.EQ.11111)RETURN1
      RETURN
      END
```

Contd.

```
$IBFTC SUB3
      SUBROUTINE LEAST
C  THIS ROUTINE PERFOFMS A POLYNOMIAL LEAST SQUARES FIT BETWEEN LOGKC
C  AND AZ. IN FACT THREE SUCH FITS ARE DONE- LINEAR(MM=1),QUADRATIC(MM=2)
C  AND CUBIC(MM=3).HIGHER POWERS ARE NOT POSSIBLE IN THIS PROGRAM.
C  THE RESULTING MATRIX EQUATION IS SOLVED BY THE DIRECT METHOD,TO
C  YIELD POLYNOMIAL COEFFICIENTS C.FOR DETAILS REFER TO INTRODUCTORY
C  COMPUTER METHODS AND NUMERICAL ANALYSIS BY R.H.PENNINGTON,PAGES 372
C      AND 289.
C  NOTE MAXIMUM POWER OF AZ IS AZ CUBED.
      DIMENSION AZ(50),AS(50),TITLE(24),ID(50),Y(50),F(4,50),A(4,4),B(4)
     1,D(5),C(3,4),FA(3,50),FB(3,50),CL(3,50),GTKA(3),AZC(49),ASC(3,49),
     1AA(5,4,4),R(3),SSS(3,50)
      COMMON TITLE,ZA,ZB,ZX,TN,NJ,N,AZ,AS,AGAM,BGAM,GRADA,GRADB,Y,C,FA,
     1FB,CL,GTKA,IND,R,CKIEL,NNN,SSS
      DO 31 J=1,N
      F(1,J)=1.
      F(2,J)=AZ(J)
      F(3,J)=AZ(J)*AZ(J)
   31 F(4,J)=AZ(J)*AZ(J)*AZ(J)
      DO 32 M=2,4
      MM=M-1
      LL=M+1
      DO 33 I=1,M
      DO 33 K=1,I
      A(K,I)=0.0
      DO 34 J=1,N
   34 A(K,I)=A(K,I)+F(I,J)*F(K,J)
   33 A(I,K)=A(K,I)
      DO 35 K=1,M
      B(K)=0.0
      DO 35 J=1,N
   35 B(K)=B(K)+Y(J)*F(K,J)
C  DIRECT METHOD OF DETERMINANT EVALUATION BEGINS.
      DO 36 L=1,LL
      DO 36 K=1,M
      DO 36 I=1,M
   36 AA(L,I,K)=A(I,K)
C  THE ARRAY AA(L,I,K) SPECIFIES THE ELEMENTS OF THE DETERMINANTS NEEDED
C TO FIND THE UNKNOWN COEFFICIENTS C. L= 1 TO M GIVE CRAMERS NUMERATORS
C  FOR C(1) TO C(M),L=M+1 GIVES THE DENOMINATOR (DETERMINANT OF
C  COEFFICIENTS OF C(L).
      DO 37 K=1,M
      DO 37 I=1,M
   37 AA(K,I,K)=B(I)
      DO 38 L=1,LL
      D(L)=1.
      NI=1
   50 CONTINUE
      NN=NI+1
      IS=NI
      IT=NI
      E=ABS(AA(L,NI,NI))
      DO 39 I=NI,M
      DO 39 K=NI,M
      IF(ABS(AA(L,I,K))-E)39,39,40                                  Contd.
   40 IS=I
      IT=K
      E=ABS(AA(L,I,K))
```

```
   39 CONTINUE
      IF(IS-NI)41,41,42
   42 DO 43 K=NI,M
      H=AA(L,IS,K)
      AA(L,IS,K)=AA(L,NI,K)
   43 AA(L,NI,K)=-H
   41 CONTINUE
      IF(IT-NI)44,44,45
   45 DO 46 I=NI,M
      H=AA(L,I,IT)
      AA(L,I,IT)=AA(L,I,NI)
   46 AA(L,I,NI)=-H
   44 CONTINUE
      D(L)=AA(L,NI,NI)*D(L)
      IF(AA(L,NI,NI))47,38,47
   47 CONTINUE
      DO 48 K=NN,M
      AA(L,NI,K)=AA(L,NI,K)/AA(L,NI,NI)
      DO 48 I=NN,M
      W=AA(L,I,NI)*AA(L,NI,K)
      AA(L,I,K)=AA(L,I,K)-W
      IF(ABS(AA(L,I,K))-0.0001*ABS(W))49,48,48
   49 AA(L,I,K)=0.
   48 CONTINUE
      NI=NN
      IF(NI-M)50,51,50
   51 D(L)=AA(L,M,M)*D(L)
   38 CONTINUE
      DO 52 L=1,M
      C(MM,L)=D(L)/D(LL)
   52 CONTINUE
   32 CONTINUE
      RETURN
      END
$IBFTC SUB4
      SUBROUTINE ZACT
      DIMENSION AZ(50),AS(50),TITLE(24),ID(50),Y(50),F(4,50),A(4,4),B(4)
     1,D(5),C(3,4),FA(3,50),FB(3,50),CL(3,50),GTKA(3),AZC(49),ASC(3,49),
     1AA(5,4,4),R(3),SSS(3,50)
      COMMON TITLE,ZA,ZB,ZX,TN,NJ,N,AZ,AS,AGAM,BGAM,GRADA,GRADB,Y,C,FA,
     1FB,CL,GTKA,IND,R,CKIEL,NNN,SSS
      DZ=0.4343*(ZB-ZA)
      DO 51 MM=1,3
      DSQ=0.
      M=MM+1
      DO 52 I=1,N
      BZ=1.-AZ(I)
      S1=0.
      S2=0.
      S3=0.
      S4=0.
      DO 53 J=1,M
      DJ=FLOAT(J)
      S=C(MM,J)*(AZ(I)**J)
      S1=S1+S
      S2=S2+S/DJ
      S3=S3+C(MM,J)/DJ
      S4=S4+S/AZ(I)
   53 CONTINUE
```

Contd.

```
      FLA=DZ*BZ+S1-S4-S2+S3
      FLB=S1-S2-DZ*AZ(I)
      CL(MM,I)=S4
      SAL=EXP(2.303*S4)
      SSS(MM,I)=SAL*(BZ**ZA)/(AZ(I)**ZB)
      GTKA(MM)=EXP(2.303*(DZ+S3))
      FA(MM,I)=EXP(2.303*FLA/ZB)
      FB(MM,I)=EXP(2.303*FLB/ZA)
      DEL=Y(I)-CL(MM,I)
      DSQ=DSQ+DEL*DEL
   52 CONTINUE
      R(MM)=SQRT(DSQ/FLOAT(N-M-1))
   51 CONTINUE
      CKIEL=C(1,2)/2.
      RETURN
      END
```

Contd.

```
$IBFTC SUB5
      SUBROUTINE OUTPUT(*)
      DIMENSION AZ(50),AS(50),TITLE(24),ID(50),Y(50),F(4,50),A(4,4),B(4)
     1,D(5),C(3,4),FA(3,50),FB(3,50),CL(3,50),GTKA(3),AZC(49),ASC(3,49),
     1AA(5,4,4),R(3),SSS(3,50)
      COMMON TITLE,ZA,ZB,ZX,TN,NJ,N,AZ,AS,AGAM,BGAM,GRADA,GRADB,Y,C,FA,
     1FB,CL,GTKA,IND,R,CKIEL,NNN,SSS
      NNN=N
      WRITE(6,600)(TITLE(J),J=1,24)
      WRITE(6,601)ZA,ZB,ZX
      WRITE(6,603)
      WRITE(6,604)(AZ(I),AS(I),Y(I),I=1,N)
      IF(IND.EQ.11111)RETURN1
      WRITE(6,605)
      WRITE(6,606)GTKA(1)
      WRITE(6,607)C(1,1),C(1,2)
      WRITE(6,615)CKIEL
      WRITE(6,614)R(1)
      WRITE(6,608)
      WRITE(6,609)(AZ(I),CL(1,I),FA(1,I),FB(1,I),SSS(1,I),I=1,N)
      WRITE(6,610)
      WRITE(6,606)GTKA(2)
      WRITE(6,611)C(2,1),C(2,2),C(2,3)
      WRITE(6,614)R(2)
      WRITE(6,608)
      WRITE(6,609)(AZ(I),CL(2,I),FA(2,I),FB(2,I),SSS(2,I),I=1,N)
      WRITE(6,612)
      WRITE(6,606)GTKA(3)
      WRITE(6,613)C(3,1),C(3,2),C(3,3),C(3,4)
      WRITE(6,614)R(3)
      WRITE(6,608)
      WRITE(6,609)(AZ(I),CL(3,I),FA(3,I),FB(3,I),SSS(3,I),I=1,N)
  600 FORMAT(1H1,12X,12A6,//13X,12A6//)
  601 FORMAT(19X,21HFOR THIS EXCHANGE ZA=,F3.1,4H,ZB=,F3.1,4H,ZX=,F3.1/
     1)
  603 FORMAT(19X,25H1.  EXPERIMENTAL  RESULTS,//24X,3H  Z,4X,3H  S,4X,5
     1LOGKC//)
  604 FORMAT(23X,F5.3,2X,F5.3,2X,F6.3)
  605 FORMAT(1H1,19X,25H2.  LEAST-SQUARES RESULTS,//19X,2HA.,5X,21HLINE
     1R FIT (KIELLAND),//)
  606 FORMAT(19X,21HGAINES AND THOMAS KA=,F8.4,//)
  607 FORMAT(19X,7HLOGKC= ,F7.3,3H + ,F7.3,3H  Z//)
  608 FORMAT(20X,3H  Z,4X,5HLOGKC,6X,3HF  ,7X,3HF  ,46X,1HS//)
  609 FORMAT(19X,F5.3,2X,F6.3,2X,F8.3,2X,F8.3,40X,F10.6)
  610 FORMAT(1H1,19X,2HB.,5X,13HQUADRATIC FIT//)
  611 FORMAT(19X,7HLOGKC= ,F7.3,3H + ,F7.3,3H  Z,3H + ,F7.3,6H  Z**2//)
  612 FORMAT(1H1,19X,2HC.,5X,10HCUBIC  FIT,//)
  613 FORMAT(19X,7HLOGKC= ,F7.3,3H + ,F7.3,3H  Z,3H + ,F7.3,6H  Z**2,3H
     1+ ,F7.3,6H  Z**3//)
  614 FORMAT(19X,29HRELIABILITY OF FIT FACTOR R =,F7.3//)
  615 FORMAT(19X,21HKIELLAND CONSTANT C =,F7.4,//)
      RETURN
      END
```

Contd.

```
$IBFTC SUB6
      SUBROUTINE REVERS
      DIMENSION AZ(50),AS(50),TITLE(24),ID(50),Y(50),F(4,50),A(4,4),B(4)
     1,D(5),C(3,4),FA(3,50),FB(3,50),CL(3,50),GTKA(3),AZC(49),ASC(3,49),
     1AA(5,4,4),R(3),SSS(3,50)
      COMMON TITLE,ZA,ZB,ZX,TN,NJ,N,AZ,AS,AGAM,BGAM,GRADA,GRADB,Y,C,FA,
     1FB,CL,GTKA,IND,R,CKIEL,NNN,SSS
      DO 990 I=1,49
      AZC(I)=FLOAT(I)/50.
      DO 990 MM=1,3
      M=MM+1
      CCLK=0.
      DO 991 J=1,M
      CCLK=CCLK+C(MM,J)*(AZC(I)**J)/AZC(I)
  991 CONTINUE
      CCK=EXP(2.303*CCLK)
      V=1.-AZC(I)
      W=CCK*AGAM*V/(BGAM*AZC(I))
      ASC(MM,I)=1./(1.+W)
  990 CONTINUE
      WRITE(6,992)
      WRITE(6,993)
      WRITE(6,994)(AZC(I),(ASC(MM,I),MM=1,3),I=1,49)
  992 FORMAT(1H1,15X,48HCALCULATED ISOTHERMS FROM LEAST-SQUARES ANALYSIS
     1//)
  993 FORMAT(24X,3H  Z,7X,3H  S,7X,3H  S,7X,3H  S/33X,8H(LINEAR),1X, 11H
     1(QUADRATIC),1X,7H(CUBIC)//)
  994 FORMAT(20X,4F10.4)
      RETURN
      END
```

```
$JOB  10014021    B.M.MUNDAY  PUFFT    0.5    500
$EXECUTE          PUFFT
$IBJOB            FIOCS
$IBFTC SVAS
C     C THIS PROGRAM TABULATES AS VS S FOR UNI-DIVALENT EXCHANGES
      DIMENSION COL(100),S(1000),TITLE(24)
      READ(5,100) NJOB
      DO 9000 NJ=1,NJOB
      READ(5,101)(TITLE(J),J=1,24)
      READ(5,102)ZA,ZB,ZX,TN,AGAM,GRADA,BGAM,GRADB
      COL(1)=0.000
      DO 1000 I=2,100
      COL(I)=(FLOAT(I)/100.)-0.010
 1000 CONTINUE
      S(1)=999.999999
      GK1A=ZB*((2.*ZB)-ZA+ZX)
      GK2A=ZA*(ZB+ZX)*(ZB+ZX)/(ZA+ZX)
      GK3A=0.5*ZA*ZB*ZX*(ZA-ZB)*(ZA-ZB)/(ZA+ZX)
      GK1B=ZA*((2.*ZA)-ZB+ZX)
      GK2B=ZB*(ZA+ZX)*(ZA+ZX)/(ZB+ZX)
      GK3B=0.5*ZB*ZA*ZX*(ZB-ZA)*(ZB-ZA)/(ZB+ZX)
      SIA=0.5*TN*ZX*(ZX+ZA)
      SIB=0.5*TN*ZX*(ZX+ZB)
      DO 2000 I=1,999
      AS=FLOAT(I)/1000.
      SI=0.5*TN*ZX*(ZX+ZB+(AS*(ZA-ZB)))
      FI=1.+1./SQRT(SI)
      AM=TN*AS/ZA
      BM=TN*(1.-AS)/ZB
      GA=AGAM+GRADA*(SI-SIA)
      GB=BGAM+GRADB*(SI-SIB)
      GLA=ALOG10(GA)
      GLB=ALOG10(GB)
      UA=GK1A*GLA-GK2A*GLB-GK3A/FI
      UB=GK1B*GLB-GK2B*GLA-GK3B/FI
      GLAX=GLA-((BM/(4.*SI))*UA)
      GLBX=GLB-((AM/(4.*SI))*UB)
      GL=(ZA*(ZB+ZX)/ZX)*GLBX-(ZB*(ZA+ZX)/ZX)*GLAX
      G=EXP(2.303*GL)
      K=I+1
      S(K)=G*(BM**ZA)/(AM**ZB)
 2000 CONTINUE
      WRITE(6,103)(TITLE(J),J=1,24)
      WRITE(6,104)
      N=1
      M=10
      DO 3000 I=1,100
      WRITE(6,105) COL(I),(S(J),J=N,M)
      N=N+10
      M=M+10
 3000 CONTINUE
 9000 CONTINUE
  100 FORMAT(40X,I5)
  101 FORMAT(12A6/12A6)
  102 FORMAT(F3.1,1X,F3.1,1X,F3.1,1X,F4.2,1X,F5.3,1X,F6.3,1X,F5.3,1X,F6
     13)
  103 FORMAT(1H1,10X,12A6//12A6//)
  104 FORMAT(7X,2HAS,5X,4H.000,7X,4H.001,7X,4H.002,7X,4H.003,7X,4H.004,
                                    ,  ,   0  ,  X,/   00 //
```

```
105 FORMAT(5X,F5.3,1X,10(F10.6,1X))
    STOP
    END
```

ION EXCHANGE IN NEVADA PHILLIPSITE

SODIUM - LITHIUM EXCHANGE AT 25 DEG. C

FOR THIS EXCHANGE ZA=1.0,ZB=1.0,ZX=1.0

I. EXPERIMENTAL RESULTS

Li_Z	Li_S	LOGKC'
C.009	C.097	-1.080
C.009	0.197	-1.438
C.017	0.294	-1.388
C.023	0.392	-1.444
0.052	C.482	-1.236
C.055	0.581	-1.384
C.081	0.672	-1.373
C.119	0.759	-1.374
C.174	0.840	-1.403
C.258	0.911	-1.476
C.365	C.980	-1.937
C.032	C.375	-1.266
C.052	0.467	-1.210
C.090	0.652	-1.284
C.156	0.825	-1.413
0.323	C.958	-1.686
0.485	0.993	-2.185

C. CUBIC FIT

GAINES AND THOMAS KA= 0.0057

$LOGKC' = -1.325 + 0.741\,Liz + -7.830\,Liz^{**2} + 5.292\,Liz^{**3}$

RELIABILITY OF FIT FACTOR R = 0.109

Liz	LOGKC′	F_{Li}	F_{Na}
0.009	-1.319	0.120	1.000
0.009	-1.319	0.120	1.000
0.017	-1.314	0.118	1.000
0.023	-1.312	0.118	1.000
0.052	-1.307	0.116	1.001
0.055	-1.307	0.116	1.001
0.081	-1.313	0.118	1.000
0.119	-1.338	0.124	0.994
0.174	-1.405	0.142	0.971
0.258	-1.564	0.188	0.897
0.365	-1.840	0.292	0.734
0.032	-1.309	0.117	1.000
0.052	-1.307	0.116	1.001
0.090	-1.318	0.119	0.999
0.156	-1.380	0.135	0.981
0.323	-1.724	0.245	0.805
0.485	-2.203	0.471	0.514

ION EXCHANGE IN NEVADA PHILLIPSITE

SODIUM - POTASSIUM EXCHANGE AT 25 DEG. C

FOR THIS EXCHANGE ZA=1.0,ZB=1.0,ZX=1.0

1. EXPERIMENTAL RESULTS

K_Z	K_S	LOGKC'
0.067	0.002	1.559
0.194	0.010	1.382
0.207	0.005	1.720
0.318	0.018	1.410
0.329	0.013	1.575
0.511	0.095	1.003
0.529	0.087	1.076
0.643	0.200	0.862
0.662	0.191	0.923
0.722	0.330	0.727
0.736	0.323	0.771
0.795	0.463	0.657
0.840	0.542	0.652
0.471	0.063	1.126
0.585	0.117	1.031
0.641	0.168	0.951
0.693	0.243	0.852
0.723	0.296	0.797
0.782	0.435	0.673
0.803	0.425	0.746
0.839	0.575	0.590
0.839	0.575	0.590
0.850	0.570	0.635
0.896	0.720	0.485
0.897	0.715	0.545
0.949	0.857	0.497
0.953	0.855	0.541
0.979	0.928	0.563

2. LEAST-SQUARES RESULTS

A. LINEAR FIT (KIELLAND)

GAINES AND THOMAS KA= 12.9012

$LOGKC' = 1.803 + -1.385\ K_Z$

KIELLAND CONSTANT C =-0.6925

RELIABILITY OF FIT FACTOR R = 0.090

K_Z	$LOGKC'$	F_K	F_{Na}
0.067	1.710	0.250	0.993
0.194	1.534	0.355	0.942
0.207	1.516	0.367	0.934
0.318	1.362	0.476	0.851
0.329	1.347	0.488	0.841
0.511	1.095	0.683	0.659
0.529	1.070	0.702	0.640
0.643	0.912	0.816	0.517
0.662	0.886	0.833	0.497
0.722	0.803	0.884	0.435
0.736	0.784	0.895	0.422
0.795	0.702	0.935	0.365
0.840	0.640	0.960	0.325
0.471	1.151	0.640	0.702
0.585	0.993	0.760	0.579
0.641	0.915	0.814	0.519
0.693	0.843	0.860	0.465
0.723	0.802	0.885	0.434
0.782	0.720	0.927	0.377
0.803	0.691	0.940	0.358
0.839	0.641	0.960	0.325
0.839	0.641	0.960	0.325
0.850	0.626	0.965	0.316
0.886	0.576	0.979	0.286
0.897	0.561	0.983	0.277
0.949	0.489	0.996	0.238
0.953	0.483	0.996	0.235
0.979	0.447	0.999	0.217

ION EXCHANGE IN SYNTHETIC PHILLIPSITE

SODIUM - POTASSIUM EXCHANGE AT 25 DEG. C

FOR THIS EXCHANGE ZA=1.0,ZB=1.0,ZX=1.0

1. EXPERIMENTAL RESULTS

K_Z	K_S	LOGKC'
C.358	0.009	1.793
C.571	C.072	1.239
C.664	0.134	1.111
C.729	0.210	1.010
C.773	C.288	0.930
C.807	0.374	C.850
C.840	C.462	0.791
C.871	0.548	0.750
0.919	0.682	0.728
C.922	0.727	0.652
0.643	0.118	1.134
C.696	0.175	1.038
C.788	0.287	C.970
C.808	0.379	0.843
0.843	0.465	0.795
C.867	0.555	0.723
C.902	0.640	C.719
C.924	0.731	0.655
0.949	0.821	0.613
C.968	0.913	0.464

2. LEAST-SQUARES RESULTS

A. LINEAR FIT (KIELLAND)

GAINES AND THOMAS KA= 28.0495

$LOGKC' = 2.402 + -1.908\ K_Z$

KIELLAND CONSTANT C =-0.9542

RELIABILITY OF FIT FACTOR R = 0.047

K_Z	$LOGKC'$	F_K	F_{Na}
0.358	1.719	0.404	0.755
0.571	1.312	0.667	0.488
0.664	1.135	0.780	0.380
0.729	1.011	0.851	0.311
0.773	0.927	0.893	0.269
0.807	0.862	0.921	0.239
0.840	0.799	0.945	0.212
0.871	0.740	0.964	0.189
0.919	0.648	0.986	0.156
0.922	0.642	0.987	0.154
0.643	1.175	0.756	0.403
0.696	1.074	0.816	0.345
0.788	0.898	0.906	0.256
0.808	0.860	0.922	0.238
0.843	0.793	0.947	0.210
0.867	0.747	0.962	0.192
0.902	0.681	0.979	0.167
0.924	0.639	0.987	0.153
0.949	0.591	0.994	0.138
0.968	0.555	0.998	0.128

ION EXCHANGE IN NEVADA PHILLIPSITE

SODIUM RUBIDIUM EXCHANGE AT 25 DEG. C

FOR THIS EXCHANGE ZA=1.0,ZB=1.0,ZX=1.0

1. EXPERIMENTAL RESULTS

Rb_Z	Rb_S	LOGKC'
C.261	0.010	1.552
C.426	0.053	1.130
0.525	0.119	0.921
C.593	0.195	0.787
C.659	0.272	0.722
C.701	0.358	0.632
C.755	0.440	0.601
C.766	0.535	0.462
0.802	0.623	0.397
C.843	0.709	0.351
C.848	0.766	0.239

2. LEAST-SQUARES RESULTS

A. LINEAR FIT (KIELLAND)

GAINES AND THOMAS KA= 10.4570

$LOGKC' = 2.037 + -2.035 Rb_Z$

KIELLAND CONSTANT C =-1.0177

RELIABILITY OF FIT FACTOR R = 0.056

Rb_Z	$LOGKC'$	F_{Rb}	F_{Na}
0.261	1.506	0.278	0.852
0.426	1.170	0.462	0.654
0.525	0.968	0.589	0.524
0.593	0.830	0.678	0.439
0.659	0.696	0.761	0.361
0.701	0.610	0.811	0.316
0.755	0.500	0.869	0.263
0.766	0.478	0.880	0.253
0.802	0.405	0.912	0.221
0.843	0.321	0.944	0.189
0.848	0.311	0.947	0.185

ION EXCHANGE IN NEVADA PHILLIPSITE

SODIUM - CAESIUM EXCHANGE AT 25 DEG. C

FOR THIS EXCHANGE ZA=1.0,ZB=1.0,ZX=1.0

1. EXPERIMENTAL RESULTS

C_{sZ}	C_{sS}	LOGKC'
C.218	0.014	1.305
C.476	C.025	1.562
C.658	C.070	1.420
C.747	0.167	1.181
C.797	0.222	1.151
C.843	C.393	1.104
0.865	0.415	0.968
C.876	0.501	0.860
C.897	0.591	0.793
C.951	0.839	0.584
0.559	0.051	1.385
C.593	0.056	1.403
0.682	0.070	1.467
0.767	0.152	1.276
0.838	0.237	1.234
C.863	0.431	0.932
0.884	0.526	0.849
C.924	C.617	0.890
0.951	0.811	0.668

ION EXCHANGE IN NEVADA PHILLIPSITE

SODIUM - CAESIUM EXCHANGE AT 25 DEG. C

FOR THIS EXCHANGE ZA=1.0,ZB=1.0,ZX=1.0

1. EXPERIMENTAL RESULTS (Smoothed)

Cs Z	Cs S	LOGKC'
C.050	0.002	1.432
C.100	0.003	1.580
C.150	0.005	1.558
C.200	0.006	1.630
0.250	0.008	1.629
0.300	0.010	1.640
C.350	0.014	1.591
0.400	0.017	1.598
C.450	0.021	1.594
C.500	0.027	1.565
0.550	0.035	1.540
C.600	0.047	1.496
0.650	0.065	1.439
C.700	0.095	1.359
C.750	0.142	1.271
C.800	0.221	1.162
C.850	0.366	1.004
C.900	0.566	0.851
C.950	0.783	0.734

C. CUBIC FIT

GAINES AND THOMAS KA= 24.2457

$LOGKC' = 1.436 + 1.024 CsZ + -1.023 CsZ^{**2} + -0.890 CsZ^{**3}$

RELIABILITY OF FIT FACTOR R = 0.029

CsZ	$LOGKC'$	F_{Cs}	F_{Na}
0.050	1.485	0.796	1.003
0.100	1.527	0.727	1.010
0.150	1.564	0.676	1.021
0.200	1.593	0.639	1.033
0.250	1.614	0.615	1.044
0.300	1.627	0.602	1.053
0.350	1.631	0.598	1.055
0.400	1.625	0.603	1.050
0.450	1.608	0.617	1.033
0.500	1.581	0.637	1.002
0.550	1.542	0.665	0.956
0.600	1.490	0.700	0.892
0.650	1.425	0.740	0.812
0.700	1.346	0.785	0.719
0.750	1.253	0.833	0.615
0.800	1.145	0.881	0.507
0.850	1.020	0.926	0.400
0.900	0.880	0.964	0.301
0.950	0.722	0.990	0.215

ION EXCHANGE IN NEVADA PHILLIPSITE

SODIUM - CALCIUM EXCHANGE AT 25 DEG. C

FOR THIS EXCHANGE ZA=2.0,ZB=1.0,ZX=1.0

1. EXPERIMENTAL RESULTS

Ca_Z	Ca_S	LOGKC'
0.072	0.075	-0.531
0.136	0.153	-0.575
0.159	0.245	-0.783
0.235	0.319	-0.731
0.292	0.399	-0.771
0.350	0.479	-0.817
0.464	0.640	-0.966
0.603	0.792	-1.153
0.669	0.815	-1.063
0.751	0.896	-1.303
0.355	0.465	-0.769
0.460	0.632	-0.952
0.588	0.792	-1.196
0.788	0.929	-1.488

2. LEAST-SQUARES RESULTS

A. LINEAR FIT (KIELLAND)

GAINES AND THOMAS KA= 0.0348

$LOGKC' = -0.451 + -1.144 Ca_Z$

KIELLAND CONSTANT C =-0.5721

RELIABILITY OF FIT FACTOR R = 0.086

Ca_Z	$LOGKC'$	F_{Ca}	F_{Na}
0.072	-0.534	0.127	1.033
0.136	-0.607	0.158	1.057
0.159	-0.633	0.170	1.065
0.235	-0.720	0.215	1.085
0.292	-0.785	0.254	1.094
0.350	-0.852	0.299	1.099
0.464	-0.982	0.401	1.094
0.603	-1.141	0.546	1.064
0.669	-1.217	0.622	1.041
0.751	-1.311	0.718	1.004
0.355	-0.858	0.303	1.099
0.460	-0.978	0.397	1.095
0.588	-1.124	0.530	1.069
0.788	-1.353	0.762	0.985

ION EXCHANGE IN NEVADA PHILLIPSITE

SODIUM - STRONTIUM EXCHANGE AT 25 DEG. C

FOR THIS EXCHANGE ZA=2.0,ZB=1.0,ZX=1.0

1. EXPERIMENTAL RESULTS

Sr_Z	Sr_S	$LOGKC'$
0.075	0.074	-0.501
0.122	0.158	-0.651
0.194	0.233	-0.619
0.262	0.310	-0.623
0.324	0.388	-0.651
0.406	0.460	-0.619
0.476	0.536	-0.634
0.542	0.613	-0.672
0.611	0.689	-0.714
0.668	0.770	-0.843
0.725	0.800	-0.780
0.804	0.889	-0.993
0.429	0.520	-0.712
0.492	0.600	-0.767
0.553	0.686	-0.868
0.729	0.842	-0.989

2. LEAST-SQUARES RESULTS

A. LINEAR FIT (KIELLAND)

GAINES AND THOMAS KA= 0.0659

$LOGKC' = -0.486 + -0.522 Sr_Z$

KIELLAND CONSTANT C =-0.2608

RELIABILITY OF FIT FACTOR R = 0.081

Sr_Z	$LOGKC'$	F_{Sr}	F_{Na}
0.075	-0.525	0.237	1.036
0.122	-0.549	0.262	1.058
0.194	-0.587	0.302	1.089
0.262	-0.622	0.345	1.117
0.324	-0.655	0.387	1.139
0.406	-0.697	0.447	1.166
0.476	-0.734	0.502	1.185
0.542	-0.768	0.558	1.201
0.611	-0.804	0.619	1.213
0.668	-0.834	0.671	1.221
0.725	-0.864	0.726	1.227
0.804	-0.905	0.803	1.231
0.429	-0.709	0.464	1.173
0.492	-0.742	0.515	1.189
0.553	-0.774	0.567	1.203
0.729	-0.866	0.730	1.227

ION EXCHANGE IN NEVADA PHILLIPSITE

SODIUM - BARIUM EXCHANGE AT 25 DEG. C

FOR THIS EXCHANGE ZA=2.0,ZB=1.0,ZX=1.0

1. EXPERIMENTAL RESULTS

Ba_Z	Ba_S	LOGKC′
0.285	0.001	2.224
0.572	0.002	2.671
0.794	0.025	2.333
0.857	0.105	1.994
0.879	0.196	1.795
0.900	0.356	1.533
0.925	0.481	1.488
0.929	0.578	1.286
0.999	0.940	3.143

ION EXCHANGE IN ZEOLITE P

SODIUM - LITHIUM EXCHANGE AT 25 DEG. C

FOR THIS EXCHANGE ZA=1.0,ZB=1.0,ZX=1.0

1. EXPERIMENTAL RESULTS

Li_Z	Li_S	LOGKC'
0.005	0.397	-2.124
0.018	0.490	-1.726
0.038	0.579	-1.548
0.069	0.662	-1.429
0.117	0.736	-1.330
0.166	0.809	-1.335
0.266	0.876	-1.297
0.319	0.944	-1.563
0.029	0.471	-1.481
0.082	0.642	-1.309
0.158	0.798	-1.330
0.285	0.927	-1.510
0.526	0.991	-2.003

B. QUADRATIC FIT

GAINES AND THOMAS KA= 0.0040

$LOGKC' = -1.521 + 1.921\,Li_Z + -5.498\,Li_{Z**2}$

RELIABILITY OF FIT FACTOR R = 0.083

Li_Z	$LOGKC'$	F_{Li}	F_{Na}
0.038	-1.455	0.116	1.003
0.069	-1.414	0.106	1.008
0.117	-1.371	0.097	1.017
0.166	-1.353	0.093	1.023
0.266	-1.399	0.101	0.998
0.319	-1.467	0.113	0.952
0.029	-1.469	0.119	1.002
0.082	-1.400	0.103	1.010
0.158	-1.354	0.094	1.022
0.285	-1.420	0.105	0.984
0.526	-2.031	0.235	0.540

ION EXCHANGE IN ZEOLITE P

SODIUM - POTASSIUM EXCHANGE AT 25 DEG. C

FOR THIS EXCHANGE ZA=1.0,ZB=1.0,ZX=1.0

1. EXPERIMENTAL RESULTS

K_Z	K_S	LOGKC'
0.087	0.052	0.244
0.155	0.114	0.158
0.159	0.112	0.180
0.250	0.163	0.238
0.383	0.190	0.427
0.525	0.211	0.621
0.648	0.244	0.761
0.657	0.238	0.792
0.755	0.284	0.895
0.829	0.345	0.968
0.878	0.417	1.007
0.906	0.501	0.987
0.968	0.829	0.800
0.973	0.787	0.994
0.072	0.082	-0.057
0.100	0.099	0.009
0.168	0.146	0.077
0.191	0.143	0.155
0.251	0.165	0.234
0.273	0.160	0.299
0.395	0.186	0.460
0.483	0.199	0.580
0.529	0.207	0.638
0.591	0.225	0.701
0.710	0.260	0.848
0.792	0.314	0.925
0.856	0.379	0.993
0.894	0.458	1.004
0.915	0.547	0.955
0.925	0.541	1.024
0.948	0.629	1.036
0.955	0.725	0.910
0.983	0.809	1.140
0.984	0.909	0.794
0.990	0.906	1.016

2. LEAST-SQUARES RESULTS

A. LINEAR FIT (KIELLAND)

GAINES AND THOMAS KA= 3.6778

$LOGKC' = -0.661 + 1.254\,K_Z$

KIELLAND CONSTANT C = 0.6268

RELIABILITY OF FIT FACTOR R = 0.034

K_Z	$LOGKC'$	F_K	F_{Na}
0.155	0.133	2.803	1.035
0.159	0.138	2.776	1.037
0.250	0.252	2.252	1.094
0.383	0.419	1.732	1.236
0.525	0.557	1.385	1.489
0.648	0.751	1.196	1.833
0.657	0.762	1.185	1.865
0.755	0.885	1.091	2.277
0.829	0.978	1.043	2.697
0.878	1.039	1.022	3.043
0.100	0.064	3.219	1.015
0.168	0.149	2.716	1.042
0.191	0.178	2.572	1.054
0.251	0.253	2.247	1.095
0.273	0.281	2.145	1.114
0.395	0.434	1.696	1.253
0.483	0.544	1.471	1.400
0.529	0.602	1.377	1.498
0.591	0.680	1.273	1.656
0.710	0.829	1.129	2.070
0.792	0.932	1.064	2.473
0.856	1.012	1.030	2.880
0.894	1.059	1.016	3.170

8. QUADRATIC FIT

GAINES AND THOMAS KA= 3.6271

$LOGKC' = -0.137 + 1.673\,K_Z + -0.419\,K_{Z**2}$

RELIABILITY OF FIT FACTOR R = 0.025

K_Z	$LOGKC'$	F_K	F_{Na}
0.155	0.112	2.928	1.045
0.159	0.118	2.893	1.047
0.250	0.255	2.252	1.117
0.383	0.442	1.677	1.279
0.525	0.625	1.331	1.549
0.648	0.771	1.159	1.885
0.657	0.781	1.149	1.913
0.755	0.887	1.069	2.273
0.829	0.961	1.032	2.604
0.878	1.008	1.016	2.856
0.100	0.026	3.481	1.019
0.168	0.132	2.817	1.053
0.191	0.167	2.637	1.068
0.251	0.256	2.247	1.118
0.273	0.288	2.128	1.139
0.395	0.458	1.639	1.298
0.483	0.573	1.413	1.458
0.529	0.630	1.324	1.559
0.591	0.705	1.227	1.716
0.710	0.839	1.101	2.097
0.792	0.925	1.049	2.432
0.856	0.988	1.022	2.739
0.894	1.023	1.012	2.944

ION EXCHANGE IN ZEOLITE P

SODIUM-RUBIDIUM EXCHANGE AT 25 DEG. C

FOR THIS EXCHANGE ZA=1.0,ZB=1.0,ZX=1.0

I. EXPERIMENTAL RESULTS

Rb_Z	Rb_S	LOGKC′
0.128	0.030	0.684
0.256	0.060	0.740
0.380	0.092	0.790
0.463	0.146	0.711
0.550	0.199	0.700
0.625	0.258	0.689
0.679	0.328	0.645
0.733	0.397	0.628
0.763	0.482	0.547
0.769	0.578	0.394
0.796	0.652	0.327
0.867	0.810	0.192

C. CUBIC FIT

GAINES AND THOMAS KA= 3.6406

$LOGKC' = 0.743 + -0.730\,Rb_Z + 3.448\,Rb_{Z**2} + -3.863\,Rb_{Z**3}$

RELIABILITY OF FIT FACTOR R = 0.065

Rb_Z	$LOGKC'$	F_{Rb}	F_{Na}
0.128	0.697	0.727	0.996
0.256	0.717	0.702	1.005
0.380	0.751	0.665	1.030
0.463	0.760	0.657	1.039
0.550	0.741	0.671	1.016
0.625	0.690	0.704	0.947
0.679	0.627	0.740	0.862
0.733	0.539	0.786	0.746
0.763	0.477	0.814	0.671
0.769	0.463	0.820	0.655
0.796	0.398	0.848	0.582
0.867	0.184	0.920	0.386

ION-EXCHANGE IN ZEOLITE P

SODIUM-CAESIUM EXCHANGE AT 25 DEGREES CENTIGRADE

FOR THIS EXCHANGE ZA=1.0,ZB=1.0,ZX=1.0

1. EXPERIMENTAL RESULTS

Cs_Z	Cs_S	LOGKC′
0.166	0.014	1.159
0.220	0.020	1.153
0.271	0.044	0.920
0.287	0.052	0.878
0.290	0.025	1.215
0.386	0.100	0.765
0.507	0.137	0.824
0.566	0.208	0.708
0.622	0.278	0.643
0.654	0.362	0.535
0.677	0.449	0.423
0.715	0.530	0.360
0.715	0.630	0.181
0.747	0.690	0.135
0.768	0.722	0.118
0.786	0.797	-0.016
0.833	0.827	0.031
0.835	0.870	-0.109
0.273	0.101	0.537
0.339	0.115	0.609
0.454	0.151	0.682
0.615	0.307	0.569
0.689	0.487	0.381
0.733	0.674	0.136
0.805	0.854	-0.139
0.865	0.938	-0.361

C. CUBIC FIT

GAINES AND THOMAS KA= 3.4601

$LOGKC' = 1.927 + -6.586 Cs_Z + 13.213 Cs_{Z**2} + -9.996 Cs_{Z**3}$

RELIABILITY OF FIT FACTOR R = 0.149

Cs_Z	LOGKC'	F_{Cs}	F_{Na}
0.166	1.152	0.214	0.879
0.220	1.011	0.279	0.826
0.271	0.913	0.330	0.782
0.287	0.889	0.344	0.769
0.290	0.884	0.346	0.767
0.386	0.778	0.407	0.707
0.507	0.681	0.461	0.640
0.566	0.619	0.492	0.593
0.622	0.537	0.532	0.529
0.654	0.475	0.560	0.483
0.677	0.422	0.583	0.446
0.715	0.319	0.627	0.377
0.715	0.319	0.627	0.377
0.747	0.213	0.669	0.316
0.768	0.134	0.699	0.275
0.786	0.059	0.727	0.241
0.833	-0.169	0.803	0.157
0.835	-0.180	0.806	0.154
0.273	0.910	0.332	0.780
0.339	0.823	0.382	0.734
0.454	0.725	0.438	0.671
0.615	0.549	0.526	0.538
0.689	0.392	0.596	0.425
0.733	0.262	0.650	0.343
0.805	-0.027	0.757	0.205
0.865	-0.354	0.856	0.110

ION EXCHANGE IN ZEOLITE P

SODIUM-STRONTIUM EXCHANGE AT 25 DEGREES CENTIGRADE

FOR THIS EXCHANGE ZA=2.0,ZB=1.0,ZX=1.0

1. EXPERIMENTAL RESULTS

Sr_Z	Sr_S	LOGKC'
0.084	0.005	0.784
0.186	0.005	1.232
0.466	0.045	1.010
0.474	0.045	1.031
0.581	0.088	0.988
0.680	0.135	1.062
0.750	0.197	1.095
0.804	0.268	1.127
0.859	0.338	1.259
0.873	0.432	1.123
0.904	0.515	1.173
0.921	0.604	1.111
0.430	0.065	0.742
0.453	0.062	0.823
0.525	0.054	1.077
0.534	0.085	0.877
0.575	0.080	1.020
0.578	0.080	1.028
0.614	0.102	1.007
0.672	0.124	1.083
0.702	0.141	1.113
0.768	0.210	1.129
0.853	0.370	1.139
0.891	0.552	0.960
0.947	0.725	1.081
0.950	0.824	0.696
0.975	0.912	0.668

ION EXCHANGE IN ZEOLITE P

SODIUM - STRONTIUM EXCHANGE AT 25 DEG. C

FOR THIS EXCHANGE ZA=2.0,ZB=1.0,ZX=1.0

1. EXPERIMENTAL RESULTS (Smoothed)

Sr_z	Sr_s	LOGKC'
0.050	0.002	0.928
0.100	0.004	0.973
0.150	0.007	0.953
0.200	0.011	0.931
0.250	0.015	0.946
0.300	0.020	0.957
0.350	0.026	0.969
0.400	0.035	0.960
0.450	0.046	0.959
0.500	0.060	0.960
0.550	0.076	0.977
0.600	0.095	1.003
0.650	0.118	1.039
0.700	0.150	1.071
0.750	0.195	1.101
0.800	0.261	1.127
0.850	0.359	1.147
0.900	0.520	1.123
0.950	0.754	1.021

2. LEAST-SQUARES RESULTS

A. LINEAR FIT (KIELLAND) (for smoothed results)

GAINES AND THOMAS KA= 3.7451

$LOGKC' = 0.900 + 0.215 Sr_Z$

KIELLAND CONSTANT C = 0.1073

RELIABILITY OF FIT FACTOR R = 0.041

Sr_Z	LOGKC'	F_{Sr}	F_{Na}
0.050	0.911	0.483	1.026
0.100	0.922	0.497	1.053
0.150	0.933	0.511	1.081
0.200	0.943	0.526	1.111
0.250	0.954	0.543	1.142
0.300	0.965	0.560	1.175
0.350	0.975	0.579	1.209
0.400	0.986	0.600	1.246
0.450	0.997	0.622	1.284
0.500	1.008	0.645	1.324
0.550	1.018	0.670	1.367
0.600	1.029	0.697	1.411
0.650	1.040	0.726	1.458
0.700	1.051	0.757	1.508
0.750	1.061	0.791	1.560
0.800	1.072	0.827	1.615
0.850	1.083	0.865	1.672
0.900	1.093	0.907	1.733
0.950	1.104	0.952	1.798

ION EXCHANGE IN ZEOLITE P

SODIUM - BARIUM EXCHANGE AT 25 DEG. C

FOR THIS EXCHANGE ZA=2.C,ZB=1.0,ZX=1.C

1. EXPERIMENTAL RESULTS

Ba_Z	Ba_S	LOGKC'
0.362	C.CC2	2.125
0.541	0.004	2.283
0.700	0.017	2.126
0.800	0.061	1.946
0.860	C.128	1.907
0.890	0.179	1.939
0.906	0.303	1.724
0.950	0.380	2.100
0.960	0.474	2.067
0.754	0.017	2.330
0.828	0.073	2.004
0.856	0.160	1.755
0.920	0.331	1.799
0.945	0.520	1.668
0.961	0.679	1.522
0.998	0.896	3.036

ION-EXCHANGE IN ZEOLITE F

SODIUM - LITHIUM EXCHANGE AT 25 DEG. C

FOR THIS EXCHANGE ZA=1.0,ZB=1.0,ZX=1.0

1. EXPERIMENTAL RESULTS

Li_Z	Li_S	LOGKC'
0.051	0.068	-0.139
0.099	0.138	-0.170
0.147	0.208	-0.190
0.218	0.264	-0.116
0.267	0.333	-0.144
0.306	0.409	-0.202
0.350	0.481	-0.242
0.410	0.545	-0.243
0.521	0.574	-0.100
0.664	0.583	0.144
0.784	0.608	0.363
0.882	0.780	0.317
0.971	0.903	0.549
0.150	0.219	-0.208
0.276	0.372	-0.198
0.332	0.430	-0.188
0.433	0.464	-0.061
0.565	0.480	0.142
0.674	0.510	0.291
0.731	0.573	0.300
0.776	0.645	0.274
0.820	0.716	0.250
0.864	0.788	0.226
0.908	0.859	0.203
0.955	0.929	0.203

ION EXCHANGE IN ZEOLITE F

POTASSIUM - LITHIUM EXCHANGE AT 25 DEG. C

FOR THIS EXCHANGE ZA=1.0,ZB=1.0,ZX=1.0

1. EXPERIMENTAL RESULTS

Li_z	Li_s	LOGKC'
0.144	0.010	1.194
0.237	0.052	0.725
0.272	0.130	0.370
0.297	0.214	0.163
0.319	0.301	0.009
0.327	0.396	-0.158
0.354	0.479	-0.253
0.376	0.565	-0.361
0.384	0.660	-0.521
0.408	0.745	-0.655
0.614	0.923	-0.905
0.313	0.340	-0.081
0.343	0.423	-0.175
0.384	0.598	-0.406
0.460	0.756	-0.589
0.564	0.898	-0.861
0.777	0.978	-1.134

ION EXCHANGE IN ZEOLITE F(CL)6.6% KCl

POTASSIUM - LITHIUM EXCHANGE AT 25 DEG. C

FOR THIS EXCHANGE ZA=1.0, ZB=1.0, ZX=1.0

1. EXPERIMENTAL RESULTS

LI_Z	LI_S	LOGKC'
0.034	0.075	-0.390
0.044	0.267	-0.926
0.075	0.444	-1.021
0.096	0.628	-1.229
0.143	0.793	-1.389
0.187	0.860	-1.455
0.244	0.909	-1.519
0.356	0.947	-1.537

ION EXCHANGE IN ZEOLITE F

SODIUM - POTASSIUM EXCHANGE AT 25 DEG. C

FOR THIS EXCHANGE ZA=1.0,ZB=1.0,ZX=1.0

1. EXPERIMENTAL RESULTS

K_Z	K_S	LOGKC'
0.128	0.035	0.612
0.166	0.055	0.539
0.214	0.080	0.500
0.288	0.132	0.429
0.337	0.201	0.310
0.386	0.268	0.239
0.420	0.348	0.137
0.443	0.366	0.144
0.456	0.423	0.063
0.489	0.502	-0.018
0.519	0.584	-0.110
0.551	0.663	-0.200
0.587	0.712	-0.236
0.612	0.737	-0.245
0.757	0.763	-0.010
0.809	0.760	0.131
0.937	0.766	0.662
0.982	0.902	0.777
0.986	0.876	1.003
0.990	0.801	1.395
0.170	0.083	0.355
0.255	0.093	0.528
0.283	0.144	0.375
0.343	0.197	0.332
0.344	0.165	0.428
0.346	0.204	0.319
0.350	0.203	0.330
0.401	0.300	0.198
0.433	0.354	0.149
0.435	0.354	0.152
0.439	0.352	0.163
0.461	0.437	0.047
0.494	0.516	-0.034
0.502	0.511	-0.011
0.523	0.598	-0.128
0.530	0.595	-0.110
0.557	0.677	-0.217
0.683	0.699	-0.028
0.688	0.695	-0.010
0.691	0.693	0.000
0.843	0.698	0.371
0.845	0.697	0.379
0.938	0.739	0.732
0.946	0.734	0.807
0.973	0.817	0.911
0.978	0.914	0.626

ION EXCHANGE IN ZEOLITE F(CL)5.80 % KCL

SODIUM - POTASSIUM EXCHANGE AT 25 DEG. C

FOR THIS EXCHANGE ZA=1.C,ZB=1.0,ZX=1.C

1. EXPERIMENTAL RESULTS

K_Z	K_S	LOGKC'
0.317	C.C65	C.838
0.336	0.076	0.802
0.463	C.C92	C.943
0.535	0.1C6	1.COC
0.597	C.114	1.C75
0.673	0.13C	1.152
0.748	C.144	1.26C
0.784	0.154	1.313
0.840	C.214	1.298
0.882	C.284	1.288
0.910	C.364	1.260
0.931	0.449	1.232
0.938	C.544	1.116
0.955	0.632	1.105
0.961	C.728	C.977
0.972	0.82C	C.895
0.983	C.912	C.760

ION EXCHANGE IN ZEOLITE F(CL)4.20 % KCL

SODIUM - POTASSIUM EXCHANGE AT 25 DEG. C

FOR THIS EXCHANGE ZA=1.0,ZB=1.0,ZX=1.0

1. EXPERIMENTAL RESULTS

K_Z	K_S	LOGKC'
0.300	0.075	0.736
0.511	0.130	0.858
0.562	0.163	0.832
0.635	0.194	0.872
0.679	0.214	0.904
0.773	0.251	1.020
0.842	0.305	1.098
0.875	0.383	1.065
0.901	0.466	1.032
0.937	0.642	0.932
0.958	0.828	0.689

ION EXCHANGE IN ZEOLITE F(CL)2.05 % KCL

SODIUM - POTASSIUM EXCHANGE AT 25 DEG. C

FOR THIS EXCHANGE ZA=1.0, ZB=1.0, ZX=1.0

1. EXPERIMENTAL RESULTS

K_Z	K_S	LOGKC'
0.228	0.099	0.443
0.526	0.304	0.418
0.655	0.421	0.430
0.715	0.483	0.442
0.782	0.540	0.498
0.847	0.598	0.584
0.902	0.663	0.683
0.936	0.741	0.722
0.958	0.827	0.692
0.981	0.912	0.711

ION EXCHANGE IN ZEOLITE F

SODIUM - CAESIUM EXCHANGE AT 25 DEG. C

FOR THIS EXCHANGE ZA=1.0,ZB=1.0,ZX=1.0

1. EXPERIMENTAL RESULTS

Cs_Z	Cs_S	LOGKC'
0.156	0.003	1.801
0.300	0.013	1.525
0.430	0.030	1.400
0.524	0.073	1.158
0.580	0.137	0.952
0.604	0.222	0.740
0.622	0.312	0.572
0.632	0.405	0.414
0.637	0.500	0.257
0.647	0.546	0.195
0.641	0.599	0.090
0.636	0.670	-0.053
0.662	0.793	-0.279
0.677	0.830	-0.355
0.593	0.141	0.961
0.621	0.330	0.534
0.646	0.421	0.412
0.642	0.623	0.048
0.704	0.902	-0.575
0.781	0.975	-1.026

Ion Exchange in Zeolite F

Potassium-Caesium Exchange at 25° C

Experimental Results

Cs_z	Cs_s	
0.010	0.095	
0.046	0.177	
0.192	0.202	
0.313	0.240	
0.370	0.310	
0.412	0.390	K ⟶ Cs
0.503	0.444	
0.587	0.501	
0.657	0.564	
0.705	0.640	
0.818	0.792	
0.919	0.907	
---	---	
0.168	0.057	
0.363	0.108	
0.587	0.171	
0.683	0.254	
0.727	0.347	
0.784	0.437	Cs ⟶ K
0.826	0.530	
0.843	0.627	
0.893	0.718	
0.911	0.815	
0.971	0.905	

Ion Exchange in Zeolite F

Sodium-Calcium Exchange at 25° C

Experimental Results

Ca_z	Ca_s	
0.160	0.0	
0.319	0.0	
0.439	0.026	
0.485	0.096	
0.510	0.181	Na ⟶ Ca
0.526	0.271	
0.552	0.354	
0.622	0.516	
0.785	0.922	
---	---	
0.978	0.914	
0.953	0.730	
0.963	0.524	
0.961	0.325	Ca ⟶ Na
0.919	0.152	
0.880	0.077	
0.786	0.022	

Ion Exchange in Zeolite F

Sodium-Strontium Exchange at 25° C

Experimental Results

Sr_z	Sr_s	
0.141	0.012	
0.157	0.002	
0.306	0.009	
0.400	0.050	
0.434	0.128	
0.477	0.202	
0.479	0.300	
0.508	0.383	Na ⟶ Sr
0.517	0.476	
0.539	0.563	
0.583	0.635	
0.582	0.709	
0.601	0.700	
0.616	0.877	
0.657	0.835	
0.673	0.933	
---	---	
0.894	0.050	
0.894	0.010	
0.898	0.060	
0.904	0.045	
0.914	0.020	Sr ⟶ Na
0.920	0.547	
0.954	0.627	
0.961	0.223	
0.975	0.815	

Ion Exchange in Zeolite F

Sodium-Barium Exchange at 25° C

Experimental Results

Ba_z	Ba_s	
0.159	0.0	
0.320	0.0	
0.481	0.0	
0.639	0.0	
0.799	0.0	
0.919	0.024	Na ⟶ Ba
0.927	0.086	
0.946	0.208	
0.956	0.302	
0.978	0.387	
1.0	0.894	
---	---	
1.0	0.999	
1.0	0.893	
1.0	0.661	
1.0	0.497	Ba ⟶ Na
1.0	0.305	
1.0	0.107	
1.0	0.013	
1.0	0.002	

Ion Exchange in Zeolite F

Potassium-Barium Exchange at 25° C

Experimental Results

Ba_z	Ba_s	
0.160	0.0	
0.321	0.0	
0.478	0.0	
0.510	0.080	
0.516	0.177	
0.503	0.286	K ⟶ Ba
0.506	0.383	
0.474	0.503	
0.488	0.594	
0.521	0.674	
0.523	0.947	
0.524	0.947	
---	---	
1.0	0.899	
1.0	0.723	
1.0	0.515	
1.0	0.309	Ba ⟶ K
1.0	0.111	
1.0	0.010	
1.0	0.00	

Ion Exchange in Zeolite K-F(Cl) (6.6% KCl)

Potassium-Barium Exchange at 25° C

Experimental Results

Ba_z	Ba_s
0.134	0.0
0.160	0.080
0.161	0.179
0.172	0.272
0.188	0.359
0.185	0.462
0.189	0.558
0.202	0.649
0.205	0.747
0.214	0.840
0.224	0.933
0.208	0.979

The above are for the exchange K ⟶ Ba.

9. References

1. H.S. Thompson, J. Roy. Agr. Soc., 11, 68 (1850).
2. J.F. Way, J. Roy. Agr. Soc., 11, 313 (1850); 13, 123 (1852).
3. J. Lemberg, Z. Deutsch. Geol. Ges. 22, 355 (1870); 28, 519 (1876).
4. G. Wiegner, J. Landwirtsch., 60, 111 (1912).
5. R.M. Barrer, Chem. and Ind. 1258 (1962).
6. C.B. Amphlett, "Inorganic Ion Exchangers", Elsevier (1964).
7. R. Gans, Jahrb. Preuss. Geol. Landesanstalt (Berlin), 26, 179 (1905).
8. W.A. Deer, R.A. Howie, J. Zussman, "Rock-forming Minerals", Vol. 4, Longmans (1963).
9. W. Loewenstein, Amer. Mineral., 39, 92 (1954).
10. W.M. Meier, in "Molecular Sieves", Society of Chemical Industry, London (1968).
11. P.B. Venuto, P.S. Landis, Advances in Catalysis, 18, 259 (1968).
12. R.M. Milton, in "Molecular Sieves", Soc. Chem. Ind. London (1968).
13. e.g., R.M. Barrer, in 'Colloque Internat. sur les Reactions dans l'Etat Solide" Paris CNRS (1948). Also (17).
14. R.M. Barrer, J.W. Baynham, J. Chem. Soc. 2882 (1956).
15. R.M. Barrer, J.W. Baynham, F.W. Bultitude, W.M. Meier, J. Chem. Soc. 195 (1959).
16. R.M. Barrer, L. Hinds, J. Chem. Soc., 1879 (1953).
17. R.M. Barrer, J.D. Falconer, Proc. Roy. Soc.(A) 236, 227 (1956).
18. R.M. Barrer, D.C. Sammon, J. Chem. Soc., 2838 (1955).
19. R.M. Barrer, J.A. Davies, L.C.V.Rees, J. Inorg. Nucl. Chem., 31 219 (1969).
20. L.L. Ames, Amer. Mineral., 49, 127 (1964).

21. L.L. Ames, Amer. Mineral., 49, 1099 (1964).

22. R.M. Barrer, R. Papadopoulos, L.V.C. Rees, J. Inorg. Nucl. Chem., 29, 2047 (1967).

23. R.M. Barrer, J. Chem. Soc., 2158 (1948).

24. R.M. Barrer, W.M. Meier, Trans. Farad. Soc., 55, 130 (1959).

25. R.M. Barrer, L.V.C. Rees, D.J. Ward, Proc. Roy. Soc.(A) 273, 180 (1963).

26. R.M. Barrer, W. Buser, W.F. Grutter, Helv. Chim. Acta., 39, 518 (1956).

27. R.M. Barrer, L.V.C. Rees, M. Shamsuzzoha, J. Inorg. Nucl. Chem., 28, 629 (1966).

28. H.S. Sherry, J. Phys. Chem. 70, 1158 (1966).

29. H.S. Sherry, J. Phys. Chem., 72, 4086 (1968).

30. H.S. Sherry, J. Phys. Chem., 72, 4095 (1968).

31. H.S. Sherry, J. Colloid. Interf. Sci., 28, 288 (1968).

32. R.M. Barrer, J.A. Davies, L.V.C. Rees, J. Inorg. Nucl. Chem., 30, 3333 (1968).

33. R.M. Barrer, J. Chem. Soc., 2342 (1950).

34. R.M. Barrer, J. Raitt, J. Chem. Soc., 4641 (1954).

35. R.M. Barrer, D.C. Sammon, J. Chem. Soc., 675 (1956).

36. F. Helferrich, Amer. Mineral., 49, 1752 (1964).

37. G. Eisenman, Proc. Symp. Membrane Transport and Metabolism, Prague 1960. Academic Press (1961).

38. H. Hoss, R. Roy, Beit. für Mineral u. Petrog., 7, 389 (1960).

39. R.M. Barrer, F.W. Bultitude, I.S. Kerr, J. Chem. Soc., 1521 (1959).

40. R.M. Barrer, J.W. Baynham, J. Chem. Soc., 2882 (1956).

41. R.M. Barrer, J.W. Baynham, F.W. Bultitude, W.M. Meier, J. Chem. Soc., 195 (1959).

42. A.M. Taylor, R. Roy, Amer. Mineral., 49, 656 (1964).

43. A.M. Taylor, R. Roy, J. Chem. Soc., 4028 (1965).

44. R.M. Barrer, J.F. Cole, H. Sticher, J. Chem. Soc. (A), 2475 (1968).

45. R.M. Barrer, N. McCallum, J. Chem. Soc., 4029 (1953).

46. H. Borer, Ph.D. Dissertation No. 4308, E.T.H. Zürich (1969).

47. F. Helferrich, "Ion Exchange", McGraw Hill, New York (1962).

48. E. Glueckauf, Nature, 163, 414 (1949).

49. J. Kielland, J. Soc. Chem. Ind., 54, 232T (1935).

50. R.H. Fowler, E.A. Guggenheim, "Statistical Thermodynamics" p.437, Cambridge University Press (1939).

51. E. Ekedahl et al., Acta. Chem. Scand., 4, 556 (1950).

52. E. Hogfeldt et al., Acta Chem. Scand., 4, 828 (1950).

53. W.J. Argersinger, A.W. Davidson, O.D. Bonner, Trans. Kansas Acad. Sci., 53, 404 (1950).

54. G.L. Gaines, H.C. Thomas, J. Chem. Phys., 21, (4), 714 (1953).

55. W.J. Argersinger, A.W. Davidson, Ann. N.Y. Acad. Sci., 57, 105 (1953).

56. E. Hogfeldt, Arkiv. Kemi, 5, 147 (1952).

57. R.L. Hay, Amer. Mineral., 49, 1366 (1964).

58. K. Harada, S. Iwamoto, K. Kihara, Amer. Mineral., 52, 1785 (1967).

59. J. Wyart, P. Chatelain, Bull. Soc. Min. Franc. 61, 121 (1938).

60. H. Strunz, Mineralog. Tabellen, Akad. Verlags., Liepzig (1957).

61. H. Steinfink, Acta. Cryst., 15, 644 (1962).

62. R. Sadanaga, F. Marumo, Y. Takeuchi, Acta Cryst., 14, 1153 (1961).

63. A.J. Regis et al., J. Phys. Chem., 64, 1567 (1960).

64. D.W. Breck, W.G. Eversole, R.M. Milton, J. Am. Chem. Soc., 78, 2338 (1956).

65. S.P. Zhdanov, M.E. Ovsepyan, Izvest. Akad. Nauk S.S.S.R., Ser. Khim. 1, 11 (1965).

66. Groves "Silicate Analysis", Allen and Unwin, London (1954).

67. A.I. Vogel, "Textbook of Quantitative Inorganic Analysis" 3rd Edn. Longmans (1961).

68. e.g., Azaroff, Buerger, "The Powder Method in X-ray Crystallography", McGraw Hill, (1958).

69. J.F. Cole, H. Villiger, Chem. Dept Imperial College, London (1968).

70. J.F. Cole, H. Villiger, Min. Mag. in press.

71. B.E. Conway, "Electrochemical Data" Elsevier (1952).

72. H.S. Harned, B.B. Owen, "Physical Chemistry of Electrolyte Solutions", A.C.S. Monograph 137, 3rd Edn. Reinhold (1958).

73. R.A. Robinson, R.H. Stokes, "Electrolyte Solutions", Butterworths (1959).

74. D.H. Freeman, J. Chem. Phys., 35(1), 189 (1961).

75. B.J. Birch, J.P. Redfern, J.E. Salmon, Trans. Farad. Soc., 63 (10), 2362 (1967).

76. J.A. Davies, Ph.D. Thesis, University of London (1967).

77. R.L. Hay, "Zeolites and Zeolitic Reactions in Sedimentary Rocks" Geol. Soc. Amer. Spec. Publ. 85, (1966).

78. B.M. Munday, unpublished work (1968).

79. D.L. Jones, Ph.D. Thesis, University of London (1969).